The effects of persistent organic pollutants (POPs) on the steroidogenesis in the mouse Y1 adrenocortical cell line

Silje Kathrine Larsen

Thesis submitted in fulfilment for the degree of Master of Science

Department of Biology

University of Bergen

October 2015

ACKNOWLEDGMENTS

The work presented in this thesis was performed in the Environmental Toxicology group at the Department of Biology at the University of Bergen and at Hormone Laboratory of the Haukeland University Hospital. This project was funded by the Norwegian Research Council, POPstress, Project 213076.

I would like to thank my supervisors Anders Goksøyr, Odd-Andrè Karlsen and Kareem Eldin Mohammed Ahmed who have been helping me through my time as a master student. Thank you Anders, for helping me in the writing process in my thesis, and for letting me attend two conferences and present a poster in one of them. Odd-Andrè, thank you for letting me knock on your door whenever I had a question and for helping me throughout my master. Kareem, I want to specially thank you for your patient teaching in the laboratory and for your dedication from day one.

Also I would like to thank Roger Lille-Langøy for giving me advice, both in the laboratory and for helping me in the writing process. A special thank you to Ralf Kellmann, for dedicating your time to teach and help me at the Hormone Laboratory

I would also like to thank all other members of the Environmental Toxicology group, including all my fellow master student, PhDs and researchers.

For all my friends who have been supporting me, you are the best!

Finally, I want to thank my family for your love and support and for always being there for me. You always believe in me no matter what.

Sotra, 01 October 2015

Silje Kathrine Larsen

Table of contents

ABSTRACT

The endocrine system refers to glands which secrets hormones that regulates a variety of physiological processes. The adrenal cortex is part of the endocrine hypothalamus-pituitary-adrenal axis, and produces and secretes steroids regulating stress reactions after stimulation by hormones secreted from the brain. Being an organ regulated by hormones, the adrenal cortex is also a potential a target for endocrine disrupting compounds that may mimic endogenous hormone receptor ligands. The Y1 adrenocortical cell line is an *in vitro* model originating from a tumour in the mouse adrenal cortex, and has maintained the ability to produce and secrete steroids. In this thesis, Y1 cells were exposed to a complex mixture of persistent organic pollutants (POPs), and the effects on steroidogenesis on steroid production and selected steroidogenic enzymes were studied with LC-MS/MS and Western blotting, respectively. Results showed that the overall steroid production in the cells was increased in the highest administered dose of the POP mixture. This indicates that POPs present in the mixture could act as endocrine disruptors and alter the steroidogenesis. More studies of the effects of this mixture might provide more information of the mechanisms behind increased steroidogenesis.

ABBREVIATIONS

Abbreviation	Full name
%	Percentage
x g	Gravitational acceleration (relative to Earth)
℃	Celcius
2D	Two-dimensional
α	Alpha
β	Beta
γ	Gamma
µg	Microgram
µL	Microlitre
µm	Micrometre
AC	Adenylyl cyclase
AC	Alternating Current
ACTH	Adrenocorticotropic hormone
ACTH-R	Adrenocorticotropic hormone receptor, also known as MC2-R
Ang II	Angiotensin II
APS	Ammonium persulfate
Arom	Aromatase
ATCC	American Type Culture Collection
ATF-1	Activating transcription factor 1
ATP	Adenosine triphosphate
AVP	Arginine vasopressin
BDE	Bromodiphenyl ether
BSA	Bovine serum albumin
CaM kinase	Calcium/calmodulin-dependent protein kinase
cAMP	Cyclic adenosine monophosphate
CBB	Coomassie brilliant blue
CID	Collision induced dissociation
CRE	cAMP response element
CREB	cAMP response element binding protein
CRF	Corticotropin releasing factor (same as CRH)
CRH	Corticotropin releasing hormone (same as CRF)
CNS	Central nervous system
CYP(P450)	Cytochrome P450 monooxygenase
DC	Direct Current
de novo	From new
DDE	Dichlorodiphenyldichloroethene
DDT	Dichlorodiphenyltrichloroethane
DMEM	Dulbecco's Modified Eagle Medium
DMSO	Dimethyl sulfoxide
DNA	Deoxyribonucleic acid

DTT	Dithiothreitol
ECL	Enhanced chemiluminescence
EDTA	Ethylenediaminetetraacetic acid
e.g	Exampli gratia (for example)
ER	Endoplasmic reticulum
ESI	Electrospray ionisation
Et al.	*Et alii* (and others)
EtOH	Ethanol
Eq	Equilibration buffer
FBS	Fetal bovine serum
Fig.	Figure
FL	Fluorescence
FLI	Fluorescence intensity
FSK	Forskolin
g	Gram
h	Hour
HB	Homogenization buffer
HBCD	Hexabromocyclododecane
HCB	Hexachlorobenzene
HCH	Hexachlorocyclohexane
HCl	Hydrochloric acid
HDL	High-density lipoprotein
HPA	Hypothalamic-pituitary-adrenal
HPLC	High performance liquid chromatography
HRP	Horseradish peroxidase
HSD	Hydroxysteroid dehydrogenase
HSL	Hormone-sensitive lipase
Hz	Hertz
IAA	Iodoacetamide
Ig	Immunoglobin
IgG	Immunoglobin G
in vitro	In glass
in vivo	Within the living
IPG	Immobilized pH gradient
IS	Internal standard
kDa	Kilodalton
LC	Liquid chromatography
LC-MS/MS	Liquid chromatography-tandem mass spectrometry
LDL	Low-density lipoprotein
LFP	Local field potential
LLE	Liquid-liquid extraction
M	Molar
mA	Milliamps
mAC	Membranous adenylyl cyclase

MC2-R	Melanocortin 2 receptor
MeOH	Methanol
mg	Milligram
min	Minute
mL	Millilitre
mm	Millimetre
mM	Millimolar
mrm	Multiple reaction monitoring
mRNA	Messenger ribonucleic acid
MS	Mass spectrometer
m/z	Mass to charge ratio
n	Mean cell number
ND	Not detectable
nm	Nanometre
nM	Nanomolar
OHP	Dihydroxyprogesterone
PAGE	Polyacrylamide gel electrophoresis
PBB	Polybrominated biphenyls
PBC	Polybrominated compound
PBDE	Polybrominated diphenyl ether
PBS	Phosphate buffered saline
PCB	Polychlorinated biphenyl
Pen-Strep	Penicillin-Streptomycin
PFC	Perfluorinated compound
PFDA	Perfluorodecanoic acid
PFHxS	Perfluorohexanesulfonic acid potassium salt
PFNA	Perfluorononanoic acid
PFOA	Perfluorooctanoic acid
PFOS	Perfluorooctane sulfonate potassium salt
PFUnDA	Perfluorododecanoic acid
PKA	Protein kinase A
PMSF	Phenylmethylsulfonyl fluoride
PMT	Photo multiplier tube
POP	Persistent organic pollutant
PVDF	Polyvinylidene difluoride
PVN	Paraventricular nucleus
Q	Quadruple
QC	Quality Controls
RIPA	Radioimmunoprecipitation assay buffer
RL	RIPA whole cell lysate
RM	RIPA mitochondria
rpm	Revolutions per minute
SB	Sample buffer
scc	Side-chain cleavage

SDS	Sodium dodecyl sulphate
SM	Sucrose isolated mitochondria
SNS	Sympathetic nervous system
SR-B1	Scavenger receptor B1
SS	Sucrose cell supernatant
StAR	Steroidogenic acute regulatory protein
TBS	Tris-buffered saline
TBST	TBS Tween-20
TEMED	N,N,N',N'-tetramethyl-ethylenediamine
TGS	Tris/Glycine/SDS
Tris	Tris(hydroxymethyl)aminomethane
UPLC	Ultra performance liquid chromatographer
V	Volt
v/v	Volume to volume
w/v	Weight to volume
Å	Angstrom

1. INTRODUCTION

1.1 The adrenal endocrine system

The endocrine system refers to glands which secrets hormones that regulates a variety of physiological processes. The adrenal gland is part of the endocrine system, and consists of the adrenal medulla and the adrenal cortex. The adrenal medulla secretes catecholamines like adrenaline and norephineprine in an immediate acute stress stimulation known as the fight-or-flight response. This is a nerve response regulated by the sympathetic nervous system (SNS). The adrenal cortex is part of the endocrine hypothalamus-pituitary-adrenal axis, and produces and secretes steroids regulating stress reactions after stimulation by hormones secreted from the brain (Rainey et al., 2004).

One way of defining stress is describing it as a state of threatened homeostasis, harmony, balance, or equilibrium (Johnson et al., 1992). A stressor may be internal factors like hypoglycaemia, or factors such as temperature, exercise or injury, or psychological factors that give rise to fear or anxiety (Johnson et al., 1992). One of the major ways of coping with stress in humans and other animals is the involvement of the hypothalamic-pituitary-adrenal (HPA) axis (Dedovic et al., 2009). This axis releases specific hormones from the brain that are transported to the adrenal gland, which produce glucocorticoids, mineralocorticoids and sex steroids from cholesterol. This axis is a vital part of maintaining homeostasis under normal basal conditions, as well as when a person or animal is faced with a stress factor or stressor.

Glucocorticoids produced in the adrenal cortex are transported to various organs throughout the body, which then binds to glucocorticoid receptors. Glucocorticoid receptors are found in many cell types in several organs and the brain, and can modify the transcription of key regulatory proteins (Herman et al., 2003). The effect of glucocorticoids in the organism are numerous, and include metabolic, cardiovascular and immune responses (Dedovic et al., 2009), as well as maintaining blood glucose levels (Bergman et al., 2013). Mineralocorticoids control and regulate water and electrolyte balance by reduction of sodium ions being excreted from the body. This occurs by stimulating reabsorption of sodium ions in the kidneys. Effects of hyper-secretion causes edema and neuromuscular dysfunction (Bergman et al., 2013). The cortex also secretes sex steroids like androgens and estrogens.

1.2 The Hypothalamus-Pituitary-Adrenal (HPA) axis

The first step in the HPA axis (Fig. 1-1) is controlled by a set of hypophysiotrophic neurons in the hypothalamic paraventricular nucleus (PVN). PVN synthesize corticotropin releasing hormone (CRH) and other factors, such as arginine vasopressin (AVP). CRH and AVP are secreted from the hypothalamus and sent via the hypophysial portal veins to the anterior pituitary. The anterior pituitary secretes adrenocorticotropic hormone (ACTH) into the bloodstream, where ACTH binds to the ACTH receptor (ACTH-R) located on the surface of cells present in the adrenal cortex. ACTH-R is also known as the melanocortin 2 receptor (MC2-R). After stimulation of the ACTH-R, the adrenal cortex secretes glucocorticoids and other steroids involved in the stress reaction (Herman et al., 2005). There is also normal secretion of glucocorticoids in a non-stressful manner, with a sharp secretion when a person or animal wakes up in the morning. The levels of glucocorticoids slowly decline throughout the day (Dedovic et al., 2009).

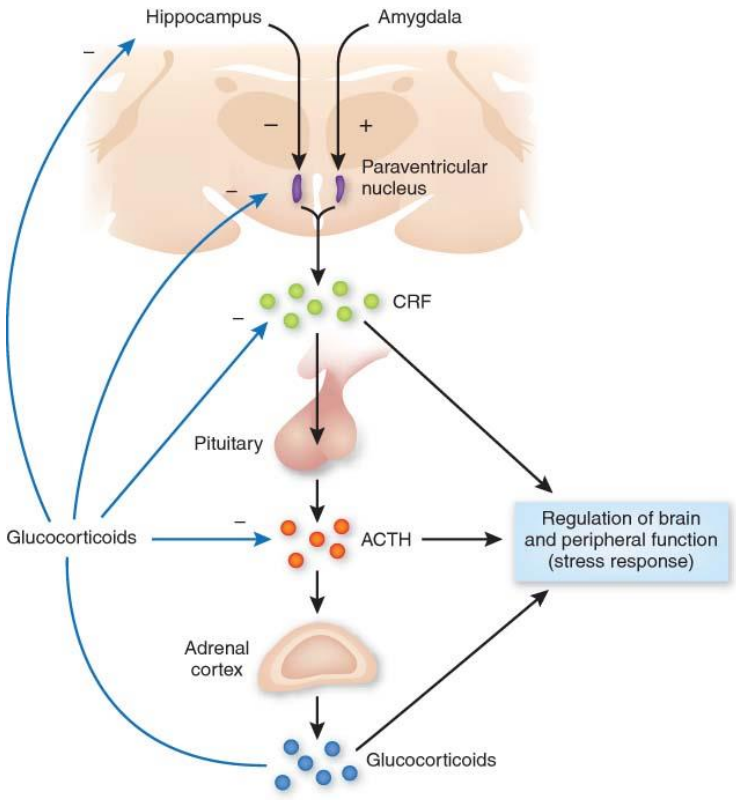

Figure 1-1: The HPA axis. CRH (CRF in the figure) are secreted from the paraventricular nucleus in the hypothalamus. CRF binds to the pituitary gland that secrets ACTH. ACTH is released into the bloodstream to reach the adrenal cortex, where it binds to the ACTH-R to produce glucocorticoids. Glucocorticoids are subsequently sent to various organs in the body. To terminate the secretion of ACTH and CRH, glucocorticoids can bind to glucocorticoid receptors in the brain in a negative feedback loop. Figure from Hyman (2009).

During acute stress, oxygen and nutrients are sent to the central nervous system (CNS) and to organs experiencing stress. The organism will increase the respiratory rate in order to deliver more oxygen to the organs, while heart rate and blood pressure increase in order to deliver sufficient nutrients. Energy mobilization is elevated by gluconeogenesis and lipolysis in the liver, which increase levels of glucose to replenish energy stores. Effects on the immune system involve suppression of innate immunity in immune organs, controlling the inflammatory response. The organism's ability to grow, reproduce and digest food is also inhibited. All these effects continue until glucocorticoids inhibit CRH- or ACTH-secretion until homeostasis is restored (Charmandari et al., 2005).

When an organism is exposed to chronic stress, the HPA axis in the body is activated for a long period of time, which results in continuous secretion of CRH and/or steroids. This prolonged secretion could cause a number of disorders such as malnutrition, Cushing syndrome and hyperthyroidism (Charmandari et al., 2005).

1.3 The adrenal cortex

The adrenal cortex consists of three zones known as zona glomerulosa, zona fasciculata and zona reticularis (Arnold, 1866). Each zone produces a different class of steroids (Fig. 1-2), depending on the enzymes that is present in each zone (Miller et al., 2010).

Enzymes involved in the steroidogenic pathway are hydroxysteroid dehydrogenases (HSDs) and cytochrome P450 (CYPP450) monooxygenase enzymes. The enzymes are found in the mitochondria and the endoplasmic reticulum (ER) (Rainey et al., 2004). The cytochrome P450 enzymes P450*scc* (CYP11A1), P450c11β (CYP11B1) and P450c11AS (CYP11B2) are located within the mitochondria. 3β-hydroxysteroid dehydrogenase (3βHSD) are found in mitochondria and ER, whilst P450c17 (CYP17A1) and P450c21 (CYP21) are located within the ER (Miller, 2013) The P450arom (CYP19) is located in the ER (Miller et al., 2010).

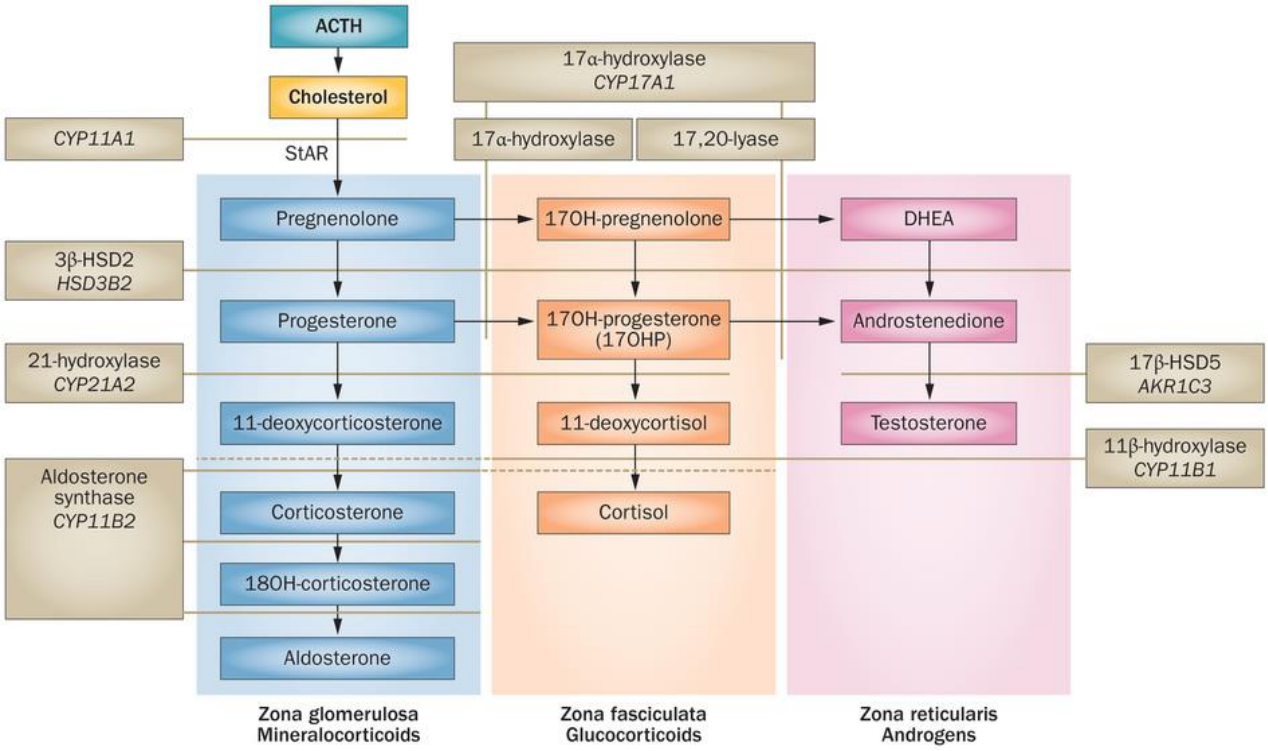

Figure 1-2: The steroidogenesis in humans that occur within the three zones in the adrenal cortex. The zona glomerulosa produces mineralocorticoids with aldosterone as the main endproduct. Glucocorticoids are synthesized in the zona fasciculata with the main product being cortisol. The androgens are synthesized in the zona reticularis, where androstenedione and testosterone can further be metabolised by CYP19 (aromatase) to give estrone and estradiol (not shown). In normal adrenal mouse cells *in vivo*, the main glucocorticoid endproduct is corticosterone (Bloch et al., 1960). Figure from T. S. Han et al. (2014).

ACTH, angiotensin II (Ang II) and potassium (K^+) regulate steroidogenesis in the adrenal cortex (Figure 1-3). Ang II and K^+ mainly regulate the synthesis of mineralocorticoids in zona glomerulosa. ACTH is the main hormone that regulates the synthesis of glucocorticoids and androgens in the zona fasciculata and reticularis (Rainey et al., 2004).

1.3.1 Mechanisms of steroidogenesis in response to ACTH

ACTH binds to ACTH-R on the cell surface (Fig. 1-3). The ACTH-R is a seven transmembrane G-protein coupled receptor (Mountjoy et al., 1992). Activation of the receptor increases the levels of cAMP (cyclic adenosine monophosphate), which in turn stimulates protein kinase A (PKA). PKA can phosphorylate target proteins by releasing an activated catalytic subunit. An important target is the cAMP response element binding protein (CREB). PKA phosphorylates CREB, which then becomes activated and binds to a specific DNA sequence called the cAMP response element (CRE) in the promotor regions of responsive genes

(Rehfuss et al., 1991). Genes that are regulated by cAMP are *CYP17, CYP11A*, *CYP11B1*, *CYP11B2* and *CYP21* (A. J. Clark et al., 1996).

However, a difference in CREB expression between adrenal cells in primary culture and the Y1 mouse adrenocortical cell line has been observed. In the Y1 cell line (chapter 1.4), the CREB protein expression is lower compared to primary cultures, while the ATF-1 (activating transcription factor 1) protein is overexpressed (Mattos et al., 2005). ATF-1 is another CRE-binding protein that is regulated by cAMP and PKA, and is expressed in a variety of cell lines. The DNA binding site for CREB and ATF-1 are quite similar with a 91 % sequence identity, thus ATF-1 probably binds to the same promoter regions as CREB (Rehfuss et al., 1991).

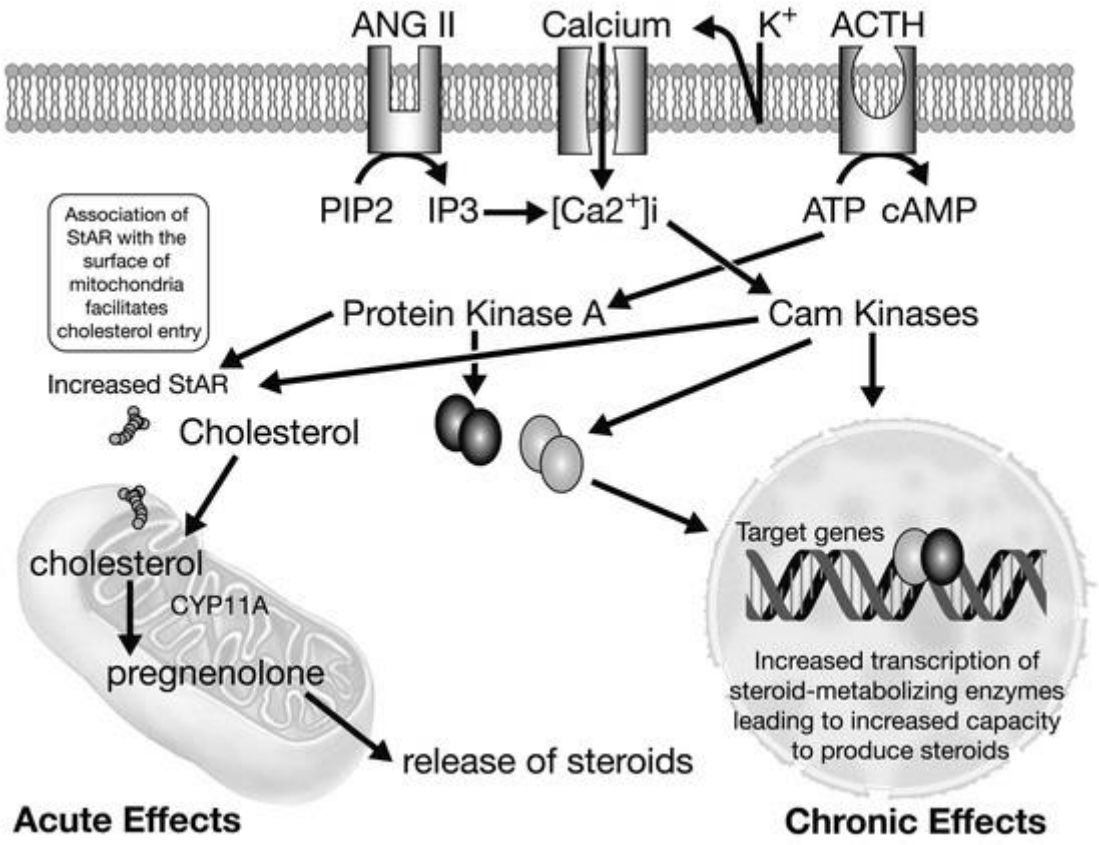

Figure 1-3: Intracellular cell signalling and mechanisms in adrenocortical cells. The agonists Angiotensin II (Ang II), K^+ and ACTH bind to membrane receptors and potassium channels**,** leading to steroid synthesis. Figure from (Parmar et al., 2011).

Cholesterol in rodents can be synthesized *de novo* from acetate in the endoplasmic reticulum, but is mainly obtained from high-density lipoproteins (HDL) via the scavenger receptor B1 (SR-B1) (Temel et al., 1997) and stored in lipid droplets. In humans, cholesterol is obtained from low-density lipoproteins (LDL) and stored in endosomes (Miller, 2013). When both

human and rodent cells is stimulated with ACTH, free cholesterol is synthesized from the lipid droplets by hormone-sensitive lipase (HSL), which is regulated by ACTH.

The rate-limiting step in the steroidogenic pathway is the translocation of cholesterol from the outer mitochondrial membrane to the inner mitochondrial membrane via the steroidogenic acute regulatory protein (StAR). Subsequently, cholesterol is converted to pregnenolone by side-chain cleavage of cholesterol via cytochrome P450scc (CYP11A1). A cell is called steroidogenic if there is presence of CYP11A1 (Miller, 2013). Pregnenolone is the precursor to all steroids produced in adrenocortical cells. Pregnenolone is translocated to the endoplasmic reticulum where most of the steroids are synthesised. Corticosterone are synthesized by hydroxylation of deoxycorticosterone via CYP11B1 (Bergman et al., 2013).

1.4 The Y1 adrenocortical cell line

The term adrenocortical carcinoma means a tumour originating from the epithelial cell layer of the adrenal cortex (Fay et al., 2014). The Y1 cell line has its origin from a tumour in an adult LAF_1 (C57L x A/HeJ) male mouse that was exposed to radiation from a test atomic bomb (Cohen et al., 1957b). Slices of the tumour was stimulated with ACTH, and the main products were mainly corticosterone and 11β-hydroxy-Δ^4-androstene-3,17-dione (Cohen et al., 1957a). The tumour was incubated in a new Laf_1 mice, and the tumour seemed to leave the adrenal medulla unchanged, but with a marked atrophy of the adrenal cortex with indication of secretion of both glucocorticoids and mineralocorticoids (Cohen et al., 1957b).

Slices of the tumour were grown in culture and mice. Cells grown in culture had a higher ability to secrete hormones than the original tumour, but production of steroids declined over time. This ability was restored when cultured cells were again administered into animals (Buonassisi et al., 1962). From these cultured cells, Yasumura et al. (1966) managed to isolate cells without a feeding layer resulting in two distinctive cell types: fibroblastic or epithelial. The epithelial cells were cloned, and the subclones were responsive to stimulation by ACTH and produced steroid hormones at varying rates. The Y1 clone had the highest secretion of hormones, and this secretion was indefinite as long as the serum concentration in the growth medium was high (Yasumura et al., 1966).

The Y1 cells do not produce steroids when treated with Ang II (Langlois et al., 1990), but produce steroids when stimulated with ACTH. The Y1 cells are one of the few adrenocortical cell lines that remains responsive to ACTH, and treatment of the Y1 cells with ACTH increases the production of ACTH-R mRNA by up to 6-fold compared to normal levels by activating cAMP (Mountjoy et al., 1994). Other analogues that induce cAMP can also start steroidogenesis in the Y1 cells. Forskolin is a diterpene (Fig. 1-4) that originates from the Indian plant *Coleus forskohlii,* and is shown to activate adenylyl cyclase and raise levels of cAMP (Schimmer et al., 1985). Membranous adenylyl cyclase (mAC) is a membrane bound protein that catalyses the conversion of ATP to cAMP. There are nine isoforms, and forskolin can activate isoform AC1-8, but not AC-9. In Y1, forskolin is suggested to activate AC-4 (Rui et al., 2004).

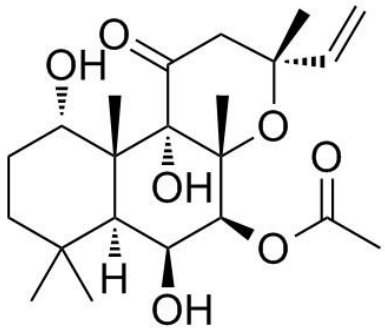

Figure 1-4: Chemical structure of forskolin. Figure obtained from MedChem Express.

In rodents, as in humans (Fig. 1-3), corticosterone is synthesized in both zona glomerulosa and in zona fasciculata by hydroxylation of deoxycorticosterone via either CYP11B2 or CYP11B1, respectively. However, the steroid profile of the Y1 cells line is different from the normal steroid adrenocortical profile in normal mouse (Fig. 1-5). The main end products produced in Y1 are 20α-hydroxy-Δ^4-pregnen-3-one (20α-dihydroxyprogesterone) and 11β,20α-dihydroxy-Δ^4-pregnen-3-one (11β,20α-dihydroxyprogesterone) (Parmar et al., 2011), instead of corticosterone and aldosterone. One reason for this deviation is that the levels of the 20α-hydroxysteroid dehydrogenase (20αHSD) enzyme are increased in Y1 cells (Pierson Jr, 1967).

The other reason for a different steroid profile is deficiency in the CYP21 enzyme in Y1 cells. In a study by Parker et al. (1985), Y1 cells were transfected with the 21-OHase gene encoding for CYP21. The transfected cells showed increased expression of adrenal 21-OHase mRNA and increased volumes of steroids synthesised by CYP21. However, no expression of the gene was found in normal untreated cells, suggesting that CYP21 is not present in the Y1 cell line.

Still, some corticosterone was detected in untreated cells, but at much lower levels compared to cells transfected with the CYP21 gene. The absence of CYP21 expression was later confirmed by Amor et al. (1988).

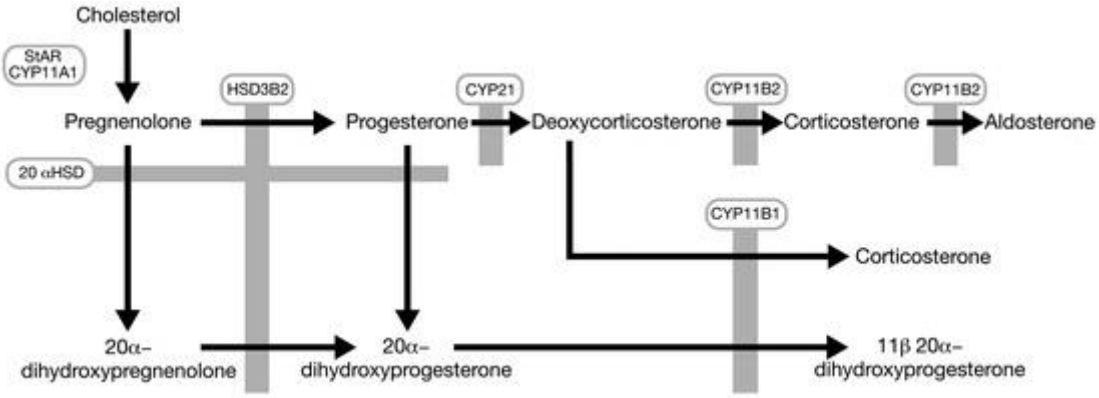

Figure 1-5: Steroid biosynthetic pathway in rodents and the special steroid profile in the Y1 cell line. The pathway in Y1 cells does not involve the CYP21 enzyme, leading to an abnormal steroid profile compared to how steroids are synthesized *in vivo*. Picture adapted from Parmar et al. (2011).

When stimulated with ACTH, forskolin or cAMP, the cell morphology changes from an epithelial cell to a round cell shape, a process called cell rounding (Fig. 1-6). This change is mediated through dephosphorylation of paxillin, a focal adhesion protein, causing paxillin to translocate from the focal adhesions to the cytoplasm, disorganising stress fibres and the rearrangement of the actin cytoskeleton (J.-D. Han et al., 1996). Actin filaments are involved in delivery of cholesterol to mitochondria (Osawa et al., 1984) and might be linked to the change of cell morphology.

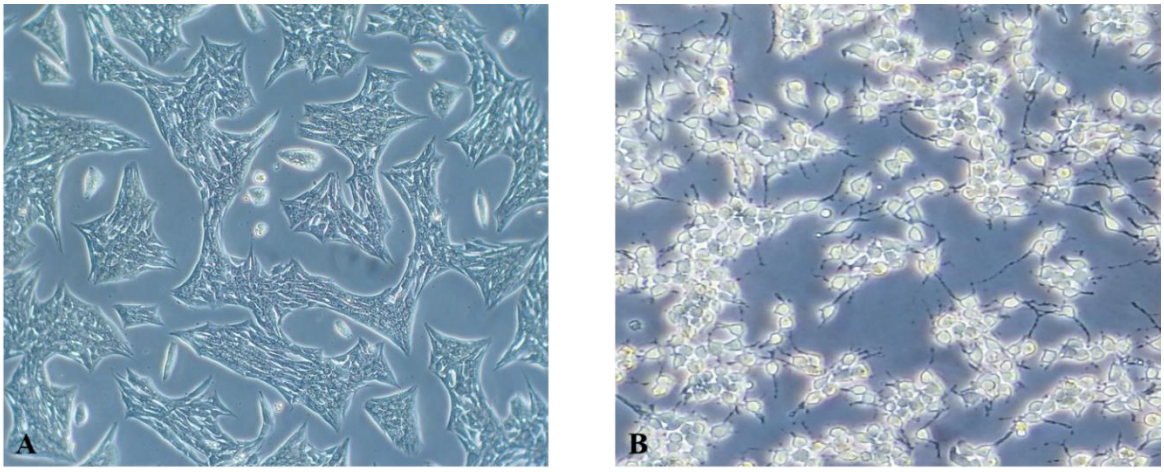

Figure 1-6: Y1 cell morphology. A) Cells after three days of incubation, showing a characteristic epithelial shape. B) The cell shape became rounded after stimulation with 0.1 % forskolin. Pictures are taken from different flasks. 10x zoom. Y1 cell growth are shown in Fig.4-1 in results. Pictures by Silje Kathrine Larsen.

1.5 Endocrine disrupting compounds

The definition for endocrine disrupting compounds (EDCs) can be described as: "An endocrine disruptor is an exogenous substance or mixture that alters function(s) of the endocrine system and consequently causes adverse health effects in an intact organism, or its progeny, or (sub) populations." Or, "A potential endocrine disruptor is an exogenous substance or mixture that possesses properties that might be expressed to lead to endocrine disruption in an intact organism, or its progeny, or (sub) populations" (Bergman et al., 2013).

Persistent organic pollutants, or POPs, is a common description used for chemicals that are persistent in the environment, with lipophilic and hydrophobic chemical properties, which often leads to POPs being stored and accumulate in fatty tissue. Storage in fatty tissue may lead to slow metabolism of the POPs that makes them persistent, and accumulation is often observed in food chains. Some POPs can alter hormone response in organs by binding to hormone receptors (Jones et al., 1999).

The adrenal cortex have high lipid content and blood supply, which makes the cortex a target for endocrine disruption as many environmental contaminants are taken up into the blood stream and distributed to target organs. Here the contaminants can become activated via biotransformation in the cells, or stored in lipids. Due to the adrenal cortex being regulated by hormones in the HPA axis, the cortex may be a target for hormone disruption by endocrine disrupting compounds binding to hormone receptors (Bergman et al., 2013).

1.5.1 Perfluorinated compounds (PFCs)

Perfluorinated compounds (PFCs) are synthetic compounds which structure consists of carbon chains bound to fluoride atoms. This is a strong bond making the chemicals highly resistant to biological degradation, and therefore these compounds can accumulate in the environment. PFCs have been detected in water and water living creatures, plants, foodstuffs and in blood and breast milk in humans. PFCs are in general used as a water and oil repellent or coating in textiles, furniture, food packaging and cooking utensils (Stahl et al., 2011).

The PFCs present in the mixture used in this thesis, include six compounds: perfluorooctanoic acid (PFOA), perfluorooctane sulfonate potassium salt (PFOS), perfluorodecanoic acid (PFDA), perfluorononanoic acid (PFNA), perfluorohexanesulfonic acid potassium salt (PFHxS), perfluorododecanoic acid (PFUnDA). Of these six, PFOS and PFOA (Fig. 1-7) are the most studied PFCs and considered the most harmful (Fromme et al., 2009).

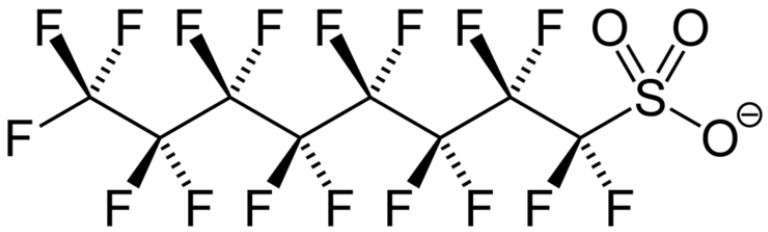

Figure 1-7: Chemical structure of PFCs represented by PFOS. Figure from Wikimedia (2015).

1.5.2 Polybrominated compounds (PBCs)

Polybrominated diphenyl ethers (PBDEs) are one of the most commonly used flame-retardants, and are found in many everyday items consisting of plastics, rubber, textiles and furnishing foam to improve fire resistance. PBDEs are aromatic bromine compounds that are favourable as flame-retardants because of their thermostability, and have weak carbon-bromide bonds that breaks at a certain temperature. The flame-retardant often decomposes at temperatures lower than the material in which it is added, as this prevents the formation of flammable gases. There are 209 possible congeners for PBDEs, and consist of an aromatic chemical structure which properties are similar to PCBs, DDT and polybrominated biphenyls (PBB) (Rahman et al., 2001).

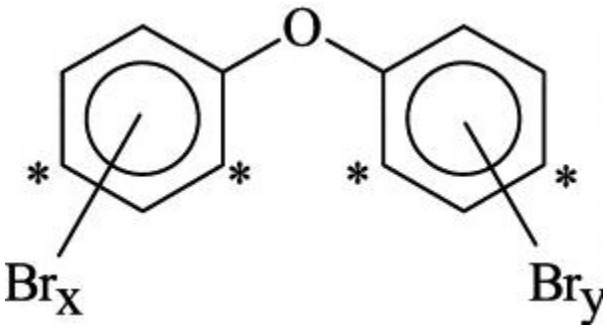

Figure 1-8: General chemical structure of PBDEs. The most active substitution sites of binding of Br is marked (*). Figure from Rahman et al. (2001).

The use of flame retardants is growing, but information of which flame retardants are produced and how they are spread into the environment is lacking, as well as their toxicity. PBDEs are extremely persistent in the environment, as they are resistant to degradation by acids, bases, heat and light (Rahman et al., 2001). PBDEs are also highly lipophilic, and combined with their stability are likely to bioaccumulate and are found more persistent than PCBs in the environment (de Boer et al., 1998). BDE-209 are found in sediments and sewage as the main PBDE and are also found in human blood serum (Alaee et al., 2003).

The PBCs in the mixture include five compounds: 2,2′,3,3′,4,4′,5,5′,6,6′-deca bromodiphenyl ether (BDE-209), 2,2′,4,4′-tetrabromodiphenyl ether (BDE-47), 2,2′,4,4′,5-pentabromodiphenyl ether (BDE-99) and 2,2′,4,4′,5,6′-hexa bromodiphenyl ether (BDE-154) and hexabromocyclododecane (HBCD).

Hexabromocyclododecane (HBCD) consists of three isomers (α, β and γ) formed from bromination of cyclododecatriene (Fig. 1-9), and is mainly used in polystyrene foam in building constructions. HBCD might be less persistent than PBDEs in nature as HBCD is less thermo stabile (Alaee et al., 2003).

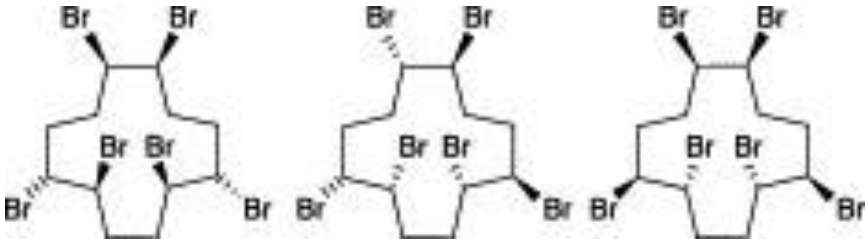

Figure 1-9: Chemical structure of HBCD. The HBCD α, β and γ isomers are shown from left to right. Figure from Alaee et al. (2003).

1.5.3 Chlorinated compounds

The polychlorinated biphenyls (PCBs) are amongst the most known and studied POPs present in the environment (Jones et al., 1999). PCBs are of an environmental and health concern because of the persistence and bioaccumulation and their carcinogenic abilities. One of the uses of PCBs have been as insulating fluids used for industrial purposes (Otchere, 2005). There are 209 possible congeners for PCBs, and consist of an aromatic chemical structure (Fig.1-10) (Rahman et al., 2001). PCB 153 is the most abundant congener in biological samples.

The PCBs in the mixture include seven compounds: PCB 138, PCB 153, PCB 101, PCB 180, PCB 52, PCB 28 and PCB 118.

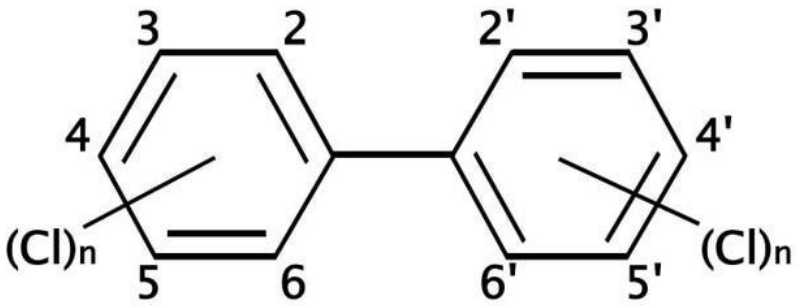

Figure 1-10: General chemical structure of PCB. referer

1.5.4 Pesticides

The pesticides in the mixture are organochlorides represented by *p,p'*-dichlorodiphenyl dichloroethene (*p,p'*-DDE), hexachlorobenzene (HCB), chlordanes (α-chlordane, oxy-chordane, trans-nonachlor), hexachlorocyclohexane (α-HCH, β-HCH, γ-HCH) and dieldrin. Like with PCBs, many of these pesticides were banned from use in from the 1970s and 1980s. But still many pesticides are found in soil (Martinez et al., 2012).

The chemical DDT is an organochlorine pesticide which also is an historically important persistent organic pollutant (Jones et al., 1999). The organochloride represented in the mixture is *p,p'*-dichlorodiphenyl dichloroethene (*p,p'*-DDE) a compound that is made during the metabolic breakdown of DDT in *e.g.* humans. Amongst the well-described effects of DDE-exposure is reduction in thickness in eggshells in birds (Jones et al., 1999). DDE is the most stable DDT metabolite, so even though use of DDT were banned in many developing countries, DDE is still being detected in human blood (Korrick et al., 2000).

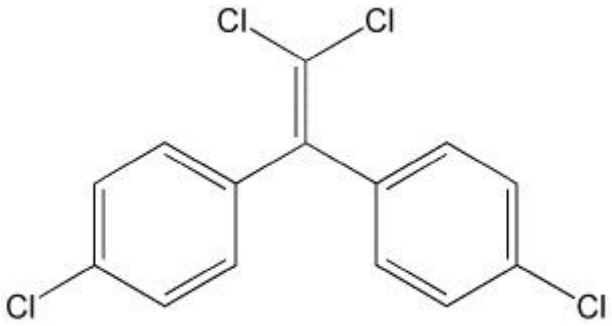

Figure 1- 11: Chemical structure of *p,p'*-DDE. Figure from Pesticideinfo (2015)

Another pesticide is hexachlorobenzene (HCB) a chlorinated compound formed as a byproduct during manufacturing of chlorinated solvents, chlorinated compounds, or pesticides (Korrick et al., 2000). HCB was introduced as a fungicide, but are not banned from use in many countries (Barber et al., 2005).

1.6 Aim of the study

This master project is part of a larger national and international project on effects of persistent organic pollutants on stress production managed by Professor Erik Ropstad at the Norwegian School of Veterinary Science (NVH). The POPstress project overall aim is to investigate the effects on POPs on the function and development of the HPA axis *in vivo* and *in vitro*. The environmental toxicology group in University of Bergen studies the effects in the human H295R and mouse Y1 adrenocortical cell lines.

The aim of this study was to investigate how a mixture of persistent organic pollutants (POPs) would affect the steroid production in Y1 mouse adrenocortical cells. This was studied under two conditions: 1) if a mixture of POPs could induce steroid production in normal cells under no stress influence and 2) if a mixture of POPs had an antagonistic, synergistic or additive effect steroid production of stress hormones in cells already being stress-induced by forskolin.

To obtain this goal, a metabolomics approach was utilized. A newly established method for studying steroids in the steroidogenic pathway at the Hormone Laboratory of the Haukeland University Hospital using LC-MS/MS was used for this purpose. Effects on enzymes by immunological detection using antibodies was also studied.

2. MATERIALS

2.1 Total concentrations of POPs in the original mixture and exposure dilutions

Chemical	1X*	1:10^{3}†	1:10^{4}†	1:10^{6}†	1:10^{6}†
	mM	mM	mM	mM	mM
PFOA	10.922	0.010922	1.0922E-06	1.0922E-11	1.0922E-17
PFOS POTASSIUM SALT	54.671	0.054671	5.4671E-06	5.4671E-11	5.4671E-17
PFDA	0.963	0.000963	9.63E-08	9.63E-13	9.63E-19
PFNA	1.724	0.001724	1.724E-07	1.724E-12	1.724E-18
PFHxS POTASSIUM SALT	7.855	0.007855	7.855E-07	7.855E-12	7.855E-18
PFUnDA	0.993	0.000993	9.93E-08	9.93E-13	9.93E-19
BDE-209	0.011	0.000011	1.1E-09	1.1E-14	1.1E-20
BDE-47	0.018	0.000018	1.8E-09	1.8E-14	1.8E-20
BDE-99	0.006	0.000006	6E-10	6E-15	6E-21
BDE-154	0.003	0.000003	3E-10	3E-15	3E-21
HBCD	0.038	0.000038	3.8E-09	3.8E-14	3.8E-20
PCB 138	0.615	0.000615	6.15E-08	6.15E-13	6.15E-19
PCB 153	1.003	0.001003	1.003E-07	1.003E-12	1.003E-18
PCB 101	0.024	0.000024	2.4E-09	2.4E-14	2.4E-20
PCB 180	0.491	0.000491	4.91E-08	4.91E-13	4.91E-19
PCB 52 (representative consumers)	0.033	0.000033	3.3E-09	3.3E-14	3.3E-20
PCB 28 (representative consumers)	0.05	0.00005	5E-09	5E-14	5E-20
PCB 118	0.196	0.000196	1.96E-08	1.96E-13	1.96E-19
p,p`-DDE	1.578	0.001578	1.578E-07	1.578E-12	1.578E-18
HCB	0.411	0.000411	4.11E-08	4.11E-13	4.11E-19
α-chlordane	0.026	0.000026	2.6E-09	2.6E-14	2.6E-20
oxy-chordane	0.052	0.000052	5.2E-09	5.2E-14	5.2E-20
trans-nonachlor	0.092	0.000092	9.2E-09	9.2E-14	9.2E-20
α-HCH	0.021	0.000021	2.1E-09	2.1E-14	2.1E-20
β-HCH	0.181	0.000181	1.81E-08	1.81E-13	1.81E-19
γ-HCH (Lindane)	0.021	0.000021	2.1E-09	2.1E-14	2.1E-20
Dieldrin	0.063	0.000063	6.3E-09	6.3E-14	6.3E-20

* Original mixture, all compounds dissolved in DMSO

† Original mixture diluted in Y1 growth media to make four doses of the mixture

2.2 General chemicals

Chemical name	Company	Catalogue No./ Lot No
Albumin, from bovine serum (BSA)	Sigma-Aldrich	A9647/051M1873V
Aluminum sulfate hydrate	Sigma-Aldrich	368458/MKBF0413V
Ammonium hydroxide solution (25 %)	Sigma-Aldrich	44273
Ammonium persulfate (APS)	Sigma-Aldrich	A9164/MKBF0028V
Bromophenol blue	Merck	108122
CHAPS hydrate	Sigma-Aldrich	C9426
Coomassie® Brilliant Blue G 250 (CBB G 250)	Merck	115444
Dimethyl sulfoxide (DMSO)	Sigma-Aldrich	D8418
Dithiothreitol (DTT)	AppliChem	A2948
Ethanol (EtOH)	Sigma-Aldrich	32221
Ethylenediaminetetraacetic acid (EDTA)	Merck	324503
Forskolin, from Coleus forskohlii	VWR International	344270
Glycerol	Sigma-Aldrich	G5516/ STBC1888V
Glycine	Sigma-Aldrich	G8898/SZBD157CV
Hydrochloric acid (HCl) 37 %	Merck	100317
Iodoacetamide	Sigma-Aldrich	I6125/030M5315V
KCl	Sigma-Aldrich	P9541/080M0091V
Methanol (MeOH)	Sigma-Aldrich	34860N
N,N,N',N'-tetramethyl-ethylenediamine (TEMED)	Sigma-Aldrich	T9281
Ortho-phosphoric acid	Merck	100573
Pharmalyte 3-10 for IEF	GE Healthcare	17-0456-01/10040852
Phenylmethylsulfonyl Fluoride (PMSF) in DMSO	Santa Cruz Biotechnology	sc-24948
Potassium dihydrogen phosphate	Merck	104873
SeaKem LE Agarose	Lonza	50004
Sodium chloride	Merck	106404
Sodium dodecyl sulfate (SDS) (20 % w/v)	Amresco	M112
Sodium Orthovanadate	Santa Cruz Biotechnology	sc-24948
Sodium phosphate dibasic dihydrate	Sigma-Aldrich	30435/SZBE0760V
Sucrose	Sigma-Aldrich	84100/SZBC0120V
Thiourea	Merck	107979
Trizma® base	Sigma-Aldrich	T1503/SLBC9023V
Urea	Merck	108487
β-mercaptoethanol	Sigma-Aldrich	M6250

2.3 General solutions, compounds, media and supplements

Chemical name	Company	Catalogue No./ Lot No
30 % Acrylamide: Bis-acrylamide solution, 37.5:1	Sigma-Aldrich	A3699
Cleaning concentrate	BIO-RAD	161-0722
Fetal Bovine Serum	Sigma-Aldrich	F6765/11H316
Ham's F-12K (Kaighn's) Medium	Gibco by Life Technologies	21127-022/1568502
Non-fat dried milk	Normilk AS	
NuSerum™ Culture Supplement	BD Biosciences	355100
Penicillin-Streptomycin (Pen-Strep)	Gibco by Life Technologies	15140-122/1469711
Pierce 660 nm Protein Assay Reagent	Thermo Scientific	22660
PlusOne DryStrip cover Fluid	GE Healthcare	17-1335-01
Protein inhibitor cocktail in DMSO	Santa Cruz Biotechnology	sc-24948
Restore PLUS Western Blot Stripping Buffer	Thermo Scientific	46430
RIPA Lysis Buffer System	Santa Cruz Biotechnology	sc-24948
Trypan Blue Stain	Cambrex Bio Science	17-942E
Trypsin-EDTA solution 0.25 %	Sigma-Aldrich	T4049/SLBG2806
Tween-20	Sigma-Aldrich	P5927

2.4 Kits

Name	Description	Company/ Catalogue No./ Lot No
SuperSignal® West Femto Maximum Sensitivity Substrate	Western blot chemiluminescence kit	Thermo Scientific /34095/PJ207501A
SuperSignal® West Pico Chemiluminescent Substrate	Western blot chemiluminescence kit	Thermo Scientific /34080/OG190590

2.5 Eukaryotic cell lines

Name	Description	Supplier
H295R	Human adrenocortical cell line	Hormone Laboratory Haukeland University Hospital
HepG2	Human liver hepatocellular carcinoma cell line	Roger Lille-Langøy
Y1	Mouse adrenocortical cell line	Hormone Laboratory Haukeland University Hospital

2.6 Molecular weight and size standard

Name	Description	Company/Catalogue No.
Precision Plus Protein™ All Blue Prestained	Ten blue-stained recombinant proteins (10-250 kDa)	BIO-RAD/161-0373

2.7 Antibodies

Antibody	Produced in	Isotype /CyDye	Reactivity	Company	Product number
Anti-beta Actin	Mouse	IgG3	Monoclonal	Abcam	ab8224
Anti-CYP11A1	Rabbit	IgG	Polyclonal	Abcam	ab175408
Anti-CYP11B2	Rabbit	IgG	Monoclonal	Abcam	ab167413
Anti-CYP19 (H-300)	Rabbit	IgG	Polyclonal	Santa Cruz Biotechnology	sc-30086
Anti-StAR (K-20)	Goat	IgG	Polyclonal	Santa Cruz Biotechnology	sc-23524
Anti-Goat IgG, Cy5 conjugate	Donkey	IgG/Cy5	Polyclonal	Abcam	ab6566
Anti-Rabbit IgG, HRP conjugate	Goat	IgG	Polyclonal	Dako Denmark A/S	P0448
ECL Plex™ anti-mouse IgG, Cy3 conjugate	Goat	IgG/Cy3	Mono reactive	GE Healthcare	PA43009 V
ECL™ anti-mouse IgG, HRP linked whole antibody	Sheep	IgG		GE Healthcare	NA931V
ECL Plex™ anti-rabbit IgG, Cy5 conjugate	Goat	IgG/Cy5	Mono reactive	GE Healthcare	PA45011 V

2.8 Consumables

Name	Company	Catalogue No.
Amersham Hybond LFP (pore size 0.2 µm) PVDF	GE Healthcare	10600060
Immobilon-p Transfer membrane (pore size 0.45 µm) PVDF	Millipore	IPVH00010
Immobiline Drystrip (IPG) pH 4-7, 7 cm	GE Healthcare	17600110

2.9 Instrumentation

Category	Name	Manufacturer
Blotting	Mini PROTEAN® Tetra Cell	BIO-RAD
Cell counting	Bürker hemocytometer	Kebo Lab
Centrifugation	CT 15RE Himac	VWR
	Galaxy MiniStar	VWR
	Heraeus Multifuge X3R	Thermo Scientific
Electrophoresis	Mini PROTEAN® 3 Cell	BIO-RAD
	Mini PROTEAN® 3 Dodeca™ Cell	BIO-RAD
Heating	Thermomixer compact	Eppendorf
Isoelectric focusing	Ettan IPGphor 3 IEF System	GE Healthcare
Imaging	ChemiDoc™ XRS+ Imaging System	BIO-RAD
	GS-800 Calibrated Densitometer	BIO-RAD
	Typhoon FLA 9000	GE Healthcare
Incubation	Galaxy 170 R	New Brunswick
LLE	Star pipetting robot	Hamilton®
Microscopy	Leica DMIL LED	Leica Microsystems
Mixing		VWR International
	Vortemp 56 EVC	Labnet
	Vortex-Genie 2™	Scientific Industries
pH measurement	pHM210 Standard pH Meter	MeterLab®
Plate reading	EnSpire™ 2300 Multilabel Reader	PerkinElmer
Power supply	PowerPac™ HC	BIO-RAD
Shaker	IKA® HS 260 basic	IKA-Werke
Sonication	Transsonic 460	Elma
	Ultrasonic Homogenizer 4710 Series	Cole-Parmer Instrument Co.
Steroid profiling	Xevo T-QS triple quadrupole mass spectrometer	Waters
	Acquity UPLC i-class	Waters
Water supply	Advantage A10	Millipore
Weighing	EK-300i	AND
	SI-64	Denver Instrument

2.10 Water quality

MΩcm@25^{0}C: 18.2
Ppb TOC: 5

Deionised type 1 ultrapure water, Milli-Q

2.11 Media, buffers and solutions

Y1 cell growth

Y1 growth media
1 x Ham's F-12K (Kaighn's) Medium
10 % FBS (v/v)
1 % Pen-Strep (v/v)

Forskolin for stimulation

Forskolin (in DMSO)
10 mM Forskolin

Mitochondria isolation

1xPBS	
NaCl	4 g
KCl	0.1 g
Na_2HPO_4	0.72 g
KH_2PO_4	0.12 g
Adjust pH to 7.4 with 6 M HCl	
dH_2O	up to 500 mL

Sucrose lysis buffer - stock solution
250 mM Sucrose
10 mM Tris-HCl pH = 7.4
0.1 mM EDTA

Sucrose lysis buffer w/inhibitors	
1 mM PMSF	1 µL
1 mM protein inhibitor cocktail	1 µL
1 mM sodium orthovanadate	1 µL
Sucrose lysis buffer	200 µL

➔ **Add inhibitors just before use**

Protein measurement

Standard (Pierce 660 assay)	
BSA (10mg/mL)	30 mg
Sucrose lysis buffer	3 mL

Whole protein lysate

RIPA	
1 mM PMSF	10 µL
1 mM protein inhibitor cocktail	10 µL
1 mM sodium orthovanadate	10 µL
RIPA buffer lysate system	1 mL

General electrophoresis

10 x TGS Running buffer
250 mM Tris
1920 mM glycine
1 % SDS (v/v)

Colloidal coomassie	
Aluminumsulfate	100 g
dH_2O	800 mL
Ethanol	200 mL
CBB G-250	0.4 g
Phosphoric acid	47 mL
dH_2O	up to 2 L

Destaining	
dH_2O	800 mL
Ethanol	200 mL
Phosphoric acid	47 mL
dH_2O	up to 2 L

Sodium dodecyl sulphate-polyacrylamide gel electrophoresis

10 % running gel (10 mL) (all amounts v/v)		**4 % stacking gel (5 mL) (all amounts v/v)**	
dH_2O	4 mL	dH_2O	3.1 mL
1.5 M Tris-HCl pH 8.8	2.5 mL	0.5 M Tris-HCl pH 6.8	2 x 625 µL
10 % SDS	100 µL	10 % SDS	50 µL
Acrylamide	3.33 mL	Acrylamide	650 µL
10 % APS	50 µL	10 % APS	25 µL
TEMED	5 µL	TEMED	5 µL

12.5 % running gel (10 mL) (all amounts v/v)		**4 % stacking gel (5 mL) (all amounts v/v)**	
dH_2O	3.3 mL	dH_2O	3.1 mL
1.5 M Tris-HCl pH 8.8	1.3 mL	0.5 M Tris-HCl pH 6.8	2 x 625 µL
10 % SDS	0.05 mL	10 % SDS	50 µL
Acrylamid	2.0 mL	Acrylamid	650 µL
10 % APS	0.05 mL	10 % APS	25 µL
TEMED	0.002 mL	TEMED	5 µL

5 x Sample buffer (5xSB)
250 mM Tris-HCl pH = 6.8
10 % SDS (
30 % glycerol
5 % β-mercaptoethanol
0.02 g bromophenolblue

1 x Sample buffer (1xSB)
5xSB 20 % (v/v)
dH_2O 80 % (v/v)

Western blot

10 x Transfer buffer	
Tris	30.3 g
Glycine	144 g
dH_2O	up to 1000 mL

1 x Transfer buffer	
10 x Transfer buffer	100 mL
Methanol	200 mL
dH_2O	up to 1000 mL

Tris buffered saline (TBS) buffers

5 x TBS	
Tris	24 g
NaCl	292.5 g
dH_2O	up to 1800 mL
Adjust pH to 7.5 with 6 M HCl	
dH_2O	up to 2000 mL

0.05 % TBS-Tween (TBST)	
5x TBS	200 mL
Tween-20	0.5 mL
dH_2O	800 mL

Blocking solution
5 % non-fat dry milk (w/v)
1 x TBST

Stripping buffer
100 mM β-mercaptoethanol
2 % SDS
62.5 mM Tris-HCl pH 6.8

LC-MS/MS

ethylacetate:hexane (80:20 % vol/vol)

Mobile phase A
dH_2O
0.05 % ammonium hydroxide solution (v/v)

Mobile phase B
Methanol
0.05 % ammonium hydroxide solution (v/v)

2D electrophoresis

Whole cell lysate

Homogenization buffer (2D HB)	
7 M Urea	4.2042 g
4 % Chaps (w/v)	0.4 g
2 M Thiaurea	1.5224 g
30 mM TrisHCl (pH = 8.5) (v/v)	600 µL
dH_2O	up to 10 mL

Standard (Pierce 660 assay)	
BSA (10mg/mL)	30 mg
2D Homogenization buffer	3 mL

5 x Rehydration buffer (fresh batch)	
8 M Urea	4.804 g
4 % Chaps (w/v)	0.4 g
Pharmalyte	100 µL
13 mM DTT	0.02 g
dH_2O	up to 10 mL

2D separation

20 % Equilibration buffer - stock solution	
50 mM 1.5 M TrisHCl pH 8.8	6.7 mL
6 M Urea	72.07 g
30 % Glycerol (v/v)	
2 % SDS (w/v)	4 g
Bromophenol blue	Few grains
dH_2O	up to 200 mL

Equilibration buffer A w/DTT	
Dithiothreitol	0.1 g
20 mL eq.buffer	

Equilibration buffer B w/IAA	
Iodoacetamide	0.9 g
20 mL eq.buffer	

12.5 % (6 gels) (all amounts v/v)	
dH_2O	20.1 mL
1.5 M Tris-HCl pH 8.8	15 mL
10 % SDS	600 µL
Acrylamid	24 mL
10 % APS	300 µL
TEMED	30 µL

Agarose for sealing IPG strip
1 % agarose
1XTGS buffer

3. METHODS

3.1 Experimental overview

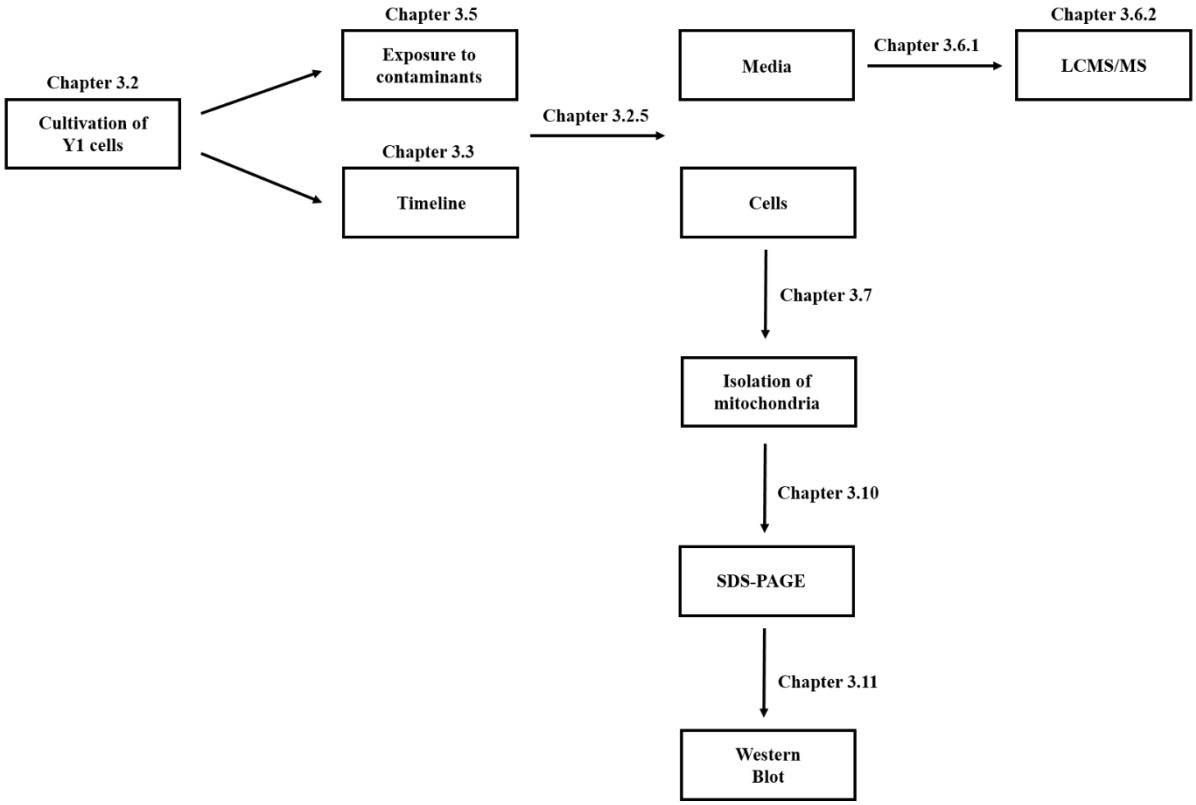

Figure 3-1: Overview of the main steps from exposures to sample analysis.

3.2 Cultivation of Y1 cells

Y1 cells were grown in HAM's F-12K (Kaighn's) medium supplemented with 10 % charcoal stripped fetal bovine serum (FBS) and 1 % Penicillin-Streptomycin (Pen-Strep). Cells were incubated in a heating cabinet adjusted to 37℃ and with 5 % CO_2 in a humified atmosphere. Media was changed every two days until reaching 70 - 80 % cell confluence. Cells were initially cultured in 75 cm^2 tissue culture media flasks before seeded into 6-well plates for the exposure and timeline experiments. Cell culture techniques previously described by Hecker et al. (2007) for the H295R cell line were used as a guideline.

3.2.1 Cultivation of parental Y1 cells

Y1 cells were obtained from Haukeland University Hospital, and this vial was used to make parental cells. Cells in the vial were thawed and then seeded in a 75 cm^2 tissue culture media flask and incubated overnight. The cells had been stored in freeze media that contained DMSO, so media was changed the next day when the cells had attached to the flask bottom. This would ensure that DMSO was removed from the growth media and not affect the cells. Media was changed every two days until reaching 70 - 80 % cell confluence. The cells were added 0.25 % trypsin-EDTA to detach cells from the flask and suspended in freeze media containing 5 % DMSO. The suspension of cells were divided into aliquots of approximately 0.5 mL and stored in – 80^0C for 24 hours before transferred to liquid nitrogen. All these vials contains parent cells, deriving from that one vial from Haukeland.

3.2.2 Cultivation of cells for experiments

One parental cell vial was thawed and cultured for three passages. For the first passage, cells were subcultured 1:5 in four new flasks. During the second passage, cells from two flasks was stored in aliquots of approximately 0.5 mL in liquid nitrogen. The other two flasks were used for further expansion by dividing the cells 1:5 into eight new flasks. For the third passage, all cells were harvested and stored in aliquots in liquid nitrogen. The number of cell vials from this one expansion was more than 40 vials. As one frozen vial was used for one experiment (pilot samples, timeline, exposure), this was enough cells for more than 40 experiments. All vials were stored in liquid nitrogen until used.

3.2.3 Subculturing

Cells were subcultured, or passaged, when the cell confluence was at 70 - 80 % per flask. Passaging was done by removing old media and washing cells with 1.5 mL 0.25 % trypsin-EDTA. 2 mL trypsin-EDTA was added to the cell flask and incubated for 5-7 minutes in 37^0C until the cells had detached. 8 mL media was subsequently added to stop the trypsinization process. The cell suspension was collected in a 15 mL falcon tube and centrifuged at 1250 rpm for three minutes (Heraeus Multifuge X3R). The supernatant was removed and the cell pellet was dissolved in 10 mL Y1 growth media. Usually, the cells was divided 1:5 by adding 2 mL of the cell pellet suspension in a new flask containing 8 mL Y1 growth media.

To ensure that the cells were stable and fully adopted to the growing conditions, cells were subcultured four times into 75 cm^2 flasks. The fourth subculture was called passage 4. Then, on the fifth subculturing, or passage 5, the cells were seeded onto 6-well plates.

3.2.4 Cell counting and seeding onto 6-well plates

After trypsinization and centrifuging the cells (chapter 3.2.3), each cell pellet was resuspended in 5 mL Y1 growth media and transferred to a 50 mL Falcon tube. 100 µL of the cell suspension was mixed with 100 µL tryptophan blue. Then the cell concentration was calculated using a Bürker hemocytometer. The cell number was determined by calculating the mean cell number from five squares on the hemocytometer.

To calculate the number of cells/mL:

n (mean cell number) x 2 x 10000 = X cells/mL.

Cells were diluted with Y1 growth media to a concentration of 1.2 x 10^6 cells/mL. Thereafter, cells were seeded by adding 1 mL to each well and incubated overnight.

3.2.5 Harvesting cell samples (6-well plates)

Both media and cells were collected for analysis. Media from each well were transferred directly to Eppendorf tubes. Cells were harvested by the trypsinization method. Any leftover media was removed by washing each well with 250 µL 0.25 % trypsin-EDTA. Each well were then added 350 µL trypsin-solution directly on the washed cells and incubated for 5 minutes. Cells were harvested by adding 800 µL Y1 growth media, and transferred to Eppendorf tubes. Suspended cells were centrifuged at 13000 x g for 5 minutes at 4^0C, and the supernatant was removed from the cell pellet. Media was stored in – 20^0C and cells in – 80^0C until further analysis.

3.3 Timeline for measuring basal steroidogenesis in stimulated cells

Cells were stimulated with forskolin in order to measure changes in the steroidogenesis pathway over time. This would give an overview of the basal steroid production in Y1 cells. Cells were forskolin-stimulated for a given time period between 0 and 48 hours, and cells and media from each well were collected for steroid analysis.

Table 1: Overview of cells and media sampling

	Time points (h)								
Timeline	0	0.5	1	2	4	8	12	24	48

Y1 cells were prepared and plated out in 6-well plates (chapter 3.2.4). The next day, old media was discarded and 1 mL Y1 growth media containing 0.1 % forskolin was added to each well. Each time point were performed in duplicates (Fig. 3-2). Cells and media from the two wells representing time 0 were collected immediately after adding media as previously described (chapter 3.2.5). Samples were collected for the remaining wells throughout the timeline. Media was stored in -20^0C and cells in -80^0C until further analysis.

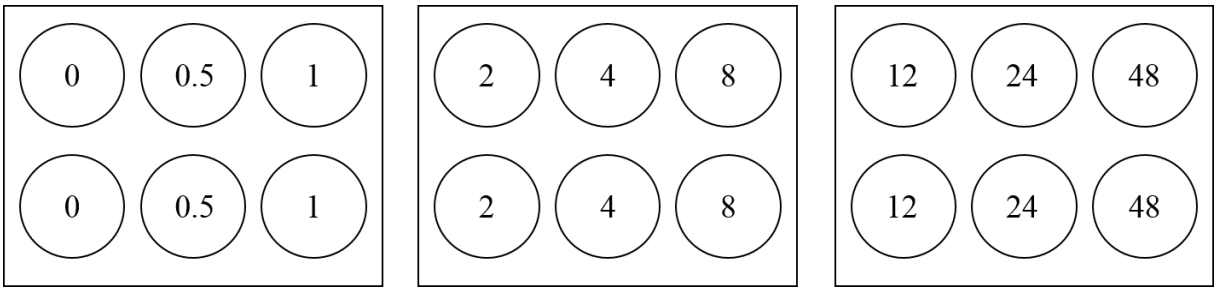

Figure 3-2: The 6-well plate setup for 48-hour time line. Three 6-well plates were used, with two wells dedicated for each time point.

One timeline was performed with longer incubation up to 72 hours. Results from this timeline is listed in Appendix D.

3.4 Cytotoxicity testing

AlamarBlue® assay (Invitrogen) was used as a cell viability test after exposures. This was performed to control if the exposure regimes are cytotoxic to the Y1 cells. This assay measures the proliferation of cells, and does so by detecting metabolic activity. Healthy and active cells convert the alamarBlue® reagent into a fluorescent and colorimetric indicator. If the cells are dead or damaged, there will be less reagent converted.

Y1 cells were grown and plated at out at passage 5 in a black 96-well fluorescent plate, in a cell density of 10000 cells/well. Every condition were measured five times, so 45 wells were plated with Y1 cells. The plate was incubated for 24 hours at 37℃. The next day the exposures was prepared by making nine different controls and mixtures (Table 2). For a positive control, cells were treated with 0.1 % Triton X-100, a detergent that disrupt the cytoplasm membranes and

cause cell death (Borner et al., 1994). Negative control was normal media (non-treated). Old media was removed and discarded, and controls and exposures were distributed on the plate at 100 µL per well. The plate was incubated for 48 hours.

Table 2: Cytotoxicity setup.

Control	DMSO	Forskolin	Mixture 10^{-3} Unstimulated	Mixture 10^{-3} Stimulated	Mixture 10^{-4} Stimulated	Mixture 10^{-5} Stimulated	Mixture 10^{-6} Stimulated	0,1 % Triton-X

After the 48 hours exposure, 100 µL of media was added to five wells as a non-cell positive control. Since this was a control without cells, this required no previous incubation before adding alamarBlue®. Afterwards, 10 µL of alamarBlue® was added to each well and the plate was further incubated for 22.5 hours. Fluorescence was measured at 540 nm excitation and 590 nm emission using an Enspire™ Multilabel Reader.

3.5 Exposures to mixture of POPs

To find out how the mixture (Materials 2.1) would influence the steroidogenic pathway, Y1 cells were exposed to four doses of the mixture (Materials 2.1) for 48 hours under two different conditions. The first condition was unstimulated cells, meaning that the cells were not treated with forskolin. With this approach, if an increase in steroid production were observed, it would indicate that one of the compounds in the mixture could activate steroid production. The second condition was exposure of stimulated cells, meaning that cells were treated with forskolin as well as the mixture. By activating the steroid production in the cell using forskolin, it could be measured if the mixture had an additive or inhibitory effect on steroid production in the cells. The mixture were distributed in four doses by serial dilution in Y1 growth media as illustrated in Figure 3-3 and 3-5.

3.5.1 Exposures on unstimulated cells

Cells were seeded in three 6-well plates (chapter 3.2.4) and incubated overnight. The next day, the mixture was diluted in Y1 growth media (Materials 2.10) resulting in four different doses of the mixture (Fig. 3-3). Control media was made separately by adding 0.1 % DMSO to Y1 growth media. Old media was removed from each well in the three 6-well plates, and the control media and the mixtures were distributed between the wells (Fig. 3-4). Plates were then incubated in 37^0C and cells and media harvested after 48 hours (chapter 3.2.5).

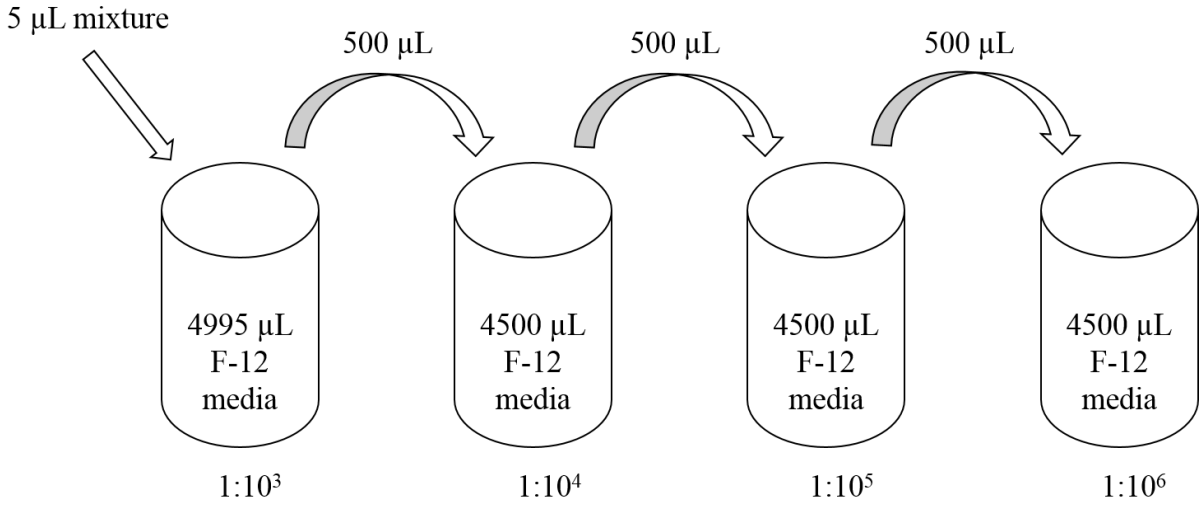

Figure 3-3: Illustration of making the four doses of the mixture in HAM's F-12K (Kaighn's) medium by serial dilution for unstimulated cells. Highest to lowest dose is 1:1000 ($1:10^3$), 1:10000 ($1:10^4$), 1:100000 ($1:10^5$) and 1:1000000 ($1:10^6$).

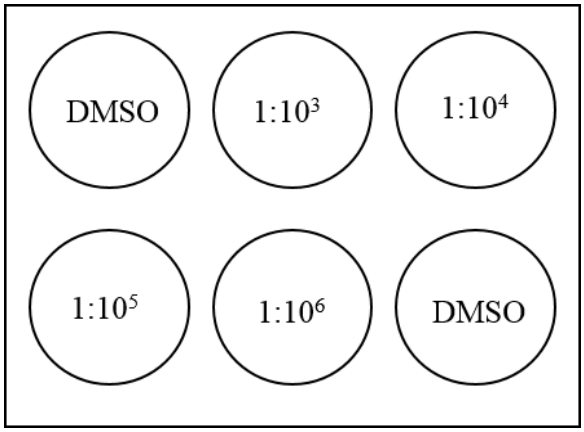

Figure 3-4: Example of one 6-well plate setup for unstimulated cells. For each exposure, the setup was rearranged to minimize the impact of cell well placement. One exposure included three 6-well plates, so that each dilution had three replicates.

3.5.2 Exposures on forskolin-stimulated cells

Cells were seeded in three 6-well plates (chapter 3.2.4) and incubated overnight. The next day, the mixture was diluted in Y1 growth media containing 0.1 % forskolin, resulting in four doses of the mixture (Fig. 3-5). Control media was made separately by adding 0.1 % forskolin to Y1 growth media. Old media was removed from each well in the three 6-well plates, and the control media and the mixtures were distributed between the wells (Fig. 3-6). Plates were then incubated in 37^0C and cells and media harvested after 48 hours (chapter 3.2.5).

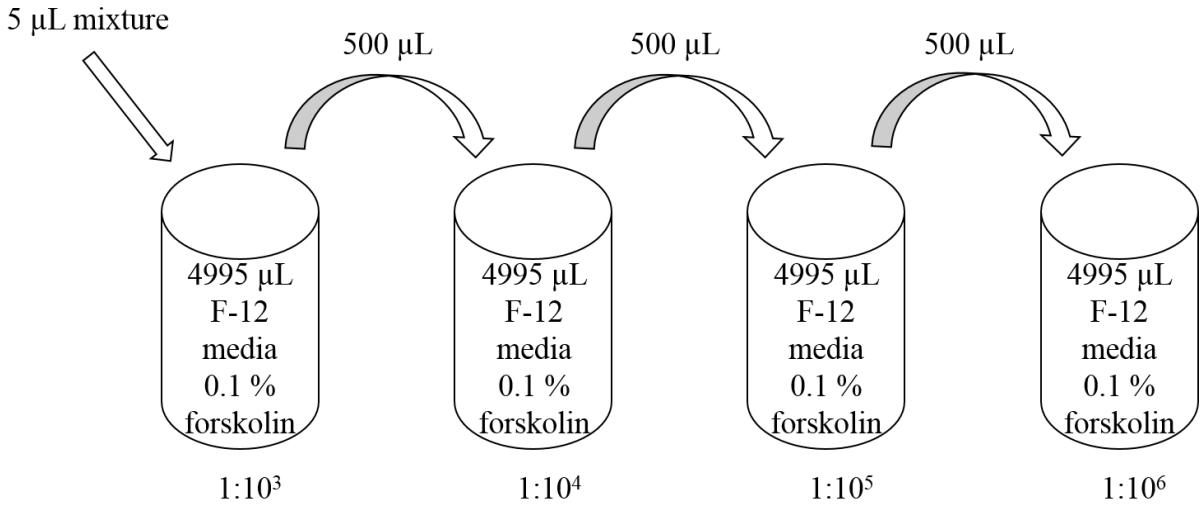

Figure 3-5: Illustration of making the four doses of the mixture in HAM's F-12K (Kaighn's) medium by serial dilution for stimulated cells. The media was added 0.1 % forskolin before mixture was diluted. Highest to lowest dose is 1:1000 ($1:10^3$), 1:10000 ($1:10^4$), 1:100000 ($1:10^5$) and 1:1000000 ($1:10^6$).

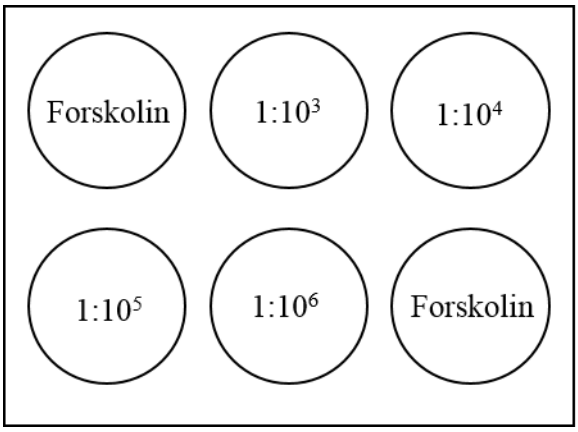

Figure 3-6: Example of a 6-well plate setup for stimulated cells. For each exposure, the setup were rearranged to minimize the impact of cell well placement. One exposure included three 6-well plates, so that each dilution had three replicates.

3.6 Steroid profiling of metabolites by liquid chromatography - tandem mass spectrometry (LC-MS/MS)

Liquid chromatography-tandem mass spectrometry (LC-MS/MS) is able to detect and determine multiple steroids at very low concentrations with high specificity in a single analytical run (Methlie et al., 2013). This method combines chromatography and mass spectrometry, by separating molecules and identify them according their mass and charge.

Samples are first injected into an ultra performance liquid chromatographer (UPLC). The analytes in that sample are moved through a column (the stationary phase) by the flow of a solvent, referred to as the mobile phase, under high pressure. Different analytes vary in their affinity and solubility to the stationary- and mobile phases, respectively, thereby they become separated as they pass through the column (Fig. 3-7). As soon as compounds elute, compounds are sent to the mass spectrometer for detection (Fig. 3-8).

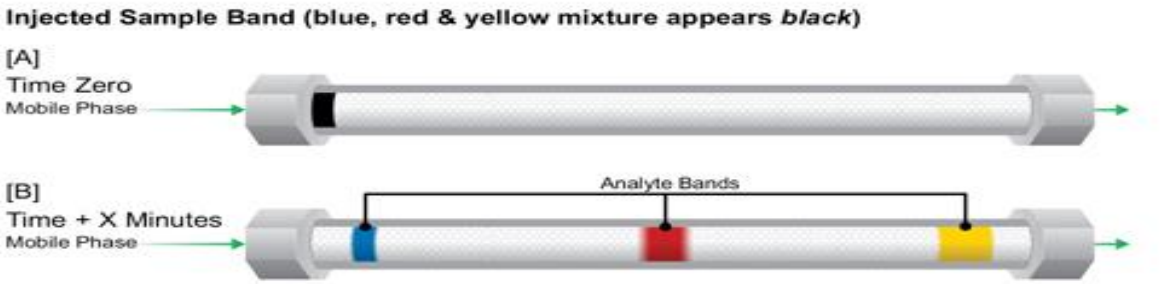

Figure 3-7: How the individual compounds in an analyte sample are separated as sample moves through the column. Mobile phase is the solvent the sample are diluted in, and the column is the stationary phase. Picture from Waters.

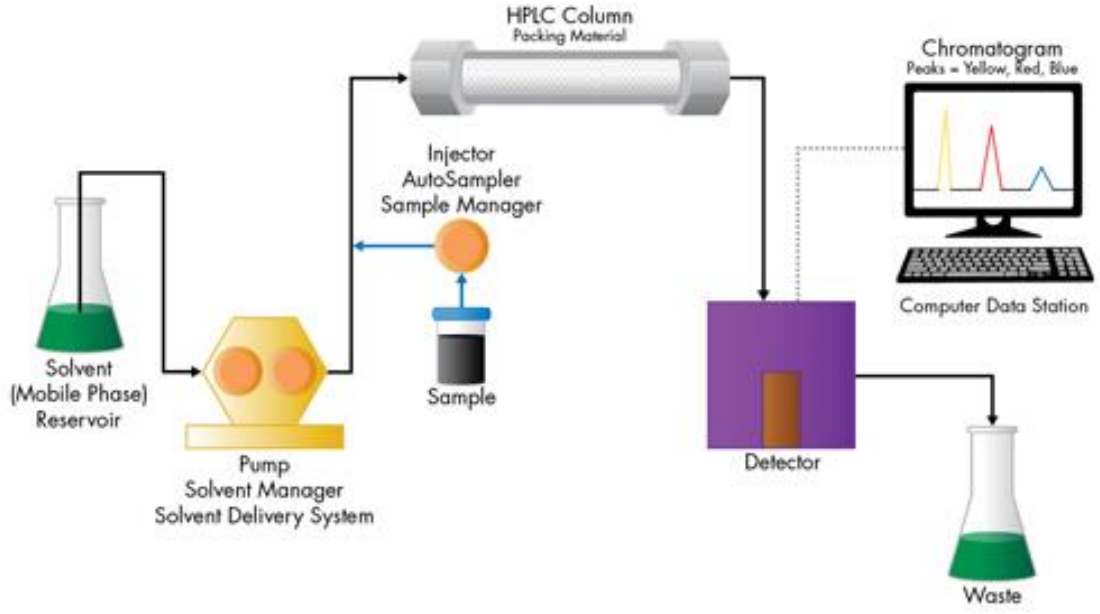

Figure 3-8: Overview of liquid chromatography, representation by high performance LC (HPLC). The principle is the same for HPLC and UPLC. The difference between the two is that the chromatogram is more sensitive and precise using UPLC. Picture from Waters.

The mass spectrometer used in this study was a triple quadrupole mass spectrometer type fitted with an electrospray ionisation (ESI) ion source. ESI is the transition stage from the UPLC to the mass spectrometer (Fig. 3-9).

After running the sample through the column, the liquid sample is pumped through a metal capillary that has a positive or a negative voltage, resulting in a positive or negative charge of the sample. At the capillary tip the charged liquid is nebulised (conversion of liquid to aerosol droplets) which gives a fine spray of charged droplets. The droplets passes down a pressure gradient, where the droplets are reduced in size by evaporation with hot nitrogen gas. This size reduction decrease droplet radius and increases the surface charge density, and the droplets enters the gaseous phase. The gas phase ions enters the mass spectrometer (Ho et al., 2003). Analysis of ions produced during the ionization process is based on mass to charge ratio (m/z) (Pitt, 2009).

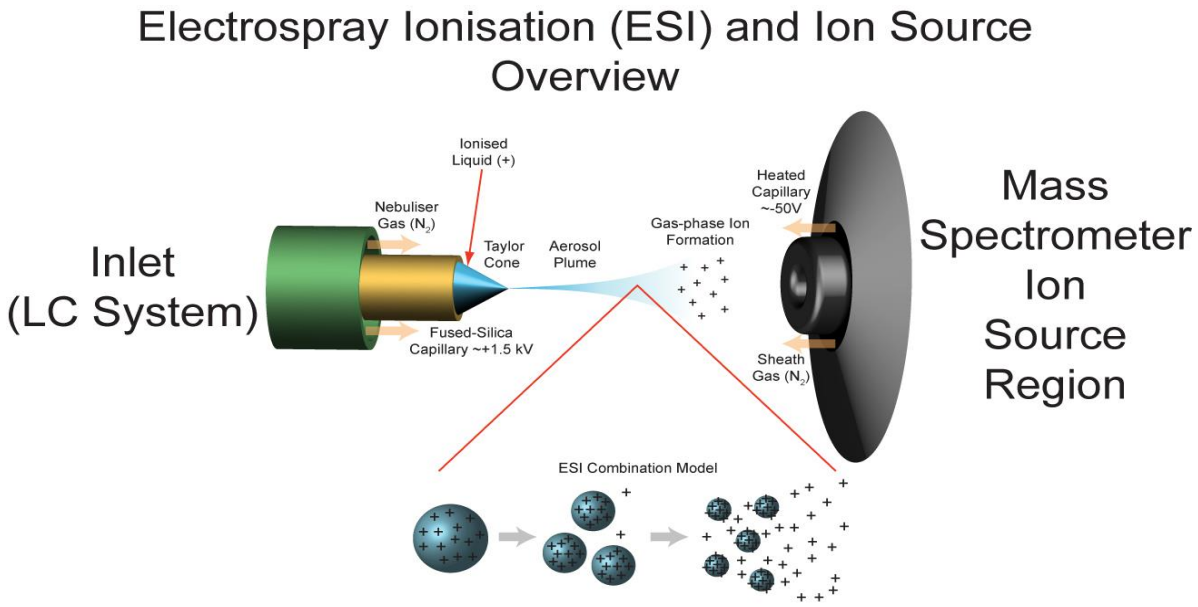

Figure 3-9: Electrospray ionisation. Picture from LamondLab.

After entering the triple quadrupole mass spectrometer, the gas phase ions travels through three sets of rods (Q1, Q2 and Q3), that each consist of four parallel metal rods, or quadrupoles (Fig. 3-10). The first metal rod, Q1, functions as a mass filter that recognize an ion of interest based in mass. The Qi sends the precursor ion to the collision cell, Q2, where the ion collide with a collision gas that fragments the ion. This is known as collision induced dissociation (CID). The resulting fragments enter the third quadruple, Q3, and one fragment at a time as scanned out

and sent to the detector. This provides structural information of the molecular ions and is the tandem system known as MS/MS.

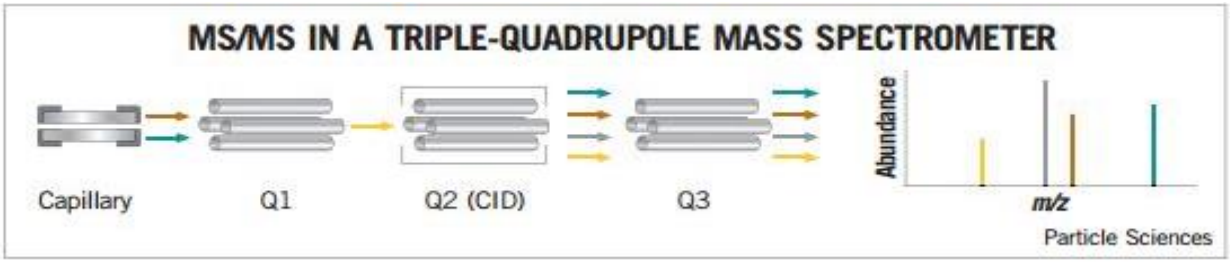

Figure 3-10: The triple quadrupole mass spectrometer. Q1 and Q3 are mass spectrometers and Q2 is the collision cell. Figure from Particle Sciences.

The ionised molecules move through the quadrupoles by an oscillating electric-magnetic field. The speed at which the molecules travel is affected by their mass over charge ratio (*m/z*). The metal rods are placed to make opposing rods that have an equal but opposite DC voltage superimposed with a radiofrequency AC voltage. By alternating the voltage and radiofrequency, ions can travel in a straight spiral through to a detector or hit the rods. Hitting the rods is a way of removing undesirable ions, as they get neutralised. (Ho et al., 2003). This method represents multiple reaction monitoring (mrm) for detection and quantitation, where the Q1 and Q3 settings are set for a selected section of precursor and product ions. The chromatograms is based on the counts per second of fragment ions.

Steroid profiling on sample media was carried out by LC-MS/MS at the Haukeland University Hospital, Bergen, Norway according to a method by Methlie et al. (2013), which was modified to quantitate all steroid hormones and their intermediate metabolites that are produced in the human adrenal gland. The modifications were done by Ralf Kellmann, in collaboration with Kareem Ahmed (not published).

3.6.1 Sample extraction

Calibrators, quality controls, and samples were extracted by liquid-liquid extraction on a Hamilton Star pipetting robot prior to LC-MS/MS analysis. A volume of 85 µl of each calibrator, quality control, and sample was transferred to a 96-well microtitre plate with 1.2 ml glass inserts. Subsequently, 10 µl internal standard (IS) solution was added to each well, during which each sample was mixed by 3 pipetting cycles of 50 µl. The plate was then incubated for one hour at room temperature to equilibrate possible interactions between isotopically labelled

steroids and binding proteins in the sample. After equilibration, 850 µl ethylacetate:hexane (80:20 % vol/vol) was added to each well, and samples were mixed with 15 pipetting cycles of 850 µl. After phase separation, 650 µl supernatant was transferred from each sample to new 96-well plate with glass inserts, and evaporated under a stream of nitrogen at 40°C. Finally, samples were reconstituted with 50 µl of 25% methanol. Calibrators, quality controls and IS are listed in Appendix C.

3.6.2 LC-MS/MS

LC-MS/MS analysis was carried out on a Waters Xevo T-QS triple quadrupole mass spectrometer that was coupled on-line to a Waters i-class Acquity UPLC. Ionisation was achieved by electrospray ionisation (ESI) in positive and negative mode.

The following LC conditions were used. Chromatographic separation was achieved on a Waters Acquity BEH-C18 column (2.1 x 100 mm, 1.7 µm particle size, pore-size 130 Å). The column temperature was set at 60°C. The mobile phases consisted of mobile phase A and mobile phase B (Materials 2.10). The injection volume was 4 µl. Steroid hormones were detected and quantitated by isotope-dilution mass spectrometry by multi-reaction monitoring (mrm). Quantifier and qualifier mrm-transitions are given in Appendix C. MS data was analysed using Waters TargetLynx™ Application Manager.

3.7 Isolation of mitochondria

As many of the enzymes of interest in the steroidogenesis pathway are present in the mitochondria, mitochondria were isolated from the cells using sonication followed by differential centrifugation. Mitochondria were isolated using a sucrose buffer as described previously (B. J. Clark et al., 1994).

3.7.1 Cell lysis by sonication

The cell pellet were washed twice by adding 1 mL of ice cold 1xPBS (Materials 2.10) and centrifuged at 13000*g* for 5 minutes at 4℃. 200 µL sucrose lysis buffer with 1 mM PMSF, 1 mM sodium orthovanadate and 1 mM protease inhibitor cocktail (Materials 2.10) was added to the cells and incubated on ice for 30 minutes. The cells were then sonicated on ice for 4 x 15 seconds on at 60 Hz and 10 seconds off.

3.7.2 Organelle enrichment by differential centrifugation

Organelle and isolation were performed based on methods described by B. J. Clark et al. (1994) and Poli et al. (2013). After sonication, the cell lysate was first centrifuged at 600 x g for 30 minutes at 4℃ to pellet heavy cell material, which then was discarded. The mitochondria-containing supernatant was transferred to a new centrifuge tube and further centrifuged at 13000*g* for 30 minutes at 4℃ to pellet mitochondria separated from the protein enriched supernatant. The mitochondria pellet were used for Western blot analyses, and the supernatant were used to measure protein concentration. Because of limited amount of mitochondria sample (not enough for both protein concentration measurement and Western blot), the protein amount of the mitochondria pellet was related to the protein concentration determined in the supernatant. The mitochondria pellet and protein supernatant were stored at – 80℃.

3.8 Preparation of whole cell lysates

Cell pellet were washed twice by adding 1 mL 1 x PBS and centrifuged at 13000 x g for 5 minutes at 4℃, before 500 µL of RIPA buffer (Materials 2.10) was added to the pellet. Pellets were then sonicated on ice for 5 x 15 seconds on, and 10 seconds off, to break the cell wall. The cell lysate were then centrifuged twice at 13000 x g for 5 minutes at 4℃ to separate cell debris and the soluble protein fraction. Protein concentration was determined with Pierce™ 660 as described in chapter 3.9.

3.9 Measurement of protein concentration

The protein concentration of the supernatant was measured using the Pierce™ 660 nm protein assay. This dye consist of a reddish-brown low pH dye-metal complex that is negatively charged. When added to proteins, the dye will bind to positively charged amino acid groups, causing the dye to turn green. This changes the absorption maximum of the dye and protein concentration can be measured at 660 nm (Thermo Scientific). Bovine serum albumin diluted in sucrose lysis buffer was used to create a protein concentration standard dilution curve (Table 3).

Table 3: Preparation of BSA protein standards

	Blank	**2000 µg/mL**	**1000 µg/mL**	**500 µg/mL**	**250 µg/mL**	**125 µg/mL**	**62.5 µg/mL**
Sucrose lysis buffer	100 µL	400 µL	100 µL	100 µL	100 µL	100 µL	100 µL
BSA (10 mg/mL)		100 µL					
2000 µg/mL			100 µL				
1000 µg/mL				100 µL			
500 µg/mL					100 µL		
250 µg/mL						100 µL	
125 µg/mL							100 µL

Protein measurements were performed in triplicates, and 10 µL of standards and unknown protein samples were added to separate wells on a 96 well Nunc clear micro plate. Next, 150 µL of Pierce™ 660 reagent were added to each well and mixed gently by shaking for 1 minute. Then the plate was incubated for 5 minutes at room temperature protected from light. After incubation the absorbance was measured at 660 nm using an Enspire™ Multilabel Reader. The concentration of each unknown sample was calculated from the standard curve.

3.10 Separation of proteins by sodium dodecyl sulphate-polyacrylamide gel electrophoresis (SDS-PAGE)

Electrophoresis is movement of charged particles in an electric field. In SDS-PAGE, negatively charged proteins are separated based on molecular weight. The reducing agent β-mercaptoethanol in the sample buffer (Material 2.10) denatures proteins by reducing disulphide binding. The detergent sodium dodecyl sulphate (SDS), which are a part of the gel, binds to protein samples to be separated and make the proteins negatively charged. This results in proteins with same shape and charge-to-mass ratio, leaving the molecular weight for each protein as the only variable.

The polyacrylamide gel consist of long polymers of acrylamide cross-linked with N,N'-methylenebisacrylamide. This cross-linked matrix resembles a grid that proteins travels through, and the density of this grid are determined by acrylamide concentration. Low concentration causes proteins to travel faster through the gel, and high concentration causes proteins to move slower. Small proteins travels faster through the gel than bigger proteins regardless of acrylamide concentration (Farrell et al., 2006).

3.10.1 Preparation of mitochondria samples

The mitochondria pellets were dissolved in 50 µL of 1 x sample buffer (Materials 2:10) and sonicated (3 x 10 seconds on and 10 seconds off). Based on the protein concentrations calculated in the corresponding protein supernatants (chapter 3.7), approximately the same amounts of mitochondrial proteins were used from each sample. Samples were denatured (95℃ for 5 minutes), then quickly spun for 10 seconds and loaded onto the gel. The concentrations were calculated according to chapter 3.7, and the approximately amount of proteins loaded on the gels are listed in Table 4 (timeline), Table 5 (unstimulated) and Table 6 (stimulated).

Table 4: Approximate quantities of samples from the timeline loaded onto 10 % SDS-PAGE gel

Sample	Quantity loaded (approx.)
0 hour pooled mitochondria fragments	10 µg
1 hour pooled mitochondria fragments	10 µg
2 hours pooled mitochondria fragments	10 µg
4 hours pooled mitochondria fragments	10 µg
8 hours pooled mitochondria fragments	10 µg
12 hours pooled mitochondria fragments	10 µg
24 hours pooled mitochondria fragments	10 µg
48 hours pooled mitochondria fragments	10 µg

Table 5: Approximate quantities of samples loaded onto 10 % SDS-PAGE gel from unstimulated cells exposed to the mixture

Sample	Quantity loaded (approx.)
DMSO control mitochondria fragment	4.2 µg
DMSO control mitochondria fragment	4.2 µg
DMSO control mitochondria fragment	4.2 µg
$1{:}10^6$ mitochondria fragment	4.2 µg
$1{:}10^6$ mitochondria fragment	4.2 µg
$1{:}10^6$ mitochondria fragment	4.2 µg
$1{:}10^5$ mitochondria fragment	4.2 µg
$1{:}10^5$ mitochondria fragment	4.2 µg
$1{:}10^5$ mitochondria fragment	4.2 µg
$1{:}10^4$ mitochondria fragment	4.2 µg
$1{:}10^4$ mitochondria fragment	4.2 µg
$1{:}10^4$ mitochondria fragment	4.2 µg
$1{:}10^3$ mitochondria fragment	4.2 µg
$1{:}10^3$ mitochondria fragment	4.2 µg
$1{:}10^3$ mitochondria fragment	4.2 µg

Table 6: Approximate quantities of samples loaded onto 10 % SDS-PAGE gel from stimulated cells exposed to the mixture

Sample	Quantity loaded (approx.)
Forskolin control mitochondria fragment	4.2 µg
Forskolin control mitochondria fragment	4.2 µg
Forskolin control mitochondria fragment	4.2 µg
$1:10^6$ mitochondria fragment	4.2 µg
$1:10^6$ mitochondria fragment	4.2 µg
$1:10^6$ mitochondria fragment	4.2 µg
$1:10^5$ mitochondria fragment	4.2 µg
$1:10^5$ mitochondria fragment	4.2 µg
$1:10^5$ mitochondria fragment	4.2 µg
$1:10^4$ mitochondria fragment	4.2 µg
$1:10^4$ mitochondria fragment	4.2 µg
$1:10^4$ mitochondria fragment	4.2 µg
$1:10^3$ mitochondria fragment	4.2 µg
$1:10^3$ mitochondria fragment	4.2 µg
$1:10^3$ mitochondria fragment	4.2 µg

3.10.2 SDS-PAGE

Four µL of protein molecular weight standard were added to each gel. The electrical voltage was slowly increased, starting with 50 V for 5 minutes, then 80 V for 5 minutes, and then 100 V for 10 minutes until the proteins had migrated from the stacking gel into the separation gel. Then current was set at 180 V for approximately 50-60 minutes until the bromphenol blue front had reached the bottom of the gel. Samples from exposures and timeline were run on 10 % gels. Some of the pilot samples were run on 12.5 % gel, which is specified in the results or Appendix B. Parallel gels were stained with Colloidal Coomassie (Materials 2.10) overnight, and destained (Materials 2.10) the next day to visualize proteins.

3.11 Transfer of proteins to membrane by Western blotting

Western blot is a method that is used to transfer proteins from a polyacrylamide gel onto a membrane through an electric current (Towbin et al., 1979). The membrane can be made of nitrocellulose, PVDF or other materials. After transferring proteins onto a membrane, proteins of interest can be detected using specific antibodies. Usually, the membrane is incubated with a primary antibody, which binds to the protein of interest. A primary antibody can be either

monoclonal or polyclonal. A monoclonal antibody is derived from a single B cell that only produces one specific antibody. A polyclonal antibody is less specific as antibodies are collected from serum instead of a cell. After primary antibody incubation, a secondary antibody are added onto the membrane that binds to the primary antibody. This secondary antibody are conjugated to an enzyme or fluorescence marker that makes the protein visible (Farrell et al., 2006). A common marker is horseradish peroxidase (HRP). Another marker used in this thesis is CyDye conjugated secondary antibodies, which are detectable when using fluorescence.

3.11.1 Protein transfer to PVDF membrane optimized for fluorescence

Originally, signal for cytochrome P450 enzymes were tested using secondary antibodies conjugated with CyDye, a fluorescent chromophore that can be detected with a Typhoon FLA 9500 scanner. This requires the use of a low fluorescent PVDF membrane suitable for fluorescent scanning (Materials 2.8). A slightly modified protocol from the manufacturer (GE Healtcare) was followed. The PVDF membrane was pre-treated for 20 seconds in methanol to activate the membrane, washed for 20 seconds in dH_2O and equilibrated for 15 minutes in cold 1 x Transfer buffer (Materials 2.10). Membrane, pads and SDS-PAGE gel was equilibrated in cold 1 x Transfer buffer for 10 minutes prior to blotting. Protein transfer was executed for 2 ½ hours at 25 V in a 4℃ cold room.

3.11.1.1 Immunological detection of proteins of interest

After protein transfer, the membrane was washed twice in 1xTBST (Materials 2.10) for 5 minutes. Then the membrane was blocked in 5 % dry milk TBST (Materials 2.10) for 45 minutes at room temperature. After blocking, the membrane was rinsed twice in water and then washed 2 x 5 minutes in 1xTBST. The membrane was then incubated with a primary antibody diluted in 5 % dry milk TBST in 10 mL 1xTBST overnight at 4℃.

Next day the membrane was rinsed twice in 1xTBST, then washed 2 x 5 minutes in 1xTBST. Membrane was probed with secondary antibody in a 1/2500 dilution in 10 mL 1xTBST without dry milk according to the manufacturer's recommendation (Amersham), and incubated for 1 hour in room temperature protected from light. After incubation, the membrane was rinsed twice in 1xTBST then washed 4 x 5 minutes in 1xTBST. Lastly, the membrane was rinsed 3 times in 1xTBS before scanning using the Typhoon FLA 9500 scanner at a PMT value of 700 V for wet membrane detection. Antibodies that were used with fluorescence detection are listed in Table 7.

Table 7: Overview of primary and secondary antibodies used for immunochemical detection of mitochondrial proteins by fluorescence.

Primary antibodies	Dilution	Secondary antibodies	Dilution
Anti-CYP11A1	1:1000	goat anti-rabbit Cy5	1:2500
Anti-CYP11B2	1:1000	goat anti-rabbit Cy5	1:2500
Anti-StAR	1:1000	donkey anti-goat Cy5	1:2500
Anti-CYP19 (Aromatase)	1:1000	goat anti-rabbit Cy5	1:2500
Anti-β-Actin	1:1000	goat anti-mouse Cy3	1:2500

3.11.2 Protein transfer to PVDF membrane used for chemiluminescence

For Western blot detection of enzymes from timeline and exposure experiments, chemiluminescence was favoured over fluorescence because of reaching higher sensitivity. This method does not require a PVDF membrane optimized for fluorescence detection, so another PVDF membrane was used instead (Materials 2.10). The PVDF membrane was pre-treated for 20 seconds in methanol for activation of the membrane, washed for 20 seconds in dH_2O and equilibrated for 15 minutes in cold 1 x Transfer buffer. Membrane, pads and SDS-PAGE gel was equilibrated in cold 1 x Transfer buffer for 10 minutes prior to blotting. Protein transfer was performed for 1 hour, set at 100 V and 300 mA.

3.11.2.1 Immunological detection of proteins of interest

After transfer, the membrane was washed twice in 1xTBST for 5 minutes. Unbound membrane was blocked with 5 % non-fat dry milk in 1xTBST for 45 minutes at room temperature, before the membrane was rinsed twice and then washed 2 x 5 minutes in 1xTBST. The membrane was then incubated with the primary antibody diluted in 0,05 % low-fat dried milk in 10 mL 1xTBST overnight at 4℃. Next day the membrane was rinsed twice and then washed 2 x 5 minutes in 1xTBST. Then the membrane was incubated with the HRP conjugated secondary antibody diluted in 5 % dry milk in 1xTBST for 1 hour in room temperature protected from light. After incubation, the membrane was rinsed twice and then washed 4 x 5 minutes in 1xTBST. Prior to chemiluminescent detection, the membrane was washed for 5 minutes in deionized H_2O. The membrane was incubated for 1 minute with a 1:1 mixture of SuperSignal® West Femto Maximum Sensitivity Substrate and SuperSignal® West Pico Chemiluminescent Substrate (Materials 2.4). Chemiluminescent signals were detected using a ChemiDoc™ XRS+ imager. Antibodies used for chemiluminescence is listed in Table 8.

Table 8: Overview of primary and secondary antibodies used for immunochemical detection of mitochondrial proteins by chemiluminescence.

Primary antibodies	Dilution	Predicted band size (kDa)	Secondary antibodies	Dilution
Anti-CYP11A1	1:1000	60	HRP goat anti-rabbit	1:2500
Anti-CYP11B2	1:1000	58	HRP goat anti-rabbit	1:2500
Anti-CYP19	1:1000	58	HRP goat anti-rabbit	1:2500
Anti-β-Actin	1:1000	42	HRP sheep anti-mouse	1:10000
Anti-StAR	-	37	Not available	-

3.11.3 Stripping of antibodies

Membranes were sometimes stripped for bound antibodies and reprobed with another primary antibody, especially during antibody testing. After ended Western blot procedure, the membrane was washed in 1xTBS for 5 minutes in room temperature. Then the membrane was covered in stripping buffer (Materials 2.10), and incubated at 50 ℃ for 30 minutes while shaking. After stripping, the membrane was washed 2 x 5 minutes in 1xTBST before blocking and incubation with primary antibody.

3.12 Separation of proteins by 2D-electrophoresis

2D-electrophoresis is a method that separates proteins in two dimensions. In the first dimension, proteins are separated by isoelectric focusing. The second dimension separates the protein by molecular weight using SDS-PAGE (Liebler, 2000). The protocol described in Amersham Biosciences Ettan DIGE User Manual (Biosciences, 2002) was followed.

3.12.1 Cell lysis by sonication and protein measurement

Cell pellet were washed twice by adding 1 mL 1xPBS and centrifuged at 13000 x g for 5 minutes at 4℃, before 600 µL of 2D-homogenisation buffer (Materials 2.10) was added to the pellet. Pellets were then sonicated on ice for 5 x 15 seconds on, and 10 seconds off, to break the cell wall. The cell lysate were then centrifuged twice at 13000 x g for 5 minutes at 4℃ to separate cell debris and the soluble protein fraction. Protein concentration was determined with Pierce™ 660 as described in chapter 3.9, but bovine serum albumin (BSA) was diluted in 2D-homogenisation buffer to make the standard (Materials 2.10).

3.12.2 1D separation by isoelectric focusing (first dimension)

In the first step of isoelectric focusing, proteins were transferred onto a 7 cm IPG strip by in-gel rehydration. 100 µL of sample containing 250 µg protein was mixed with 25 µL 5 x rehydration buffer (Materials 2.10) and pipetted onto a rehydration tray. The strip was placed face down onto the protein sample then added cover fluid to avoid dehydration. The IPG strip was left to rehydrate overnight in room temperature protected from light. The next day the isoelectric focusing was performed with an Ettan IPGphor 3 Isoelectric Focusing unit for 3 hours.

3.12.3 2D separation by SDS-PAGE (second dimension)

As soon as the isoelectric focusing was done, the strip was put in a rehydration tray. Then 10 mL equilibration buffer A (Materials 2.10) was added to the strip, and shaken for 10 minutes in room temperature before buffer A was discarded. The strip was incubated next with 10 mL equilibration buffer B (Materials 2.10) for 10 minutes in room temperature while shaking. After incubation, the IPG strip was soaked in the TGS running buffer (Materials 2.10) before placed on top of a 12 % SDS-PAGE gel (1.0 mm) for separating proteins by size. Four µl of the molecular weight standard was pipetted onto a small filter paper and placed next to the IPG strip. The top was sealed with 1 % agarose (Materials 2.10). The electrophoresis was run at 180 V until the dye front reached the bottom of the gel. The resulting gel was stained with Colloidal Coomassie (Materials 2.10) overnight, and destained (Materials 2.10) the next day to visualize proteins.

3.13 Statistical analysis

The statistical analyses of LC-MS/MS data from exposure experiments were performed in R using one-way Anova. Tukey multiple comparison test was performed when more than two samples indicated significant p-values. Statistical significance was set with a p-value at 0.05. Intensity of antibody signal on the western blot was analysed with ImageJ. For each sample, the antibody signal for one enzyme was normalised with the β-actin signal (housekeeping protein) of the same sample.

4. RESULTS

4.1 Establishing growth conditions for Y1 cells

The Y1 cells did not grow according to recommended type of serum supplements, which were a combination of 2.5 % fetal bovine serum (FBS) and 15 % horse serum (American Type Culture Collection (ATCC) web site). Therefore, a different type of serum supplementation had to be considered. Yasumura et al. (1966) showed that Y1 cells need high serum concentration in order to maintain high steroid production, and in a relatively recent study, Whitehouse et al. (2002) used 10 % FBS to grow Y1 cells successfully. Taking these studies into account, 10 % charcoal stripped FBS was used as the only serum supplement to grow the Y1 cells. Charcoal stripping has previously been shown to efficiently remove hormones from serum (Cao et al., 2009), and therefore charcoal stripped FBS was chosen to avoid interference from steroids in the serum supplement in the downstream steroid profiling analysis. Prior to use, the serum was analysed with LC-MS/MS, and the charcoal-stripped FBS were confirmed free of hormones (performed by Ralf Kellmann and Kareem Ahmed).

Several papers report the cultivation of Y1 cells in Ham's F10 medium (Colonna et al., 2005; Pagotto et al., 2014) or DMEM (Aumo et al., 2010; Whitehouse et al., 2002), or a combination of these. The medium used in this study was Ham's F-12K (Kaighn's) medium supplemented with 10 % FBS and 1 % Penicillin-Streptomycin (Pen-Strep). To monitor cell growth in this medium, pictures of cells were taken each day until cells reached 80-90 % confluence (approximately 4 days). While the cells initially were irregular shaped, their morphology changed into the characteristic epithelial shape two days after seeding (Fig. 4-1). This observation is in accordance to the descriptions given by ATCC (2015). Since the cells apparently grew as expected in 10 % FBS and HAM's F-12K media, this growth media combination was used throughout the cell expansion procedure and for growing cells for exposure experiments (Materials 2.10).

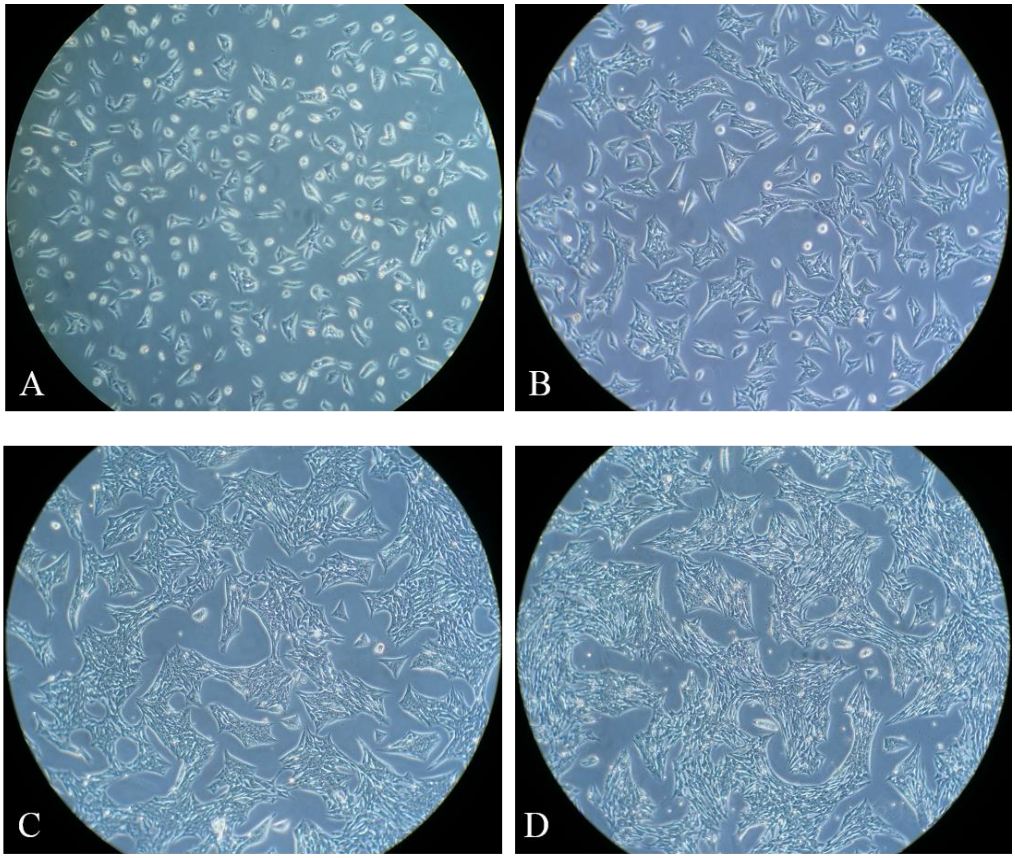

Figure 4-1: Development of Y1 cells grown in Ham's F-12K growth media supplemented with 10 % fetal bovine serum. Pictures show Y1 cells at 10x magnification on A) day one after seeding, B) day two after seeding, C) day three after seeding and D) day four after seeding.

4.2 Choosing the sample buffer for SDS-PAGE protein separation based on antibody affinity testing

4.2.1 Mitochondria enrichment or total protein cell lysates

Many of the enzymes that are part of the steroidogenesis are found in the mitochondria, suggesting that mitochondria enrichment should be considered for optimal enzyme detection. Cells were lysed in either RIPA (whole cell lysates) or sucrose buffer (mitochondria enrichment). By using antibodies against various steroidogenic enzymes, the success and need for performing mitochondria enrichment would be indicated if antibodies only bound to mitochondria samples.

Antibody specificity was tested on forskolin stimulated Y1 cells before the real exposure and time line samples were to be analysed in Western blots (chapter 3.11.2). In addition to Y1 cells,

human cell lines (HepG2 and H295R) have previously been shown to express some of the proteins of interest, and were therefore included as possible positive controls on the Western blots. The human hepatocytes, HepG2 cells, were lysed in RIPA, while human and mouse adrenocortical cells, H295R and Y1 cells, were lysed in either RIPA or sucrose buffer (Materials 2.10). Both the supernatant with soluble proteins and the mitochondria enriched pellet were loaded onto the SDS-PAGE gel. One sample of isolated Y1 mitochondria fraction lysed in RIPA was also added. This sample was prepared before the sucrose buffer was made, as a test to see if mitochondria could be isolated using RIPA buffer and differential centrifugation.

Using an anti-CYP11B2 antibody, the mitochondrial protein CYP11B2 was detected in total protein fraction of human hepatocytes (HepG2 cells), as well as in total protein preparation (RL) and enriched mitochondria (SM) in human adrenocortical cells (Fig. 4-2). No CYP11B2 were detected in Y1 cells. Thus, CYP11B2 could be detected in both total protein fraction and enriched mitochondrial fractions.

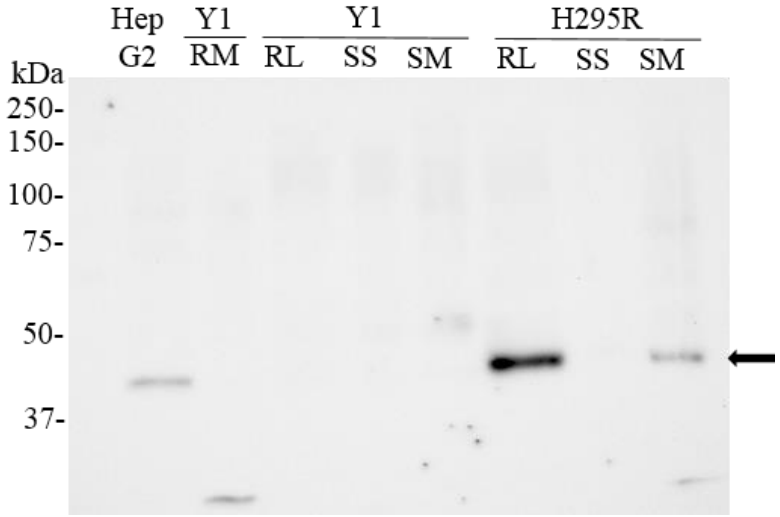

Figure 4-2: Immunochemical detection of P450c11AS (CYP11B2) in HepG2, Y1 and H295R. Proteins separated on a 10 % SDS-PAGE gel. RM = RIPA isolated mitochondria. RL = RIPA whole cell lysate. SS = sucrose supernatant. SM = sucrose isolated mitochondria. Membrane was incubated with rabbit monoclonal anti-CYPB2 IgG primary antibody (1:1000) and detected with a goat anti-rabbit IgG HRP-conjugated secondary antibody (1:2000). Chemiluminescence was detected with a 1:1 mixture of SuperSignal® West Femto Maximum Sensitivity Substrate and SuperSignal® West Pico Chemiluminescent Substrate.

CYP11A1, a protein located in the inner mitochondrial membrane with a molecular weight at 60 kDa, was detected in human hepatocytes (HepG2), isolated Y1 mitochondria (Y1 RM), and in the enriched mitochondrial fraction of adrenocortical cells from mouse (Y1 SM) and both in

total protein and mitochondrial fraction of human cells (H295R RL and SM) (Fig. 4-3). Mouse CYP11A1 appeared to migrate slightly shorter than CYP11A1 from human cells. Thus, CYP11A1 could be detected in both total protein fraction and enriched mitochondrial fractions in the human cells, but only in the mitochondria fragment in Y1 cells.

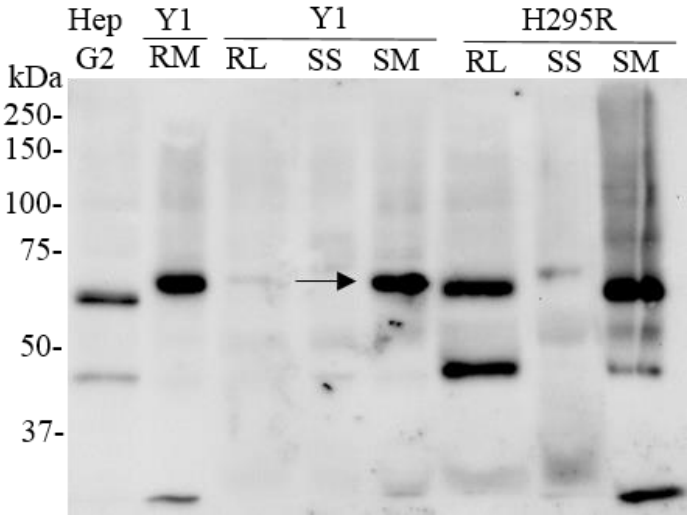

Figure 4-3: Immunochemical detection of P450scc (CYP11A1) in HepG2, Y1 and H295R. The membrane was incubated with rabbit polyclonal anti-CYP11A1 IgG primary antibody (1:1000) and detected with a goat anti-rabbit IgG HRP-conjugated secondary antibody (1:2000). Signal in Y1 marked with an arrow.

The same membrane was stripped for 30 minutes and incubated with anti-CYP19. CYP19, a peripheral membrane protein with a molecular weight 58 kDa, was detected in total protein fraction, sucrose supernatant and enriched mitochondrial fraction of Y1 cells (Fig. 4-4) but not in human H295R cells. The antibody detected two proteins, one migrating according to a size of approximately 60 kDa, and one of 50 kDa. Thus, CYP19 could be detected in both total protein fraction and enriched mitochondrial fractions, meaning that Y1 cells can be lysed in RIPA and sucrose and there will be no difference regarding detection of CYP19.

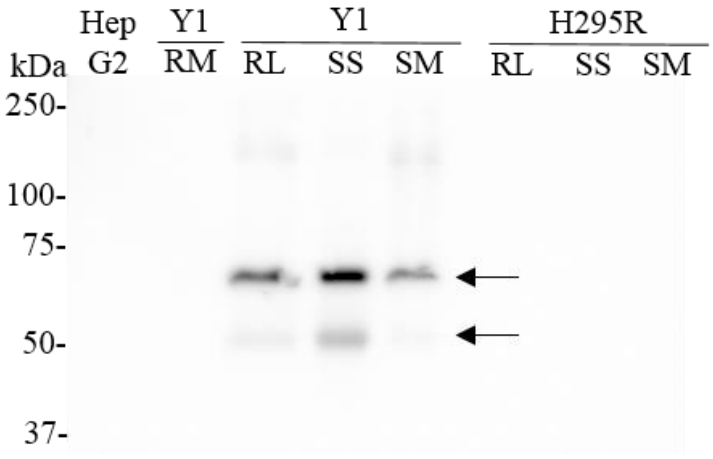

Figure 4-4: Immunochemical detection of P450arom (CYP19 aromatase) in HepG2, Y1 and H295R. The membrane was incubated with rabbit polyclonal anti-CYP19 IgG primary antibody (1:1000), and detected with a goat anti-rabbit IgG HRP-conjugated secondary antibody (1:2000). Signal for two bands marked with arrows.

4.2.2 Using sucrose lysis buffer for mitochondria enrichment

Since CYP11A1 could only be detected in the enriched mitochondrial fraction of Y1 cells, and CYP19 and CYP11B2 were detected in either fraction, sucrose enrichment of mitochondrial fraction was used for the remaining Western blots of this study.

4.2.3 Determining antibodies to use on exposed cells and timeline experiments

Two antibodies appeared to work with the Y1 cells; the anti-CYP11A1 and anti-CYP19. These antibodies were therefore used on cells from the exposure experiments and cells from the timeline assays.

CYP11B2 was decided to be tested on timeline cells in addition to the three antibodies. Signal for CYP11B2 was in the previous experiments only detected in the human cells, and this suggested that CYP11B2 were not present in Y1 cells. However, signal for CYP11B2 was tested on the timeline cells to investigate if this enzyme might be present in an earlier stage in the steroidogenic pathway.

For Western blot detection of enzymes from timeline and exposure experiments, chemiluminescence was favoured over fluorescence because of reaching higher sensitivity. Relevant results from fluorescence immunological detection are listed in Appendix B.

4.3 Basal steroidogenesis in stimulated Y1 cells

The basal steroidogenesis in Y1 cells were measured by three timeline experiments as described in chapter 3.3. This would help identify a suitable time window to measure metabolites in media in cells exposed to the mixture. Steroid profiling of media and enzyme levels in cells were studied with LC-MS/MS and Western blot.

4.3.1 Immunological detection of steroidogenic enzymes

During the 48h time line experiments, steroidogenic enzymes were detected using antibodies. Since Western Blot is semi-quantitative, this could reveal changes in enzymes concentrations over time as steroids are being produced in the cells. Cell samples for Western blot and parallel SDS-PAGE were prepared according to chapter 3.10 and Western blot were performed as described in chapter 3.11.

From the parallel gel (Fig. 4-5) there seems to have been loaded more proteins from hour 1 and hour 4 on the gel. The same protein amounts were loaded on the gel used for Western blot and immunological detection. However, the membrane was incubated with anti-beta actin as a loading control, and were used for normalization of signal detection of CYP11A1 and CYP19. Because three samples from each time point were pooled together, difference in signal could not be analysed for statistical significance.

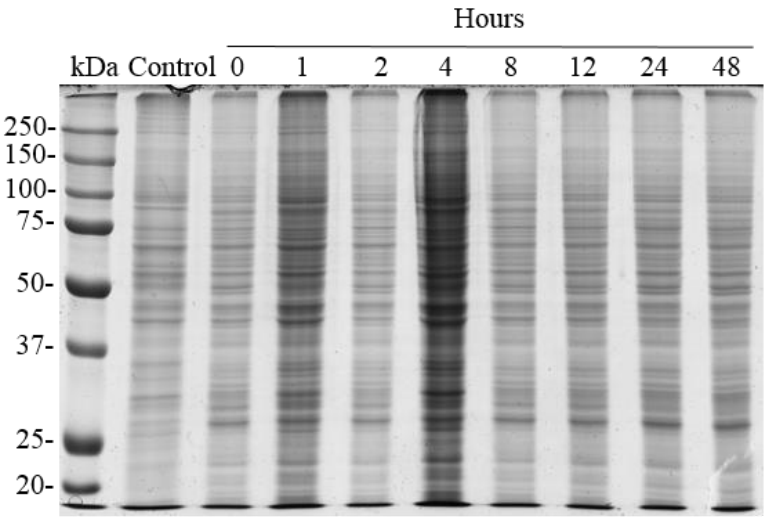

Figure 4-5: Parallel SDS-PAGE gel of the samples collected in the timeline experiment. Mitochondria fraction of three pooled cell samples for each time point (0, 1, 2, 4, 8, 12, 24, 48 hours, respectively) separated on a 10 % gel. Gel stained with colloidal coomassie for protein visualisation.

CYP19 was detected after 12, 24 and 48 hours. Two protein bands were detected that migrated according to masses of approximately 65 kDa and 50 kDa as previously detected (Fig. 4-6). Based on band intensity (Fig. 4-7), there seems to be slightly more CYP19 in the cells after 48 hours.

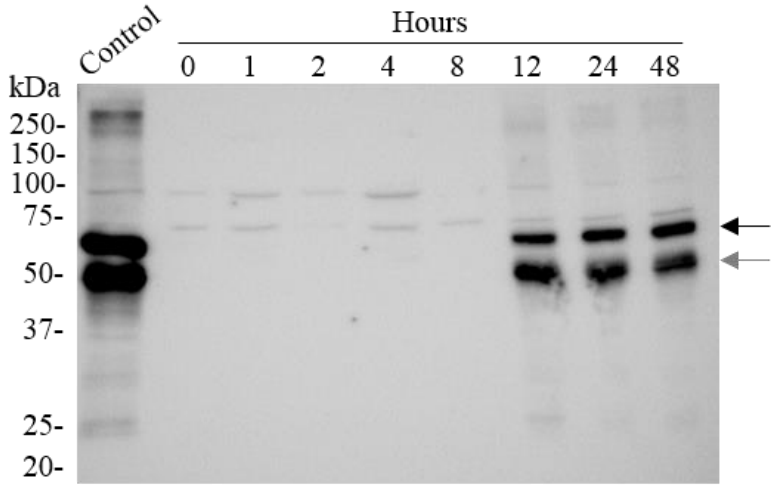

Figure 4-6: Immunochemical detection of P450arom (CYP19 aromatase) in Y1 cells. Three mitochondria enriched fractions were pooled for each time point (0, 1, 2, 4, 8, 12, 24, 48 hours, respectively) where transferred to a PVDF membrane. A universal antibody control was prepared by mixing whole cell lysates of forskolin stimulated H295R and Y1 cells. Membrane was incubated with rabbit polyclonal anti-CYP19 IgG primary antibody (1:1000) and primary antibody binding detected with a goat anti-rabbit IgG HRP-conjugated secondary antibody (1:2000). Chemiluminescence was detected with a 1:1 mixture of SuperSignal® West Femto Maximum Sensitivity Substrate and SuperSignal® West Pico Chemiluminescent Substrate.

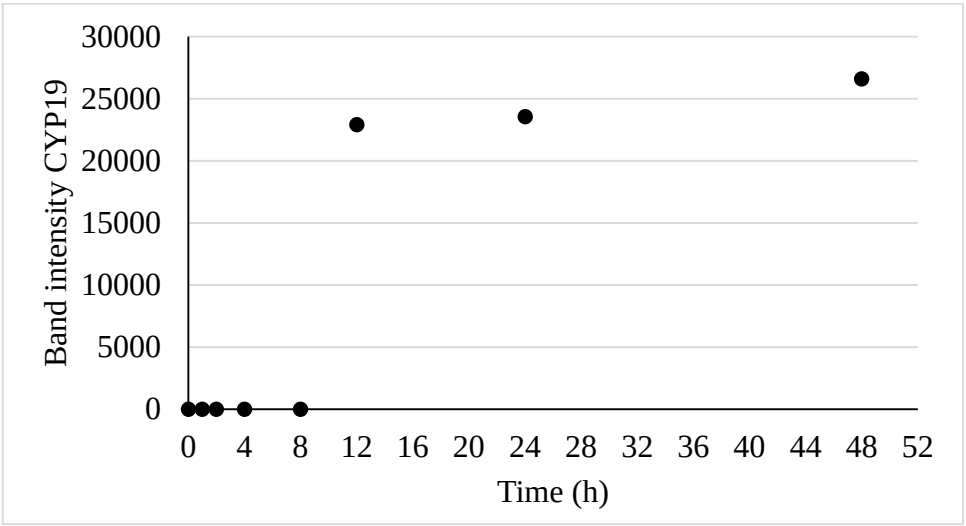

Figure 4-7: Band intensity of P450aro (CYP19). Band intensities were measured in ImageJ and signals were adjusted against beta actin. Band intensity represent the mean of the upper and lower band.

When the same membrane was stripped (chapter 3.11.3) and incubated with anti-CYP11B2, no CYP11B2 was detected in the timeline samples (Figure 4-8) except for in the antibody control that is probably binding of H295R as previously detected (Fig. 4-4).

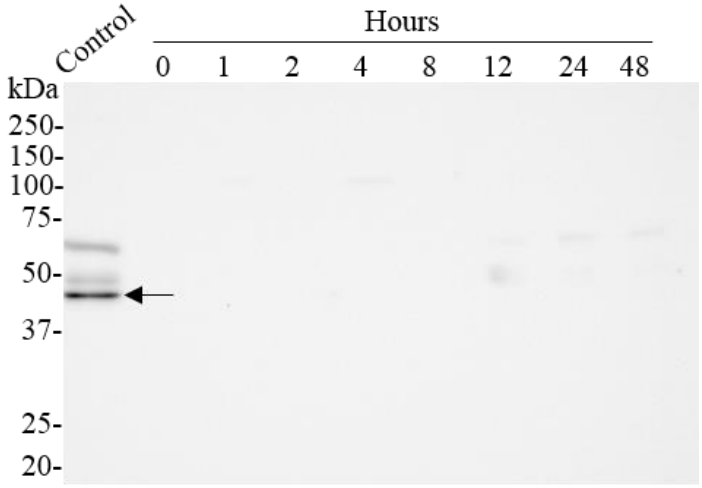

Figure 4-8: Immunochemical detection of P450c11AS (CYP11B2) in Y1 cells. Mitochondria enriched fractions of three pooled cell samples for each time point (0, 1, 2, 4, 8, 12, 24, 48 hours, respectively) were transferred to a PVDF membrane. Antibody control is a mixture of forskolin induced H295R and Y1 whole cell lysates. Membrane was incubated with rabbit monoclonal anti-CYP11B2 IgG primary antibody (1:1000) and detected with a goat anti-rabbit IgG HRP-conjugated secondary antibody (1:2000).

The membrane was then incubated with anti-CYP11A1, and CYP11A1 were detected in all the cell samples in the time line. The membrane was then incubated with anti-beta actin. Figure 4-9 shows the signals for both CYP11A1 and β-actin. Based in band intensity (Fig. 4-10), signal for CYP11A1 was strongest at 24 hours. As seen in the parallel gel, detection of β-actin showed more protein loaded from hour 1 and 4.

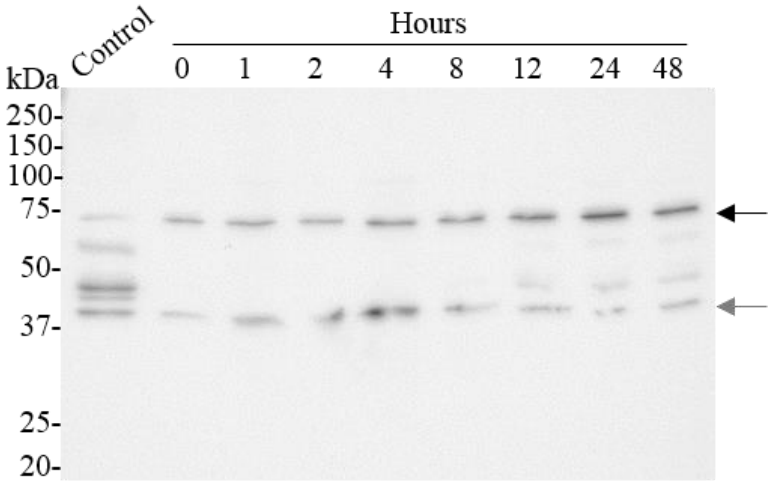

Figure 4-9: Immunochemical detection of P450scc (CYP11A1) and β-actin loading control in Y1 cells. Mitochondria enriched fraction of three pooled cell samples for each time point (0, 1, 2, 4, 8, 12, 24, 48 hours, respectively) where transferred to a PVDF membrane. Antibody control is a mixture of forskolin induced H295R and Y1 whole cell lysates. Membrane was first incubated with rabbit polyclonal anti-CYP11A1 IgG primary antibody (1:1000) and detected with a goat anti-rabbit IgG HRP-conjugated secondary antibody (1:2000). Then the membrane was incubated with a mouse monoclonal anti-beta actin IgG primary antibody (1:1000) and detected with a sheep anti-mouse HRP-conjugated secondary antibody (1:10000). Black arrow is CYP11A1, grey arrow is β-actin.

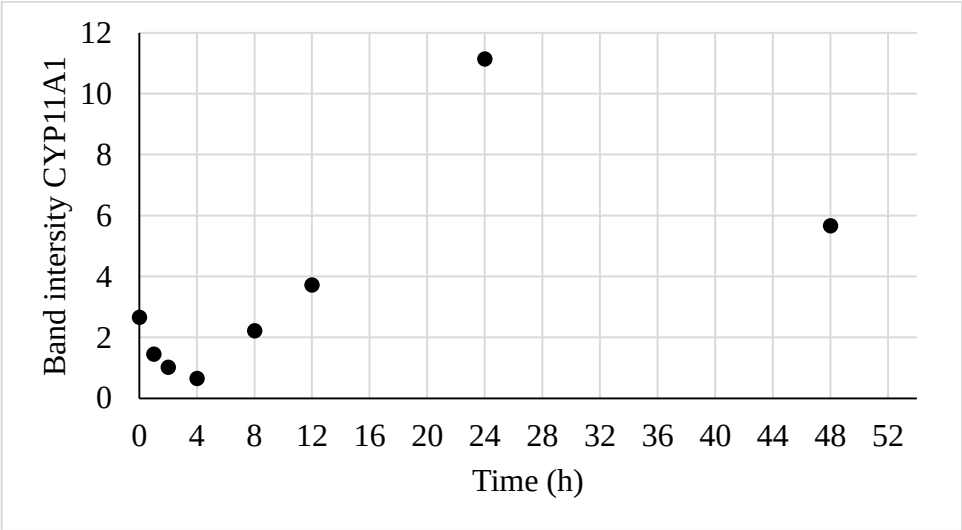

Figure 4-10: Band intensity of P450scc (CYP11A1). Band intensities were measured in ImageJ and signals were adjusted against beta actin.

4.3.2 Steroid profiling of metabolites in Y1 media

Media collected from three timeline experiments with two replicates of each time point were analysed with LC-MS/MS (chapter 3.6). All time points were measured six times and absolute values is listed in Appendix A. One timeline was performed with longer incubation up to 72 hours. Results from this timeline is listed in Appendix D.

Initially there were no detectable levels of pregnenolone until two hours after stimulation, and then concentrations increased slowly from 9 nM to 48 nM at eight hours. After twelve hours, the concentration increased quite rapidly from 152 nM to 411 nM at 24 hours before dropping down to 11 nM at 48 hours (Fig. 4-11). Pregnenolone is synthesised from cholesterol via CYP11A1, and is the rate-limiting step in steroidogenesis.

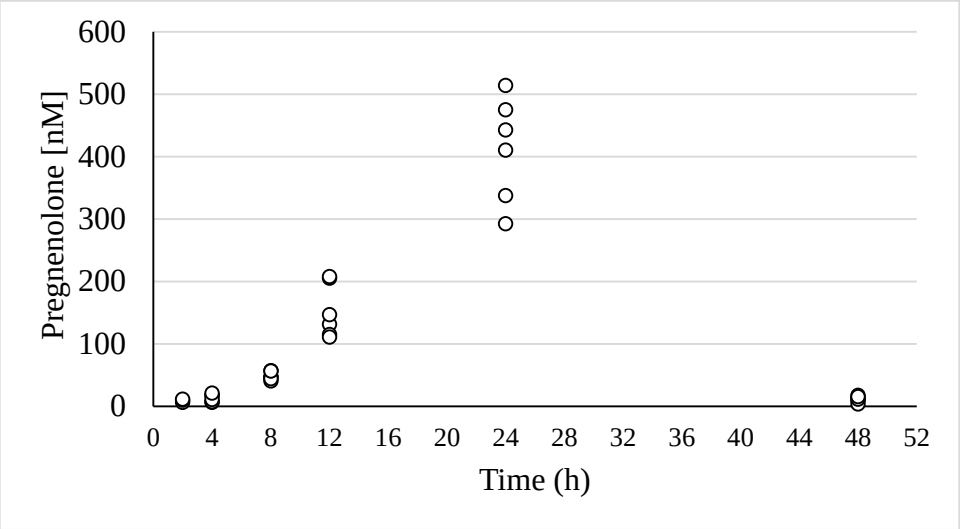

Figure 4-11: Levels of pregnenolone in medium of forskolin stimulated Y1 cells.

There were detectable levels of progesterone at time 0, and the concentration rapidly increased after two hours from 12 nM up to 619 nM at 24 hours, before decreasing to 74 nM after 48 hours (Fig. 4-12). The concentration of progesterone were higher than pregnenolone for each time point, but the trend of pregnenolone and progesterone were similar with the highest concentration of both metabolites at 24 hours.

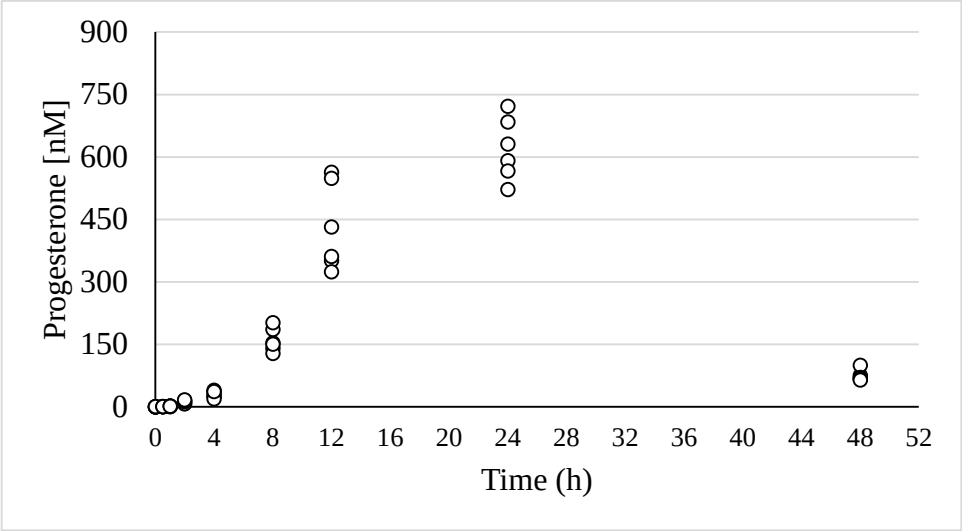

Figure 4-12: Levels of progesterone in medium of forskolin stimulated Y1 cells.

Levels of 20α-dihydroxyprogesterone (20αOHP), one of the main metabolites produced in Y1 cells, steadily increased in concentration after 12 hours (Fig. 4-13). There were low detectable levels of 20αOHP after 8 hours, which increased after 12 hours from 2 nM to 39 nM at 48 hours. The data from the timelines indicate linear increase of 20αOHP.

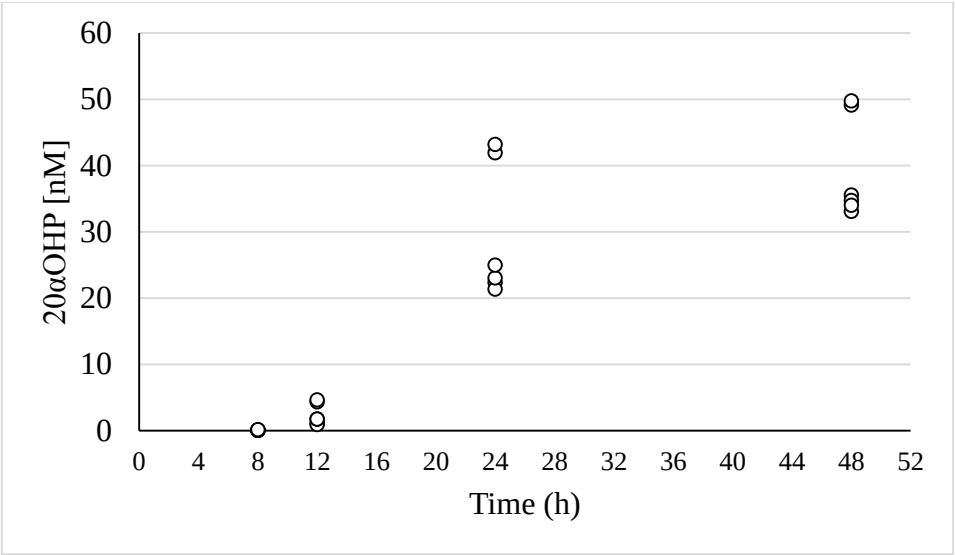

Figure 4-13: Levels of 20α-dihydroxyprogesterone (20αOHP) in medium of forskolin stimulated Y1 cells.

Corticosterone was detected after 12 hours, and concentration increased from 0.08 nM to 7.9 nM at 48 hours of incubation (Fig. 4-14). Both end products, 20α-dihydroxyprogesterone and corticosterone, reached detectable levels in media after approximately 12 hours. Comparing the two metabolites, levels of 20α-dihydroxyprogesterone were higher than of corticosterone.

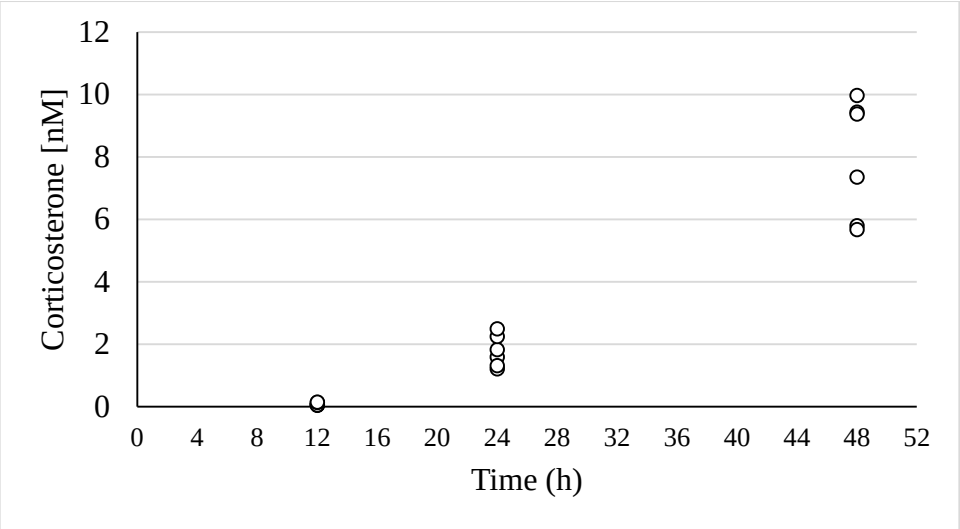

Figure 4-14: Levels of corticosterone in medium of forskolin stimulated Y1 cells.

Androstenedione, an androgen, were detectable at time 0, However there was no clear trend of increasing concentration until after four hours (Fig. 4-15). Then concentration increased slowly from 0.94 nM to 2.2 nM at 48 hours.

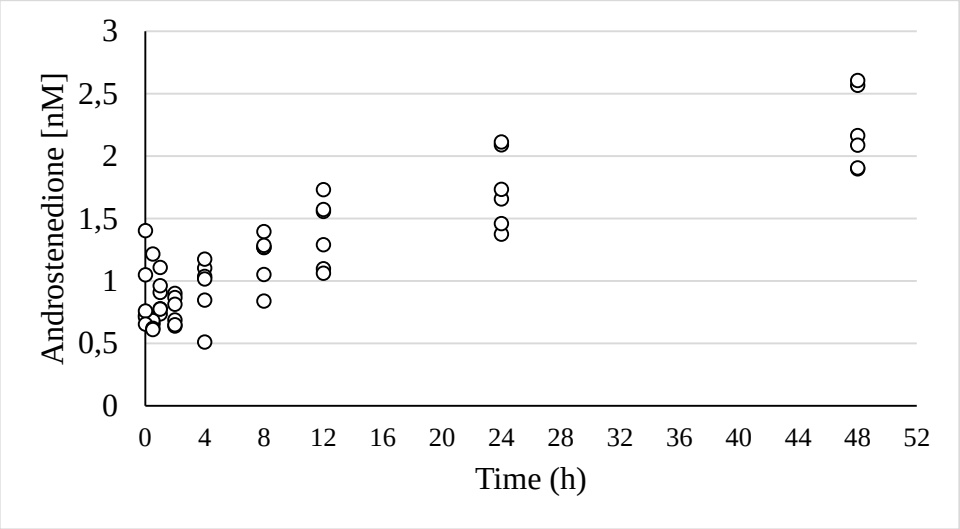

Figure 4-15: Levels of androstenedione in medium of forskolin stimulated Y1 cells.

When quantifying testosterone with LC-MS/MS, an interference was detected in the mass spectrometry. This was shown as a widening of the peak in the mass spectrometry, as well as two peaks instead of one peak. However, since the interference were the same for all samples, the measured concentrations were comparable. Like with androstenedione, there were

detectable levels of testosterone from time 0. However, levels decreased from 0.08 nM at 1 hour to 0.04 nM at 48 hours (Fig. 4-16).

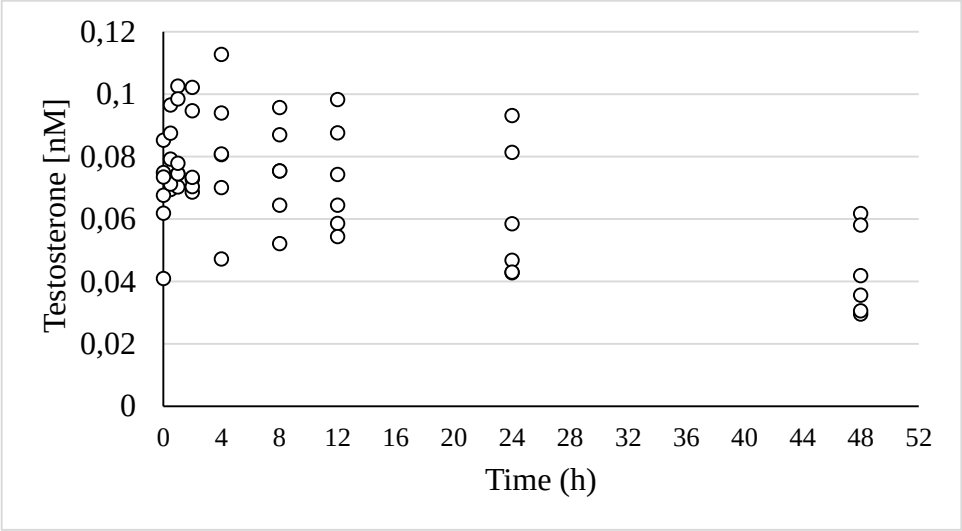

Figure 4-16: Levels of testosterone in medium of forskolin stimulated Y1 cells.

Estradiol, an estrogen synthesised from androstenedione via CYP19, were detected after 24 hours at 0.06 nM. Concentration increased to 1.2 nM at 48 hours (Fig. 4-17).

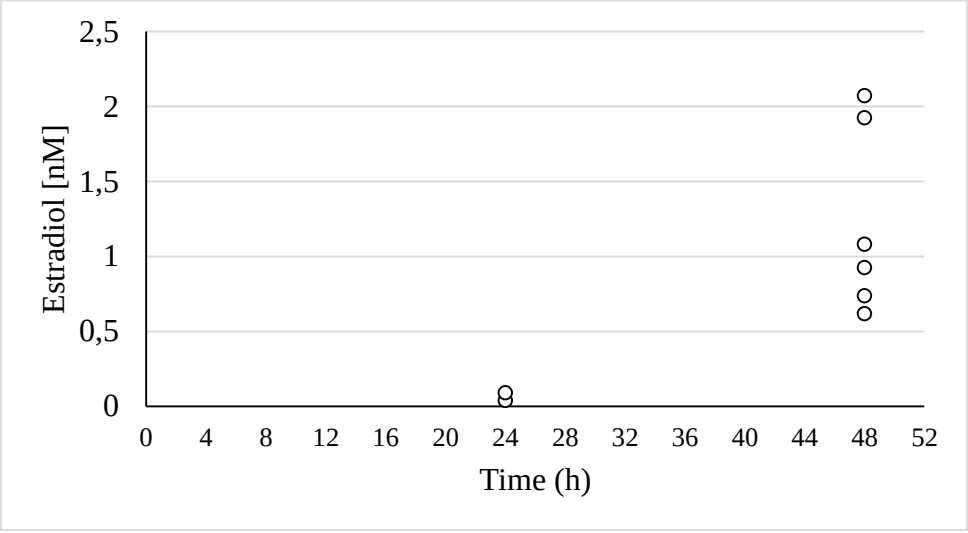

Figure 4-17: Levels of estradiol in medium of forskolin stimulated Y1 cells.

Estrone, an estrogen synthesised from testosterone via CYP19, were first detected after 24 hours at 0.03 nM (Fig.4-18). The concentration increased to 0.27 nM after 48 hours.

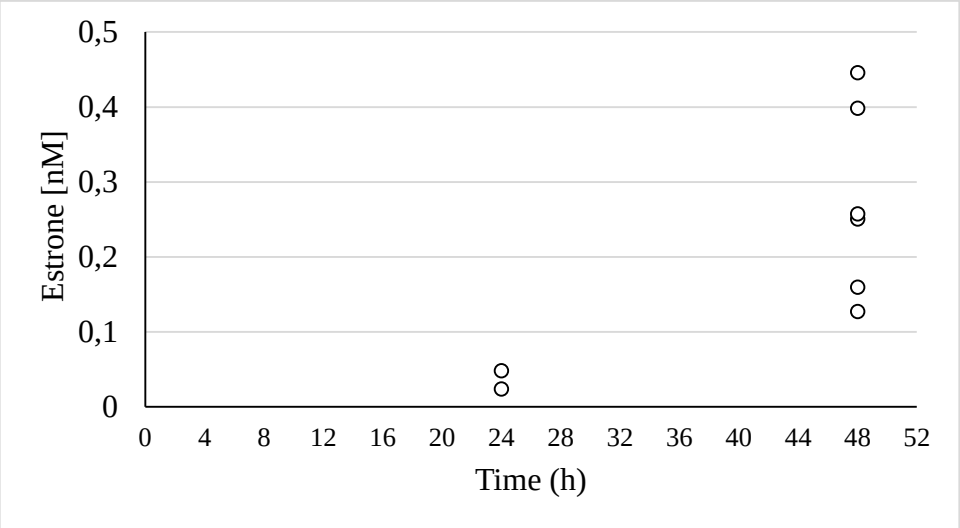

Figure 4-18: Levels of estrone in medium of forskolin stimulated Y1 cells.

The measured concentrations of androgens (androstenedione, testosterone) and estrogens (estradiol, estrone) were much lower than the measured concentrations of 20α-dihydroxyprogesterone and corticosterone.

4.4 Testing the cytotoxicity of the four mixture doses

The cytotoxicity of the diluted POP-mixture doses on the Y1 cells was tested using alamarBlue®. Not all the doses were tested for the unstimulated conditions because of limited amount of POP-mixture to make dilutions.

As expected, Triton X-100 and media blank (positive controls) had low fluorescent intensity (Fig. 4-19). Measured fluorescence intensity was high in the negative control cells treated with normal growth media (12000 FL 590). Similar intensities were observed in unstimulated cells supplemented with 0.1 % DMSO, unstimulated exposed cells (1:10^3 mixture dilution), 0.1 % forskolin stimulated cells and exposed stimulated cells (1:10^3, 1:10^4 and 1:10^5 mixture dilutions). This indicated that neither DMSO, forskolin nor the different POP-mixture concentrations were cytotoxic or induced apoptosis in Y1 cells.

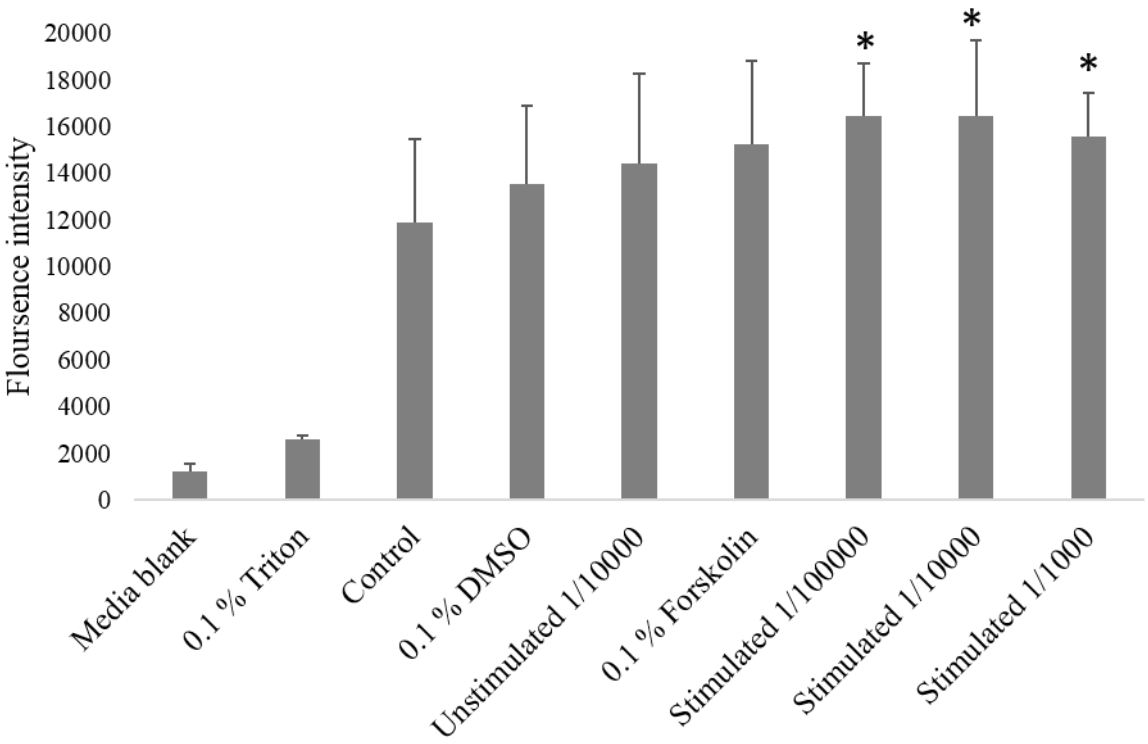

Figure 4-19: Cell cytotoxicity test of the mixture after incubation with alamarBlue®. Fluorescence measured at 540 nm excitation and 590 nm emission using an Enspire™ Multilabel Reader.

4.5 Effects of the mixture of POPs on steroidogenesis in Y1 cells

To study the effects on steroidogenesis in Y1 cells by contaminant mixtures, Y1 cells, either stimulated by forskolin or not, were exposed to the contaminant mixture. Subsequently, steroid profiling of media and enzyme levels in cells were studied with LC-MS/MS and Western blot.

4.5.1 Effects in unstimulated cells

The effects of the mixture in unstimulated cells were measured in three exposure experiments as described in chapter 3.5.1.

4.5.1.1 Immunological detection for effects on steroidogenic enzymes

Cell samples for Western blot and parallel SDS-PAGE were prepared according to chapter 3.10 and Western blot were performed as described in chapter 3.11.2.

From the parallel gels (Fig. 4-20) there seems to have been loaded more protein from the $1{:}10^6$ sample from the first exposure. The same protein amounts were loaded on the gels used for Western blot and immunological detection. However, the membranes were incubated with anti-beta actin as a loading control, and were used for normalization of signal detection of CYP11A1 and CYP19.

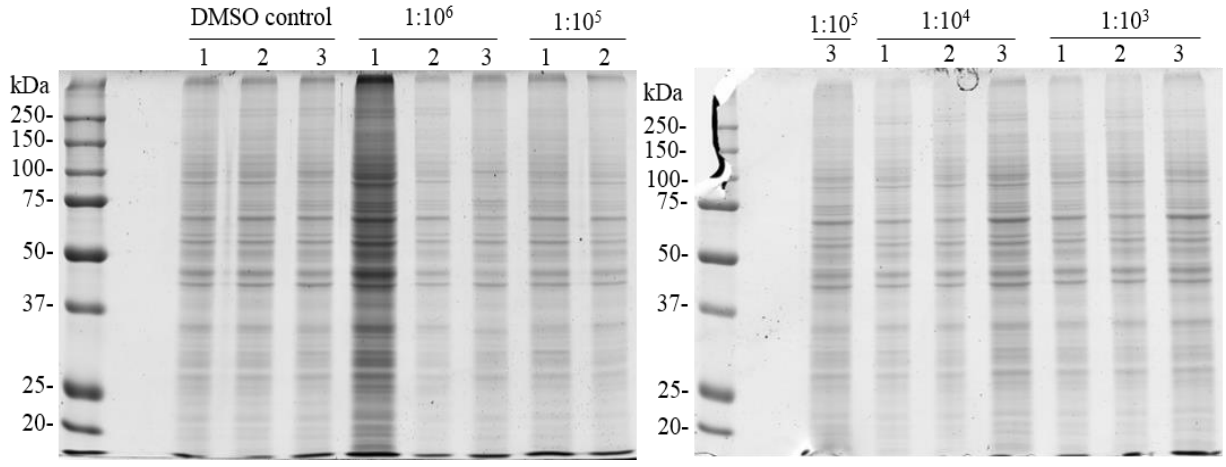

Figure 4-20: Parallel SDS-PAGE gels of unstimulated Y1 cells exposed to the mixture. Mitochondria fragment of one cell sample for each exposure (1st, 2nd and 3rd repeated exposure, respectively) run on two 10 % gel. Left to right is the lowest dose to the highest dose tested on the Y1 cells ($1{:}10^6$, $1{:}10^5$, $1{:}10^4$ and $1{:}10^3$). Gels stained with colloidal coomassie for protein visualisation.

As expected, two proteins reactive to the anti-CYP19 antibody were detected in the Y1/H295R control (black and grey arrow). However, no CYP19 was detected in unstimulated Y1 cells or in non-stimulated cells exposed to the contaminant mixtures (Fig. 4-21).

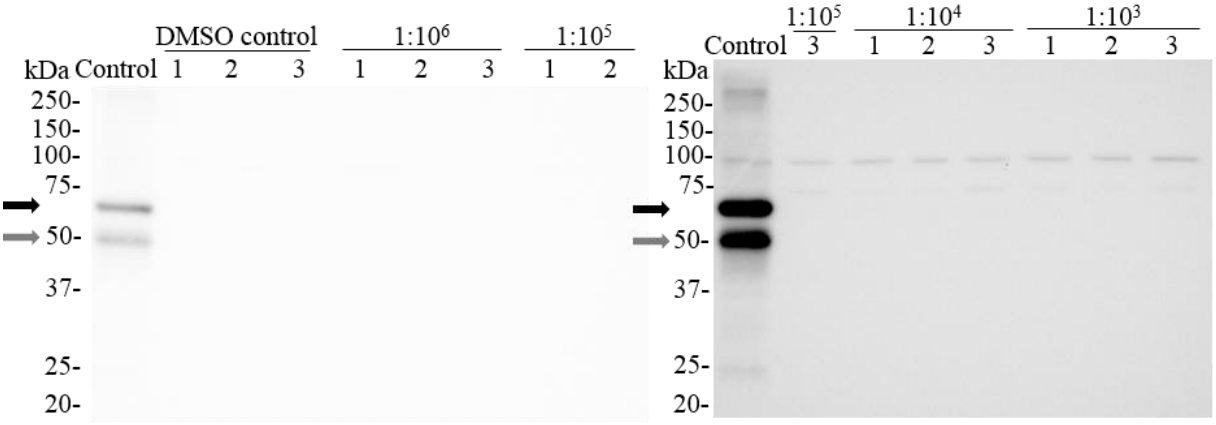

Figure 4-21: Immunochemical detection of P450arom (CYP19 aromatase) in unstimulated Y1 cells exposed to contaminant mixtures. Mitochondria fraction of one cell sample for each exposure (1st, 2nd and 3rd repeated exposure, respectively) transferred to PVDF membranes. Left to right is the lowest dose to the highest dose tested on the Y1 cells ($1:10^6$, $1:10^5$, $1:10^4$ and $1:10^3$). Antibody control is a mixture of forskolin induced H295R and Y1 whole cell lysates. Membranes were incubated with rabbit polyclonal anti-CYP19 IgG primary antibody (1:1000) and detected with a goat anti-rabbit IgG HRP-conjugated secondary antibody (1:2000). Chemiluminescence was detected with a 1:1 mixture of SuperSignal® West Femto Maximum Sensitivity Substrate and SuperSignal® West Pico Chemiluminescent Substrate.

The membranes were then incubated with anti-CYP11A1, and CYP11A1 was detected in all the samples (Fig. 4-22). The membranes were then incubated with anti-beta actin. Figure 4-22 shows the signals for both CYP11A1 and β-actin. Based in band intensity but there was no significant difference between levels in unstimulated cells and cells exposures to the mixtures (Fig. 4-23). As seen in the parallel gels, detection of β-actin showed more protein loaded from the $1:10^6$ sample from the first exposure compared to other samples on the same membrane. Nevertheless, the amount seems to be the same as loaded on the other membrane. However, detection of β-actin showed less protein loaded from the $1:10^6$ sample from the second exposure.

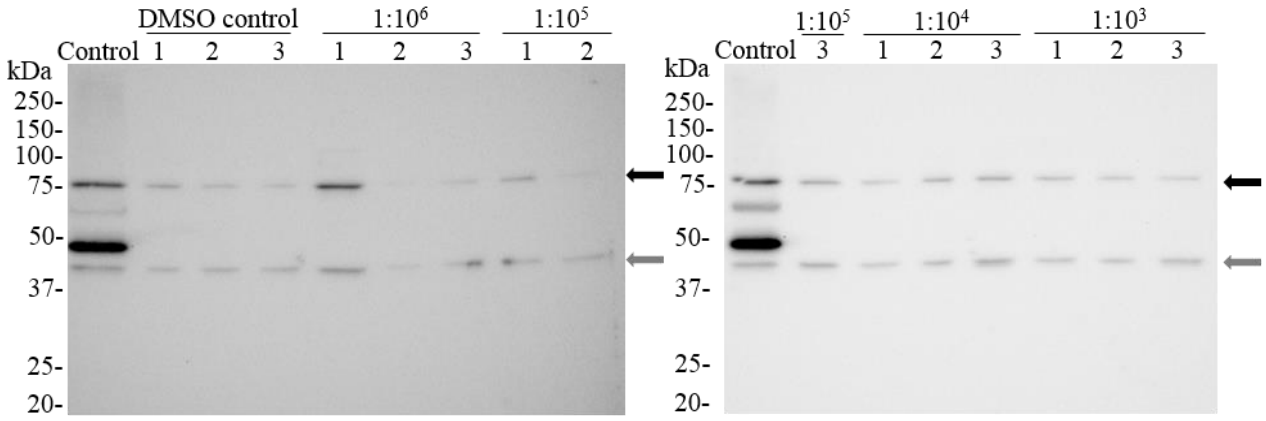

Figure 4-22: Immunochemical detection of P450scc (CYP11A1) and β-actin loading control in unstimulated Y1 cells exposed to the mixture. Mitochondria fraction of one cell sample for each exposure (1st, 2nd and 3rd repeated exposure, respectively) transferred to PVDF membranes. Left to right is the lowest dose to the highest dose tested on the Y1 cells ($1:10^6$, $1:10^5$, $1:10^4$ and $1:10^3$). Antibody control is a mixture of forskolin induced H295R and Y1 whole cell lysates. Membranes were first incubated with rabbit polyclonal anti-CYP11A1 IgG primary antibody (1:1000) and detected with a goat anti-rabbit IgG HRP-conjugated secondary antibody (1:2000). Then the membranes were incubated with a mouse monoclonal anti-beta actin IgG primary antibody (1:1000) and detected with a sheep anti-mouse HRP-conjugated secondary antibody (1:10000). Black arrow is CYP11A1, grey is β-actin.

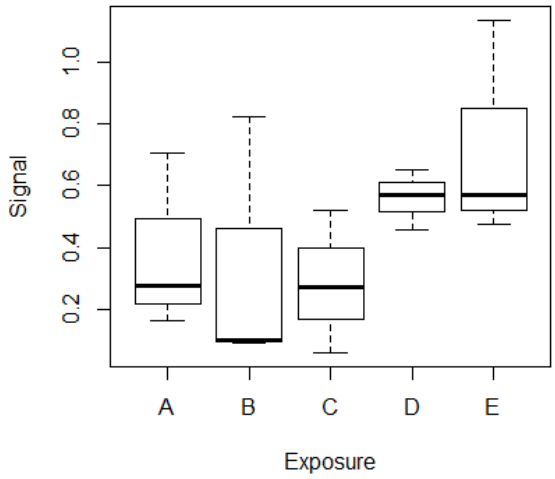

Figure 4-23: Band intensity for CYP11A1 in unstimulated Y1 cells exposed to the mixture, all doses included. Band intensities were measured in ImageJ and signals were adjusted against beta actin.

4.5.1.2 Steroid profiling for effects in metabolites

For the unstimulated cells, only two metabolites where possible to quantify. Those were the two precursors, pregnenolone and progesterone (Fig. 4-26). The levels of progesterone in unstimulated cells were lower than that in stimulated cells (2.89 nM vs 148.09 nM). Moreover, the levels of pregnenolone and progesterone increased above the lowest detection limit at the highest concentration of contaminants used (Appendix C), indicating that some environmental toxicant in the mixture stimulated steroidogenesis.

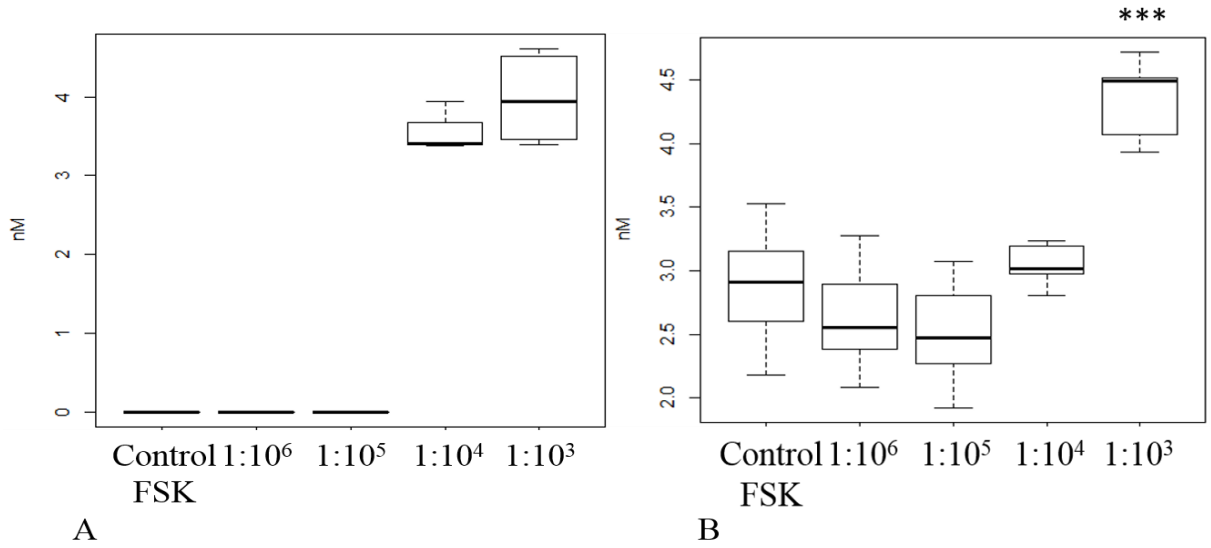

Figure 4-24: Measured levels of pregnenolone and progesterone in medium. There was detectable levels of A) pregnenolone in cells exposed to the two highest doses however. There is a significant increase in B) progesterone in cells exposed to the highest dose, $p < 0{,}001$.

4.5.2 Effects in forskolin-stimulated cells

The effects of the mixture in unstimulated cells were measured in three exposure experiments as described in chapter 3.5.2. Y1 cells were inspected for cell rounding upon forskolin stimulation before and after exposures (Fig.4-25).

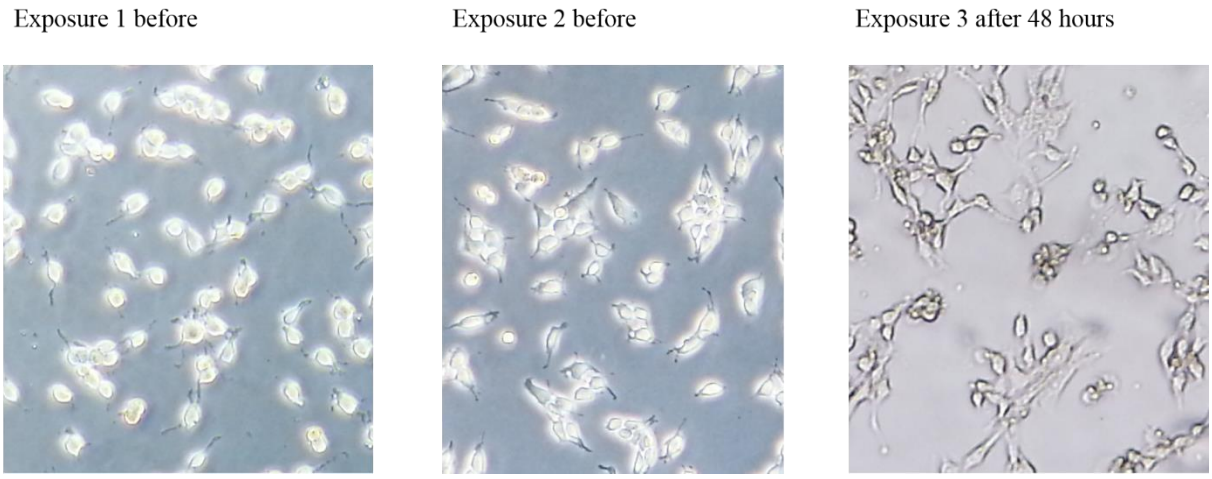

Figure 4-25: Y1 cells stimulated with forskolin for exposure experiments. First picture is the first exposure before adding the mixture. Second picture is the second exposure before adding the mixture. Thrid picture is Y1 cells after mixture exposures for 48 hours. 10x zoom. Picture by Silje Kathrine Larsen.

4.5.2.1 Immunological detection for effects on steroidogenic enzymes

Cell samples for Western blot and parallel SDS-PAGE were prepared according to chapter 3.10 and Western blot were performed as described in chapter 3.11.2.

From the parallel gels (Fig. 4-26) there seems to have been loaded less proteins from the $1{:}10^6$ and $1{:}10^5$ samples both from the second exposure. The same protein amounts were loaded on the gels used for Western blot and immunological detection. However, the membranes were incubated with anti-beta actin as a loading control, and were used for normalization of signal detection of CYP11A1 and CYP19.

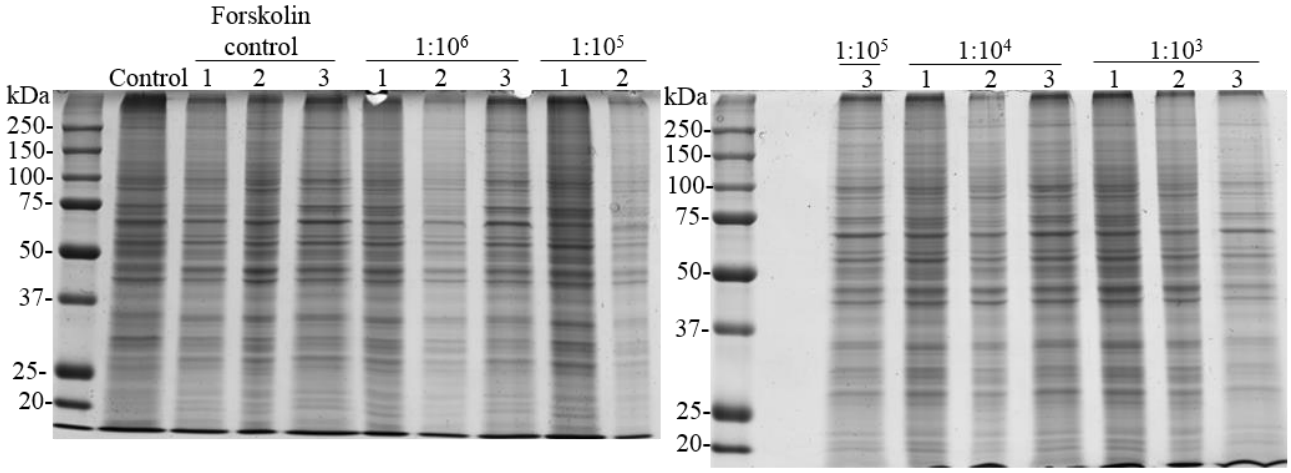

Figure 4-26: Parallel SDS-PAGE gels of stimulated Y1 cells exposed to the mixture. Mitochondria fraction of one cell sample for each exposure (1st, 2nd and 3rd repeated exposure, respectively) transferred to PVDF membranes. Left to right is the lowest dose to the highest dose tested on the Y1 cells ($1:10^6$, $1:10^5$, $1:10^4$ and $1:10^3$). Antibody control is a mixture of forskolin induced H295R and Y1 whole cell lysates, and only added to the first parallel SDS-PAGE gel due to restricted amounts of control. Gel stained with colloidal coomassie for protein visualisation.

Based on the parallel gels (Fig. 4-26) there seems to be the same amount loaded on both gels of almost every sample. Detection of β-actin (Fig. 4-27) however showed more protein loaded on the second membrane containing samples exposed to the higher doses ($1:10^4$ and $1:10^3$).

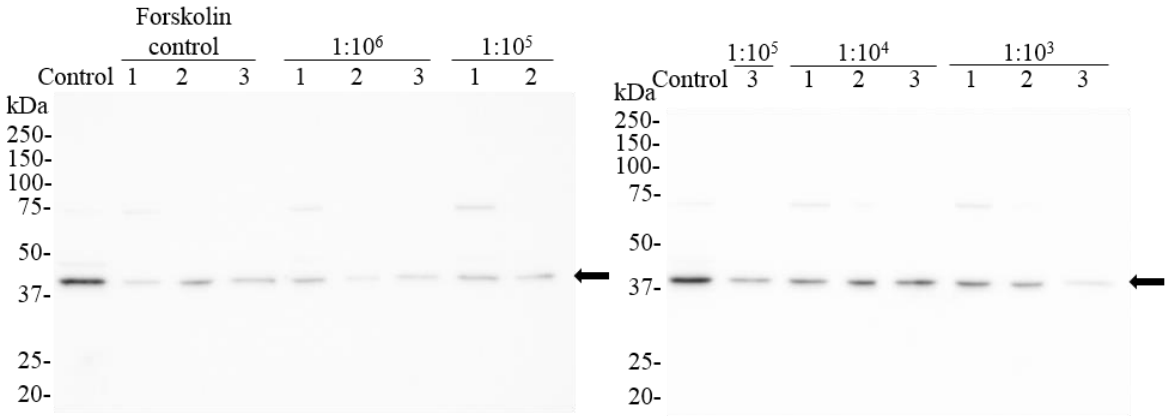

Figure 4-27: Immunochemical detection of β-actin loading control in stimulated Y1 cells exposed to the mixture. Mitochondria fraction of one cell sample for each exposure (1st, 2nd and 3rd repeated exposure, respectively) run on a 10 % gel. Antibody control is a mixture of forskolin induced H295R and Y1 whole cell lysates. Membrane was incubated with mouse monoclonal anti-beta actin IgG primary antibody (1:1000) and detected with a sheep anti-mouse HRP-conjugated secondary antibody (1:10000). Chemiluminescence was detected with a 1:1 mixture of SuperSignal® West Femto Maximum Sensitivity Substrate and SuperSignal® West Pico Chemiluminescent Substrate.

CYP19 was detected in the Y1/H295R-control sample, but not in Y1 cells stimulated by forskolin, nor in forskolin-stimulated cells co-exposed with contaminant mixtures at different concentrations (Fig. 4-28). The signal however was quite strong in the antibody control, so signal on the exposures and forskolin control might have been undetected due to saturation.

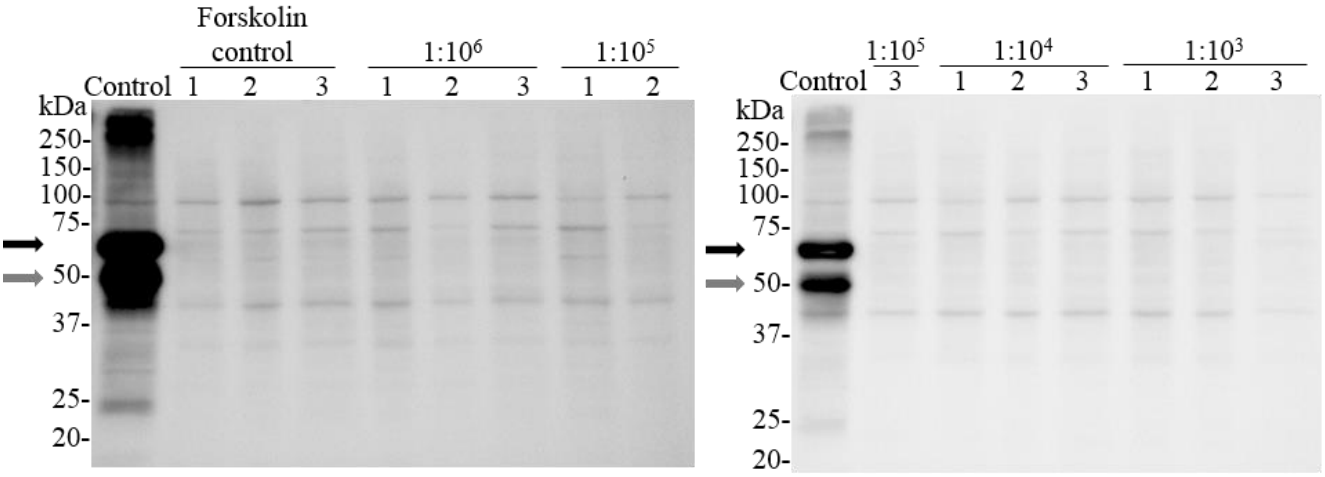

Figure 4-28: Immunochemical detection of P450arom (CYP19 aromatase) in stimulated Y1 cells exposed to the mixture. Mitochondria fraction of one cell sample for each exposure (1st, 2nd and 3rd repeated exposure, respectively) transferred to PVDF membranes. Antibody control is a mixture of forskolin induced H295R and Y1 whole cell lysates. Membranes were incubated with rabbit polyclonal anti-CYP19 IgG primary antibody (1:1000) and detected with a goat anti-rabbit IgG HRP-conjugated secondary antibody (1:2000).

Since CYP19 and CYP11A1 differ in size, the membranes were incubated with anti-CYP11A1 without stripping to remove anti-CYP19. In cells from experiment 1 and 2, CYP11A1 (appr. 75 kDa) was detected in forskolin-stimulated Y1 cells and in stimulated cells exposed to various concentrations of contaminant mixtures (Fig. 4-29). The signal intensity for exposure 1 was calculated in Figure 4-30. Because only samples from the first exposure were used analysing signal intensity, difference in signal could not be analysed for statistical significance.

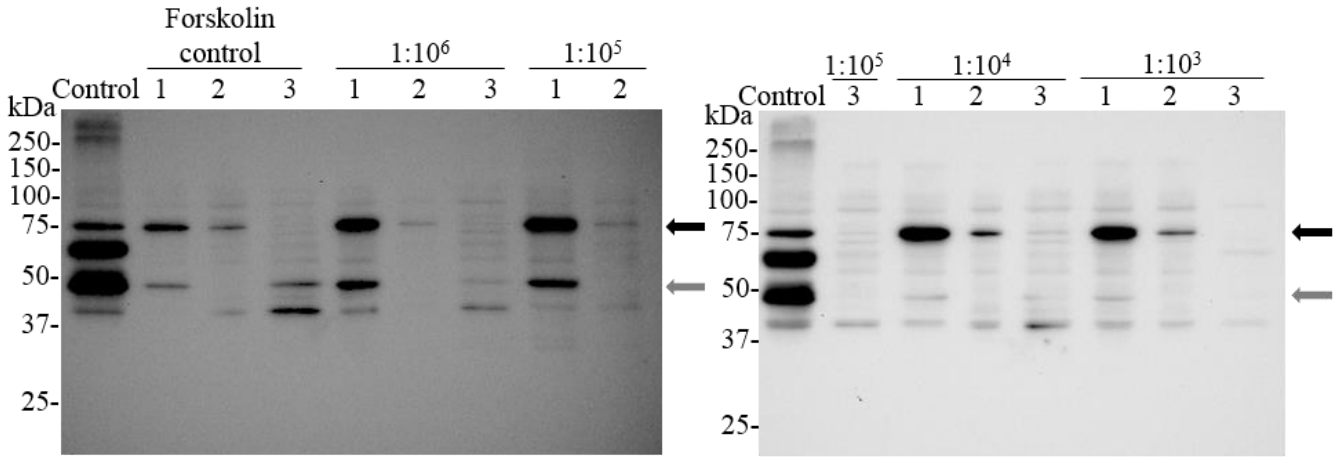

Figure 4-29: Immunochemical detection of P450scc (CYP11A1) in stimulated Y1 cells exposed to the mixture. Mitochondria fraction of one cell sample for each exposure (1st, 2nd and 3rd repeated exposure, respectively) transferred to PVDF membranes. Antibody control is a mixture of forskolin induced H295R and Y1 whole cell lysates. Membranes were incubated with rabbit polyclonal anti-CYP11A1 IgG primary antibody (1:1000) and detected with a goat anti-rabbit IgG HRP-conjugated secondary antibody (1:2000). Black arrow is CYP11A1, grey arrow is the lower band of CYP19 which seems to become detectable.

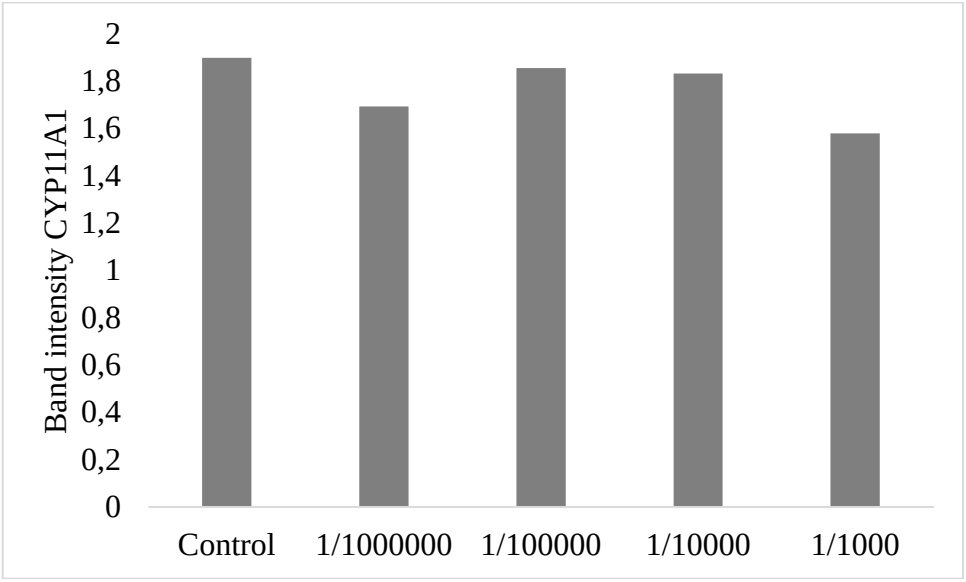

Figure 4-30: Relative quantification of CYP11A1 in Y1 cells. Band intensity of CYP11A1 in exposure 1 was measured with ImageJ and signals were adjusted against beta actin.

After incubation with CYP11A1, visible bands for CYP19 were still detectable on the blot (Figure 4-23, grey arrow) and band for CYP19 appeared in control samples and exposure samples. This might be due to more washing, making the anti-CYP19 binding more visible. As seen for CYP11A1, there were also some difference in band intensity between exposure 1, 2 and 3 for CYP19. The strongest bands are the ones from exposure 1, at least in the membrane

with the controls. The band intensity was calculated based on the lower band at approximately 50 kDa, since the band at approx. 65 kDa that had previously been detected in Y1 cells could not be detected on the blots in Figure 4-29. Because only samples from the first exposure were used analysing signal intensity, difference in signal could not be analysed for statistical significance (Fig.4-31).

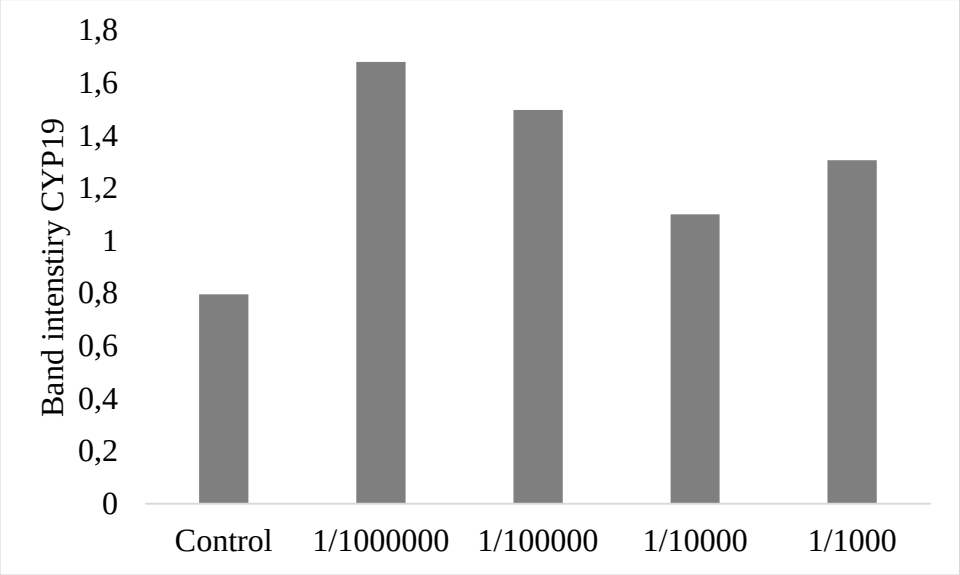

Figure 4- 31: Relative quantification of CYP19 in exposure 1. Band intensity of CYP19 in exposure 1 was measured with ImageJ and signals were adjusted against beta actin.

Based on the difference in band intensity between the exposures (1, 2 and 3) it might indicate that the forskolin stimulation has been more successful in the first exposure, and something might have gone wrong with exposure 2 and 3.

4.5.2.2 Steroid profiling for effects in metabolites

The difference sin enzyme levels between the three independent experiments indicated that steroid production was induced to various degrees. Steroid profiling also showed difference between experiments; with stimulated cells in exposure 2 that showed no stimulation, data from exposure 3 show an irregular pattern and data from experiment 1 giving the most reliable results. Based on this, only the data from exposure 1 will be presented. The results from steroid profiling shows that cells exposed to the highest dose of the environmental pollutants increased steroid production. Five of eight steroids measured in media had significant increase in levels compared to forskolin controls.

In the Y1 cells, levels of progesterone was the highest measured metabolite followed by 20α-dihydroxyprogesterone (20αOHP), pregnenolone and corticosterone (Fig. 4-32). This matched the basal steroid profile at 48 hours (chapter 4.3.2). All metabolites had elevated concentration levels in cells exposed to the highest mixture dose ($1:10^3$).

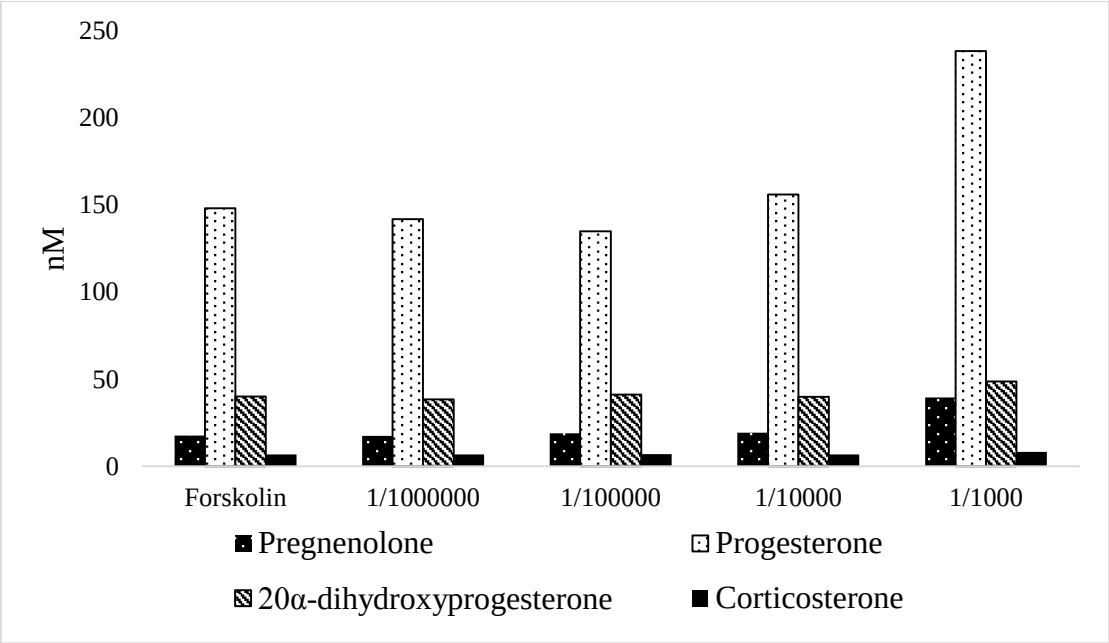

Figure 4-32: Overview of main steroids produced in Y1 cells after 48 hour exposure.

In Y1 cells exposed to the highest exposure dose of the mixture ($1:10^3$), the production of all four metabolites were significantly increased compared to the control (Fig. 4-33). Levels of progesterone was increased by 60 % compared to forskolin controls. The levels of 20α-dihydroxyprogesterone was increased by 20 %. Pregnenolone levels had the highest increase in production with a 122 % elevated levels compared to the controls. The corticosterone levels was increased by 30 %. There was no significant effects in cells exposed to the other doses.

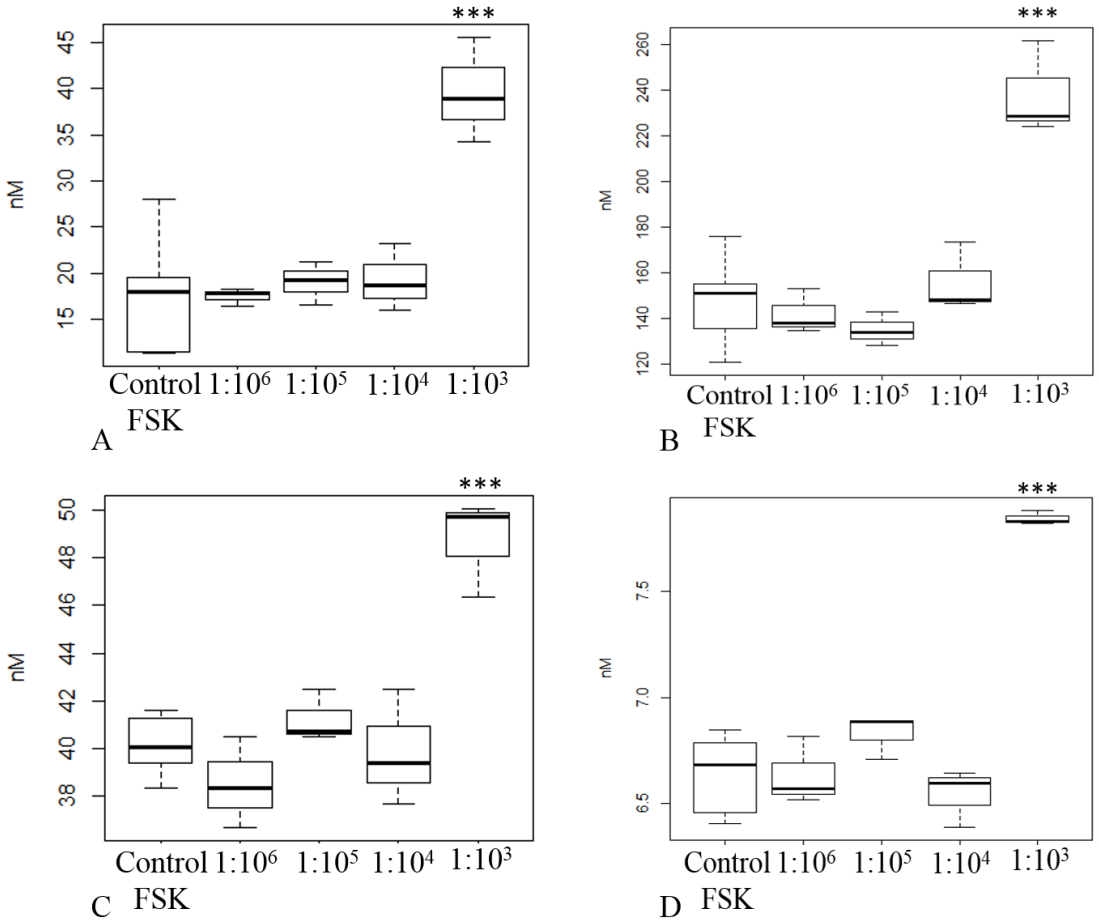

Figure 4-33: Levels of main steroids produced in zona fasciculata in medium of stimulated Y1 cells exposed to the mixture for 48 hours. Control is cells only treated with forskolin (FSK). Pregnenolone A) had significant increased production in the highest dose, $p < 0.001$. Progesterone B) had significant increased production in the highest dose, $p < 0.001$. 20α-dihydroxyprogesterone (20αOHP) C) had significant increased production in the highest dose, $p < 0.01$. Corticosterone D) had significant increased production in the highest dose, $p < 0.001$.

For the androgens measured in the Y1 cells, androstenedione was the highest measured metabolite followed by estradiol, estrone and testosterone (Fig. 4-34). This also matched the basal steroid profile at 48 hours (chapter 4.5.2). Levels of androgens and estrogens appeared to be independent of exposure concentration.

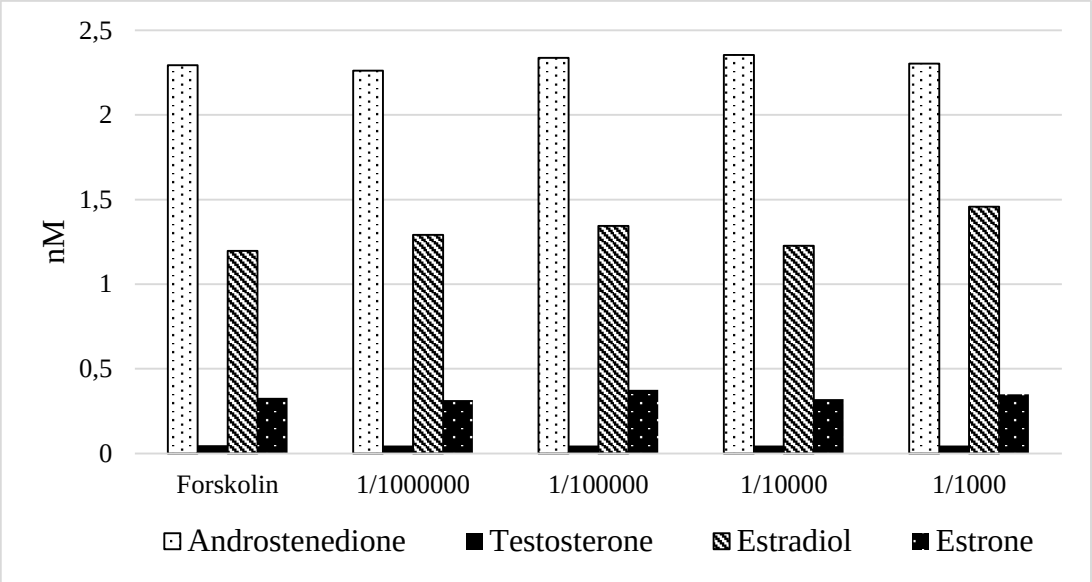

Figure 4-34: Overview of androgens and estrogens in Y1 cells in exposure 1 after 48 hour exposure.

Among the androgens and estrogens, only estradiol levels were significantly increased in cells exposed to the highest dose (Fig. 4-35). Levels of estratiol increased by 21 % compared to the controls. There was no significant effects in cells exposed to the other doses.

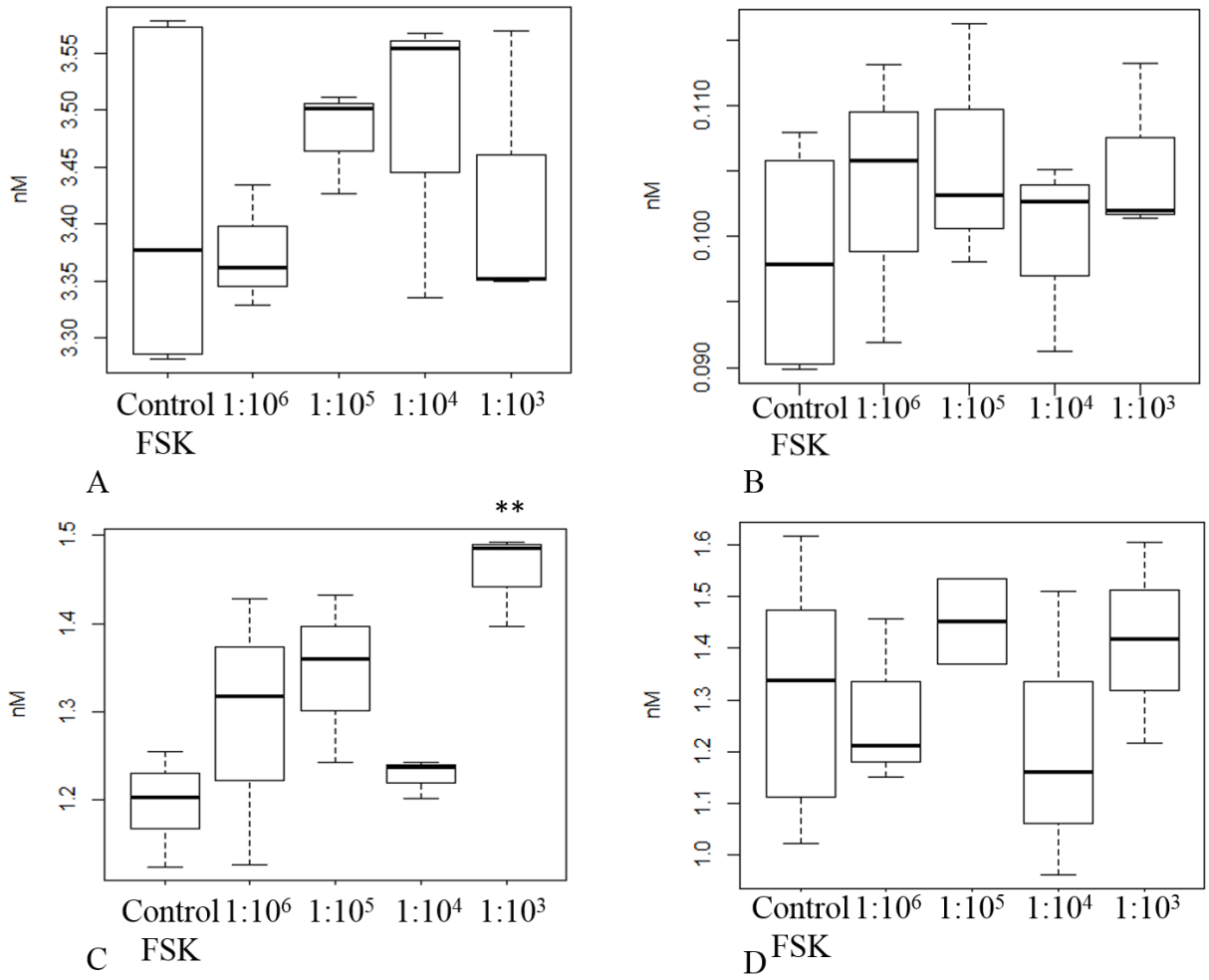

Figure 4-35: Levels of main steroids produced in zona reticularis in medium of stimulated Y1 cells exposed to the mixture for 48 hours. A: Androstenedione, there are no significant difference between the exposures and control. B: Testosterone, there are no significant difference between the exposures and control. C: Estradiol, significant increase in the highest dose, $p < 0.01$. D: Estrone, there are no significant difference between the exposures and control.

4.6 Pilot experiments on 2D-electrophoresis for Y1 cells

2D-electrophoresis was originally chosen as a method for separating and analyse how all proteins in the cells would respond when exposed to contaminants, and not only the specific steroids involved in steroidogenesis. 2D-electrophoresis was performed as described in chapter 3.12. The 2D electrophoresis was successful with good separation of proteins in the Y1 cells (Fig. 4-36). Due to time limitations, this method was not used further in this thesis for analysis of exposed samples.

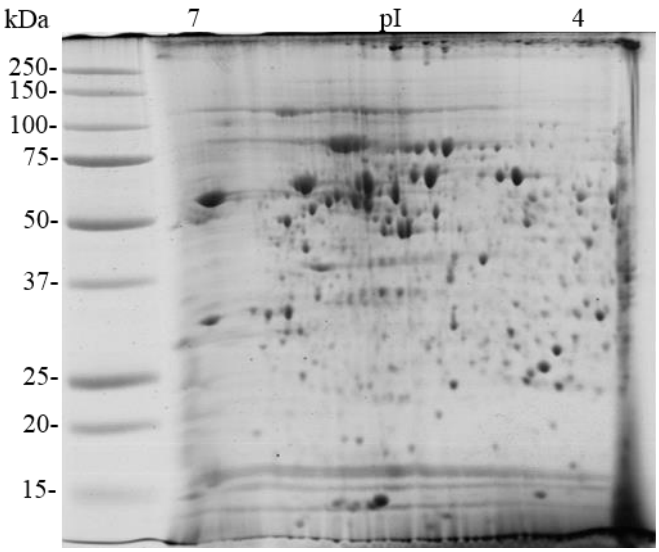

Figure 4-36: 2D electrophoresis of an untreated Y1 pilot sample. Whole cell sample of Y1 lysed in 2D homogenisation buffer, and rehydrated onto a 7 cm IPG strip pH 4-7. 12.5% gel stained with colloidal coomassie for protein visualisation.

5. DISCUSSION

The Y1 adrenocortical cell line is widely used for studying the pathways regulated by ACTH (Rocha et al., 2003) as Y1 remains responsive to ACTH. Because of this, many studies involving Y1 cells mostly focus on the effect of ACTH on gene expression (Schimmer et al., 2006), cell cycle control (Rocha et al., 2003), cell proliferation (Mattos et al., 2005) and various diseases linked to abnormal adrenal gland functions. There are also studies using Y1 to investigate the effects of drugs on steroid production (Brion et al., 2011). The cell line is an important model to characterise regulation of gene expression in the adrenal cortex because of the cell lines amenability to transfection with exogenous DNA (Rainey et al., 2004).

In this thesis, the aim was to study how a mixture of POPs would influence the steroid production in Y1 adrenocortical cells in a dose-response manner. Effects were detected in both unstimulated and forskolin stimulated cells exposed to the highest dose. The concentration of progesterone and pregnenolone were elevated in unstimulated cells, whilst most of the steroids were elevated in stimulated cells. The combination of the effects seen in both cell conditions may indicate that the POPs mixture has an inductive effect on Y1 cell steroidogenesis which may be additive or synergetic in cells stimulated with forskolin.

5.1 The effects of the mixture in unstimulated cells

Results from steroid profiling on exposure of unstimulated cells showed that levels of pregnenolone were increased when exposed to the two highest doses, and progesterone increased significantly when exposed to the highest dose. Event though concentrations increased, the levels were lower than what is produced in normal stimulated cells. This indicates that the mixture can induce pregnenolone and progesterone synthesis. However, there was no significant difference in the production of CYP11A1.

Similar induction of steroidogeneis have been found in unstimulated H295R adrenocortical cells exposed to other mixtures of POPs. Montaño et al. (2011) extracted POPs from crude cod liver oil, commercial oil and industrial waste where PCBs was the main component, followed by DDTs. Mixtures from crude cod liver oil and industrial waste containing high concentration of POPs induced production of progesterone, cortisol, estradiol and testosterone. Only estradiol levels were induced by incubation with the commercial oil, which was the oil containing low levels of POPs. All mixtures however induced gene expression of enzymes (CYP11B1,

CYP11B2) and the adrenocortical receptor (*M2CR*). The authors concluded that PCBs in the mixture were associated with the induction of steroidogenesis.

Compared to the results in this thesis, there was no detection of steroids produced later in the steroidogenic pathway (estradiol, corticosterone) in unstimulated Y1. This might be due to the doses used in the Y1 cells contained very low concentrations of PCBs compared to the high doses from cod liver oil and industrial waste that increased steroid production in the H295R cells (Montaño et al., 2011). This may indicate that high levels of PCBs in a mixture can induce steroid production more significantly. Nevertheless, there was increased metabolic activity in the H295R cells that was exposed to the commercial oil with low levels of PCBs and HCB. It is therefore likely that the metabolic activity in Y1 cells have increased as well, since the mixture induces pregnenolone and progesterone.

The results from the cell viability test further support this hypothesis. The mixture did not cause apoptosis in the cells, however the cell activity was increased in cells exposed to the mixtures, and for stimulated cells the raised activity were significant. Another consideration is the difference in mixture compositions. The mixtures used by Montaño et al. (2011) did not contain perfluorinated compounds, which is the main component in the mixture used on Y1. Therefore, induction of pregnenolone and progesterone production in Y1 cells might be a combination of perfluorinated compounds and PCBs in the mixture.

Increased steroid production has also been reported in H295R cells exposed to two mixtures of POPs from two polluted lakes by Zimmer et al. (2011). These mixtures contained similar POPs used in this thesis (HCB, HCHs, chlordanes, DDTs, PCBs, BDEs and HBCD). The results showed increased production of cortisol and estradiol and reduction on testosterone levels in H295R. The study also revealed upregulation of *CYP11B1*, *CYP11B2* and *CYP19A1* genes. The *MC2R* gene that encodes the ACTH receptor was upregulated even though the cells were not ACTH stimulated before exposures. The steroid responses overall was thought to be caused by PCBs and DDT in the mixture.

5.2 The effects of the mixture in forskolin stimulated cells

Even though the effects of the mixture on unstimulated cells might be minimal, more effects was observed on stimulated cells exposed to environmental pollutants. The effects observed in stimulated Y1 cells are more similar to the effects seen in unstimulated H295R cells (Montaño et al., 2011; Zimmer et al., 2011). Five of eight steroids measured in media had significant increase in levels compared to forskolin controls. The steroid profile does not seem to have been inhibited by the pollutants in the mixture, as the measured amounts of steroids in exposed cells were similar to those measured in the timeline experiment. The levels of pregnenolone, progesterone, 20α-dihydroxyprogesterone and corticosterone and estradiol were significantly increased.

Increased levels of estradiol in Y1 cells was found to be the only steroid with increased levels in H295R cells exposed to a mixture with low concentration of POPs (Montaño et al., 2011). Since basal levels of estradiol in H295R cells is low, estradiol was argued to be a sensitive endpoint for induction. Estradiol has also been found to slightly increase H295R cell proliferation (Jaroenporn et al., 2008), which may explain why there was a slight increase in metabolic activity (Montaño et al., 2011). Since the basal levels of estradiol in forskolin stimulated Y1 is low, the effects of estradiol may be the same in Y1 as in H295R even though estradiol was not induced in unstimulated Y1 cells. This increased that might explain why estradiol was the only estrogen with increased levels in stimulated cells.

Induction of estradiol might be due to HCB in the mixture. This was the compound that was thought to contribute to induction of estradiol levels (Zimmer et al., 2011) when administered in lower concentrations than PCBs and DDTs in H295R cells, showing that observed effects are caused not only by the compounds with the highest concentrations.

There are some studies on Y1 testing single compound and effects on steroidogeneis. Studies have been performed with forskolin stimulated Y1 cells to investigate CYP11B1 and corticosterone inhibition by single compounds with and without a methyl sulfone group (-$MeSo_2$). A study by Johansson et al. (1998) showed that p,p`-DDE, PCB 118 and PCB 153 did not affect corticosterone synthesis, but $MeSo_2$-PCBs and $MeSo_2$-DDEs inhibited CYP11B1 in Y1 cells. It was concluded that the methyl sulfone group was needed for inhibition of CYP11B1. Further studies of single compounds 3-$MeSO_2$-DDE and o,p'-DDD added to forskolin induced Y1 cells showed to bind irreversibly on cells. It was suggested that forskolin is able to activate these pollutants via CYP11B1 (Hermansson et al., 2007). Since the mixture

in this thesis contains p,p`-DDE and some of the PCBs tested, these studies have shown that these compounds does not inhibit or affect steroidogenesis when tested in single doses in Y1 cells. The pesticide p,p`-DDE have also been found not to affect steroidogenesis in the H295R cell line as well (Sanderson et al., 2002).

Testing of single compounds in the H295R cell line has also resulted in increases in steroid production. Xu et al. (2006) tested single doses of four different PCBs (PCB 101, 110, 126 and 149) on H295R cells, where all PCBs tested resulted in upregulation of steroidogenic enzymes with exception of CYP11A1 and CYP17. CYP17 is however not present in Y1 cells for comparison. Upregulation of steroidogenic enzymes were also observed when testing single polybrominated diphenyl esters (PBDEs) in H295R cells, where 5-OH-BDE-47 was found to induce CYP19 (He et al., 2008). PBDEs did not seem to effect the regulation of CYP11A1 (Song et al., 2008).

Upregulation of steroids was also detected on H295R cells exposed to PCB 118, 153 and 126 (Kraugerud et al., 2010). Focusing on PCBs that are in the mixture, PCB 118 increased levels of estradiol, progesterone, cortisol (human glucocorticoid) and aldosterone, while PCB 153 increased levels of estradiol and aldosterone but downregulated testosterone. In this study, the levels of testosterone were not significantly changed. Studies have found that some compounds are inhibitors of CYP19. One study showed that perfluorinated compounds (PFOS, PFOA and PFBS) were aromatase inhibitors in the human placental choriocarcinoma JEG-3 cell line (Gorrochategui et al., 2014). This is a different result than what have been observed in this thesis where CYP19 activity seems to have been raised in stimulated cells. There is no detection of CYP19 in the unstimulated Y1 cells in both control and exposures, so if perfluorinated compounds in the mixture have inhibited CYP19 is uncertain.

There are groups of POPs where the effect on steroidogenesis are not fully understood or lack in published data. There is little data on effects by chlordanes, and in vitro effects of HCB have not been studied (Zimmer et al., 2011). Testing chlordanes on the human placental choriocarcinoma JEG-3 cell line showed to induce CYP19 in the cells (Laville et al., 2006).

Data suggests that there might not be a correlation between low dose administration of a mixture and low dose exposure of a single compound. Administration of single compounds may not have an adverse effect in a system, but adverse effects are detected after low dose exposure to mixtures and vice versa (Fisher, 2004). The doses administered to Y1 in this thesis are low, and effects are observed in both unstimulated and stimulated cells. When testing different mixtures

i*n vitro*, even though there is similarities in the composition of POPs, small differences in concentration or components in the mixture may change the effects observed (Zimmer et al., 2011). The levels of perfluorinated compounds used in this mixture might be causing induction of pregnenolone and progesterone in unstimulated Y1 cells in the highest dose. Testing groups of perfluorinated compounds would be of interest in further testing to understand how the PFCs might affect steroidogenesis, both alone and in combination with PCBs.

The results in this thesis show upregulation of steroidogenesis when administered with the highest dose and no evident sign of enzyme inhibition. These findings correspond with previous findings when testing single compounds of PCBs, chlordanes and DDE on enzyme gene expression or steroid production in the H295R cell line, as well of mixtures of similar POPs. Even though the results correspond with studies done on single compounds and mixtures, there might be other factors that are responsible for upregulation of steroidogenesis in Y1 that cannot be explained by individual chemical properties.

It is important to note that the results from steroid profiling are based on three replicates from one exposure on stimulated cells. Detection of CYP11A1 in the first exposure showed a slight decrease in the highest dose and the lowest dose, and detection of CYP19 showed that there are upregulated levels of CYP19 in all the exposed cells compared to the control. Statistical significance could not be calculated since only cell samples from one exposure could be used for semi-quantification. Steroid profiling and western blots will have to be repeated to confirm the findings from the first exposure.

5.3 Choice of exposure doses

An interesting aspect of the levels of toxicants is what concentrations an effect can be observed, meaning the dose-response curve for this mixture of POPs on Y1 cells. There is a gap between the highest dose and the second highest dose, from no effect to a significant effect. Thus, it cannot be determined if the highest dose of the POPs tested is a possible threshold for increase in steroidogenesis. Based on not finding any significant difference between the control and the three other lower doses, adjusting to higher doses to see where effects are observed might be a suggestion for further determining the toxicity of the mixture.

5.4 Basal steroid production in stimulated Y1 cells

In the steroidogenic pathway, the rate limiting step is the conversion of cholesterol into pregnenolone. Pregnenolone was detected in media eight hours after stimulation with forskolin. Pregnenolone is the precursor of progesterone, and progesterone was measured in cells at all time points. It is likely that pregnenolone was not detectable shortly after induction as most were used to synthesize progesterone. As the concentration of pregnenolone increases, more progesterone build up in the cell. The highest measured steroid was progesterone, which is the most abundant steroid in the Y1 cells (Brion et al., 2011).

Increased levels of progesterone have also been shown in clones of ST5-L mouse cells induced with cAMP for 24 hours in culture media. The production varied depending on the clone type: 1) basal high progesterone production which was minimally stimulated by cAMP, 2) low basal production of progesterone which increased 5-fold with cAMP stimulation, and 3) both basal and cAMP had minimal progesterone secretion (Compagnone et al., 1997). The results in this thesis correspond with what was observed in pattern 2, with low basal production that increased up to 24 hours.

CYP11A1 was present in all timeline cells, and signal increased slightly over time. However, since samples from three replicates were pooled together, the results cannot be tested for statistical significance. The strongest signal was at 24 hours, which is the time when pregnenolone concentration was highest in the cells. This might indicate that the best time to measure CYP11A1 and pregnenolone activity is between 12 and 24 hours.

5.4.1 Steroids produced in the zona fasciculata

After 24 hours, the concentration of the end products increased in the cells, and the concentration of pregnenolone and progesterone decreased as more is being used to synthesise end products. As expected, 20α-dihydroxyprogesterone was more abundant in the Y1 cells than corticosterone. This suggests that the best time point to measure end products is after 24 hours.

As is reported previously using in rat adrenal cells, CYP11B1 is not expressed in rat zona glomerulosa cells, but is expressed in zona fasciculata cells (Mukai et al., 1995). This supports why CYP11B2 was not detected in the Y1 cells, as Y1 cells mainly contains cells from zona fasciculata (Rainey et al., 2004). Also CYP11B1 is highly expressed in Y1 cells (Domalik et al., 1991), suggesting that corticosterone is synthesised by CYP11B1 via deoxycorticosterone.

The cells are producing corticosterone in stimulation with forskolin (Johansson et al., 1998), so cells should be tested for CYP11B1 signal in western blot. Since the have been no testing with CYP11B1 antibody in this thesis, the effect the mixture might have on CYP11B1 expression is unknown.

A question that arises from this thesis is how corticosterone is synthesised from deoxycorticosterone when normal Y1 cells have a deficiency in the CYP21 enzyme (Parker et al., 1985). CYP21 is the enzyme that converts progesterone to deoxycorticosterone in mice (Fig. 1-5). The same lack in CYP21 expression found in Y1 cells was found in a study by Mellon et al. (1994) to make new adrenocortical cell lines (ST5R and ST5L) from two transgenic female mice. Progesterone and deoxycorticosterone were detected, but there was no measurement of CYP21 mRNA. Further work by Compagnone et al. (1997) confirmed that ST5L clones produced progesterone and corticosterone and expressed CYP11A1 and CYP11B1, but no CYP21 was detected. The authors proposed a hypothesis that an unidentified enzyme converts deoxycorticosteone to corticosterone.

5.4.2 Steroids produced in the zona reticularis

Interestingly, there were low levels of androstenedione and testosterone detectable in cells at all time points. Estradiol is metabolised from testosterone via CYP19, and levels of estradiol were detectable and increasing even though testosterone levels were constant. CYP19 was detected in western blots 12 hours after forskolin stimulation. This corresponds with the late synthesis of estrone and estradiol, which is metabolised from androstenedione and testosterone via CYP19. Some enzymes are being synthesized from target genes when cells are being stimulated with a steroid inducing compound (Introduction Fig 1-3). This delays conversion of the androgens into estrogens. These results suggest that effects on sex steroids in Y1 cells is best investigated after exposure for minimum 12 hours.

5.4.3 Deciding length of exposure to POPs depends on steroids of interest

How long to expose cells to the mixture seems to depend on the steroids of interest. Effects on early metabolites might be better studied after maximum 24 hours exposure when the activity is highest. Effects on late metabolites like corticosterone and sex steroids might be better studied after 48 hours exposure. However, there seems to be an intermediate at 24 hours, where there is a shift in expression of early and late steroids. However, results form timeline

lasting 72 hours showed that levels of pregnenolone and progesterone was highest after 30 hours (Appendix B). This might be taken into consideration for future exposures.

The length of exposure was decided based on results from LC-MS/MS method on the first timeline. This reading was done before calibrators and internal standards were made for measuring steroids in adrenocortical cells, so these results were semi-quantitative. The first run of a timeline showed a continuous increase in end products after 48 hours, as well as pregnenolone. Progesterone was higher at 24 hours and levels went down after 48 hours. A 48 hour exposure was chosen based on the increasing levels of end products.

However, the results from the exposures on forskolin stimulated cells showed that the levels of pregnenolone and progesterone were the most upregulated, with increased production of 122 % and 60 %. These two steroids were the only elevated metabolites in exposed unstimulated cells. Taking both cell conditions and the common effects into consideration, the impact of the mixture might be involved around the early stages of the steroidogenesis. Therefore, it might be interesting to test shorter exposure times more suitable for detecting pregnenolone and progesterone in media and enzymes and factors involved early in the steroidogenic pathway (CYP11A1, StAR).

5.5 Evaluation of steroid profiling

The LC-MS/MS method used in this thesis is newly established at the Hormone Laboratory of Haukeland University Hospital (unpublished), based on LC-MS/MS previously established for measuring glucocorticoids and androgens in human serum (Methlie et al., 2013). This method was stablished for studying multiple steroids found in the H295R steroidogenic pathway, which is a cell line secreting steroids similar to the profile in humans than the Y1 cell line. Since this method is based on the H295R steroid profile, this method proved to be a powerful tool to measure steroids also in Y1 cells. Not all steroidogenic metabolites could be measured however, as there are some steroids not produced in H295R cells (*e.g.* 20α-dihydroxypregnenolone) which have not been included in the calibrators as of yet (Appendix C). The standards have not been fully adjusted for errors when preparing calibrators (*e.g.* pipetting), meaning that the measured concentrations might deviate until the standards are fully calibrated.

5.6 Evaluation of Western blots

The band size in for CYP11A1 in the western blots gave signal at approximately 75 kDa in a 10 % SDS-PAGE gel opposed to the theoretical value for 60 kDa for CYP11A1. However, during antibody testing signal for CYP11A1 have been observed at both 75 kDa and 50 kDa (Appendix B). The inconsistency of signal for CYP11A1 might be due to "gel shifting," which can be common for membrane bound proteins and the reasons are not fully understood. However, a mechanism behind might be proteins have not been fully denatured, and thusly binding to SDS is not complete. Binding to SDS is necessary in order to negatively charge the proteins which enables proteins to migrate through the SDS-PAGE gel (Rath et al., 2009).

The *Cyp19* gene in mice encodes for 503 amino acid residues (Terashima et al., 1991) and the CYP19 enzyme have a molecular mass of 57.8 kDa. In all western blots, there was two bands visible for CYP19. To my knowledge, there have not been published studies where detection of two CYP19 bands have previously been shown. However, in a product photo of a CYP19 antibody (LS-C312646) from LifeSpan Biosciences Inc. (Appendix D) shows two bands on a western blot from human placenta. Two CYP19 genes, cyp19a and cyp19b, have been detected in ovaries and brains in zebrafish, respectively (Chiang et al., 2001), but CYP19 is encoded by only one gene in both humans and mice. Since two bands are detected in both controls and exposed cells, it is unlikely that the bands could be explained by post-translational modification of CYP19 by the mixture. The unexpected detection of two CYP19 bands might be a subject for further studies.

There was a lot of background noise in the western blots for stimulated cells, which is probably due to the incubation with CYP19. The first image of CYP19 in stimulated cells had positive detection off two bands in antibody control, but the rest of the blot had no detectable signal of CYP19. This could be due to the signal being oversaturated. Detection of CYP19 was possible after washing and incubation with CYP11A1. Extra washing steps might have improved on the signal for CYP19 by washing away excess secondary antibody, making the signal visible on all the samples. This is had an effect in the antibody control, where signal became less saturated. However, only the lower CYP19 band was possible to distinguish on controls and exposed cells.

5.7 Evaluation of experimental setup

Results from timeline and exposures gave rise to evaluation of the exposure setup. There was also suggestions for how to improve the results or what other antibodies should be tested to investigate how the mixture affects steroidogenesis.

5.7.1 Fixed DMSO concentration in unstimulated cells

In the experiment for unstimulated cells, only the control cells were added 0.1 % DMSO in the media. When diluting the mixture to make the four doses to be used on unstimulated cells, DMSO was not added to the dilutions. This was a mistake discovered after all three replicates were completed. All doses should ideally have been added 0.1 % DMSO as was done with the control. By adding 0.1 % DMSO in both control and exposures, the only variable to explain possible deviations from the control would be the mixture. This was not an issue with stimulated cells. Forskolin at a fixed concentration of 0.1 % forskolin was added to all doses and control for stimulated cells.

5.7.2 Using forskolin to induce steroidogenesis

Upon forskolin stimulation the cell shape got the characteristic rounded cell shape, which is a well known response to forskolin (Whitehouse et al., 2002). The change in cell shape was observed on all cells stimulated with forskolin used for pilot samples, timeline and exposures (Appendix A). However, the combined results from western blots and LC-MS/MS turned out to be an important tool to determine if the cells indeed had been stimulated.

The results from steroids profiling initially showed that steroids were being produced in two of the repeated exposures, exposure 1 and 3. Exposure 3 had irregular pattern of steroid concentration, which were either lower or much higher than levels measured in exposure number one and timeline experiments. The second exposure, exposure 2, showed no indication of steroid production since levels were the same as found in untreated DMSO control cells. Based on steroid profiling, exposure 1 and 3 seemed to have been successful. However, results of the western blots gave indication of inefficient forskolin stimulation. Studying the forskolin induced controls on CYP11A1 detection (Fig.4-29), the signal was strong in the sample from exposure 1, weaker in exposure 2 and barely detectable in exposure 3 and the same trend are observed in the exposures. From immunodetection in exposed unstimulated cells (Fig. 4-22),

CYP11A1 is present in cells in a dormant state, which might explain that CYP11A1 are detected in exposure 2 and 3. Since there was correlation between the signal in the controls and exposures, it was likely that the results were due to the forskolin rather than an inhibition of steroidogenesis due to the mixture. Based on this, even though cells seem to have reacted to forskolin and steroidogenesis have started, this alone might not indicate that cells are producing steroids.

One cause of failed steroidogenesis might be a combination of human failure and too many thaw-freeze cycles of forskolin. The first exposure were stimulated with forskolin that had not been thawed previously, and the results seem to show that this exposure have been successful. Exposure 2 and 3, which were unsuccessful, the same vial of forskolin was used. Consequently, forskolin should be used fresh in order to prevent contamination and loss of properties.

5.7.2.1 Difference in using forskolin compared to ACTH

Differences between forskolin and ACTH have been described previously in Y1 cells stimulated to forskolin or ACTH (Schimmer et al., 1985). Steroid production were measured over a six hour period, and the production of steroids increased three-fold in response to either compound. Therefore, using forskolin instead of ACTH to stimulate Y1 cells does not seem to make a difference in steroid production in the cells. However, the steroid production were measured for six hours, which is shorter than the time line for 48 and 72 hours in this thesis.

As mentioned in chapter 5.1, elevated levels of the MC2R gene was measured in unstimulated H295R cells exposed to mixtures of POPs (Zimmer et al., 2011), a response that was thought to be related to PCBs in the tested mixtures. The authors argued that upregulation of the *MC2R* gene was not responsible for raise in hormone levels measured in the H295R cells, but might increase responsiveness to ACTH. One of the advantages in using Y1 is the intact ACTH receptor (same as MC2R). In the HPA axis in humans and rodents, ACTH is the main hormone that binds to the ACTH receptor in the cell surface (Tsigos et al., 2002). Therefore, using ACTH would be a more biologically accurate *in vitro* model to the steroidogenesis *in vivo,* and would be a way to investigate if the mixture acts like a ligand to the ACTH receptor. Since forskolin does not bind to the ACTH receptor, it is impossible to indicate if the increase in steroid production is due to binding to the ACTH receptor. Using ACTH would be interesting as a refinement to the experiment to see if some of the POPs binds to the ACTH receptor. However, there are reported Y1 mutants that are not responsive to ACTH (Schimmer et al., 1995) and the

current Y1 passage at ATCC is unresponsive to ACTH (Rainey et al., 2004), so steroid production should be tested before doing exposure experiments to ensure that Y1 cells react to ACTH stimulation.

5.7.3 Immunological detection of StAR

During antibody testing using fluorescence (Appendix B), StAR and CYP11A1 were not detected. A disadvantage of using fluorescence is that signal is dependent on amount of secondary antibody, and some proteins might require higher concentration of secondary antibody in order for a signal to be detected. Using chemiluminescence, which involves an enzymatic reaction for immunodetection, signal might be easier to detect by using sensitive substrates. This was the case with CYP11A1, as signal for CYP11A1 were observed with chemiluminescence. Unfortunately, signal for StAR was not possible to test with chemiluminescence, as a suitable HRP-secondary antibody was not available. However, considering that CYP11A1 was detectable using chemiluminescence, this method might be a good option for detection of StAR.

5.8 Conclusions

The production of pregnenolone and progesterone were upregulated in unstimulated cells exposed to the highest dose of the mixture of POPs. The production of CYP11A1 were slightly elevated, but there was no significant difference between the dose mixtures and the controls. CYP19 was not detected in neither control nor the dose mixtures, suggesting that the mixture did not induce CYP19 production. This was confirmed by not detecting the CYP19 metabolised estradiol and estrone in media. However, the due to the detection limit of the LC-MS/MS method the levels might be too low to measure in the current method. Previous studies have shown upregulation of genes involved in steroidogenesis encoding steroidogenic enzymes (*e.g.* CYP11A1 and CYP19) in H295R cells exposed to low dose mixture, but these upregulations were not detected in protein levels (Montaño et al., 2011). Therefore the effects on POPs in unstimulated cells might be of interest to investigate in further studies, especially regarding the composition of persistent organic pollutants in the mixture in regards to testing individual groups (*e.g.* perfluorinated compounds).

The production of most steroids measured in media were upregulated in forskolin-stimulated cells exposed to the highest dose of the mixture of POPs in one of three exposures measured.

The steroids that were upregulated included pregnenolone, progesterone, 20α-dihydroxyprogesterone, corticosterone and estradiol in all triplicates of one exposure. The production of CYP11A1 appeared unaffected, and signal for CYP19 in cells exposed to all mixture doses appeared to be elevated. Statistical analysis could not be performed for enzyme detection due to only one exposure being reliable for semi- quantitative analysis. Repetition of exposures will have to be conducted to confirm the effects of the mixture in stimulated cells. Nevertheless, the results indicated a synergetic or additive effect of the POPs mixture in forskolin-stimulated cells. These results are similar to studies on unstimulated H295R cells exposed to a higher concentrated mixture of POPs resulting in increased gene expression of steroidogenic enzymes and steroid production (Zimmer et al., 2011).

5.9 Future perspectives

A further step to investigate which compounds contribute to the increase of steroids would be to test the effects of individual pollutant groups. The most abundant group in the mixture, the perfluorinated compounds, would be of interest as there are lacking data of how they interfere with steroidogenic cells. Existing data of perfluorinated compounds shows evidence of enzyme inhibition, which is not found in this thesis. An important modification to the method would be to stimulate Y1 cells with ACTH to investigate how the POPs would compete with an ACTH receptor ligand. The mixture might also affect other cell components and enzymes unrelated to steroid synthesis, which have not been measured in this thesis. One suggestion for obtaining more information on mechanisms would be shorter exposures, in combaination with analyses of the proteome and the genome.

One way of investigating a wider effect on the proteome would be analysis with 2D electrophoresis, which would separate all proteins within the cells. Combined with gel analysis of up or downregulated protein proteins affected by the mixture can be identified by protein sequences. The 2D electrophoresis tested for use with Y1 cells in this thesis and is ready to be used for further analyses. A protein that could be interesting to investigate further is the CYP19 enzyme. The two protein bands could be analysed by MS/MS to see if there is a difference in sequence between the two bands, or whether or not CYP19 have been modified by phosphorylation. Studies are being performed using *in vivo* models exposed to mixtures and single compounds, as well as other *in vitro* models. Studying the wider physiological impact of POPs in relation to stress will be of high relevance in the future.

APPENDIX A

Table A 1: Levels of steroids measured in exposures on stimulated cells

	Pregnenolone	Progesterone	20α-OHP	Corticosterone	Androstenedione	Testosterone	Estradiol	Estrone
Control	17.75±6.14	148.09±18.68	40.12±1.21	6.89±0.18	2.29±0.10	0.05±0.003	1.20±0.05	0.33±0.02
$1/10^6$	17.49±0.97	141.86±9.75	38.51±1.92	6.89±0.16	2.26±0.06	0.05±0.004	1.29±0.15	0.31±0.03
$1/10^5$	19.03±2.35	134.87±7.39	41.24±1.09	7.12±0.10	2.34±0.05	0.05±0.003	1.35±0.10	0.38±0.04
$1/10^4$	19.26±3.64	155.98±15.10	39.86±2.42	6.87±0.14	2.35±0.07	0.05±0.003	1.23±0.02	0.32±0.02
$1/10^3$	39.55±5.69	238.19±20.49	48.72±2.06	8.24±0.03	2.30±0.08	0.05±0.004	1.46±0.05	0.35±0.02

Table A 2: Levels of steroids measured in exposures on unstimulated cells

	Pregnenolone	Progesterone
Control	0	2.89±0.37
$1/10^6$	0	2.63±0.39
$1/10^5$	0	2.53±0.38
$1/10^4$	3.58±0.32	3.05±0.15
$1/10^3$	3.98±0.58	4.35±0.29

Table A 3: Levels of steroids measured in timeline from 48 and 72 hour timelines

Time (h)	Pregnenolone	Progesterone	20α-OHP	Corticosterone	Androstenedione	Testosterone	Estradiol	Estrone
0	0	0.13±0.08	0	0	0.84±0.26	0.08±0.03	0	0
0.5	0	0.65±0.22	0	0	0.74±0.23	0.08±0.01	0	0
1	0	1.35±0.41	0	0	0.88±0.14	0.08±0.01	0	0
2	8.93±2.50	12.05±3.79	0	0	0.76±0.12	0.08±0.01	0	0
4	13.20±6.22	30.56±8.03	0	0	0.95±0.24	0.08±0.02	0	0
8	48.63±6.70	160.23±28.08	0.06±0.04	0	1.18±0.20	0.07±0.02	0	0
9	88.89±2.06	263.96±2.97	0.26±0.003	0	1.44±0.06	0.11±0.005	0	0
12	176.02±56.69	462.38±106.09	2.05±1.53	0.06±0.01	1.44±0.25	0.08±0.02	0	0
24	513.47±201.15	720.17±196.72	36.89±16.22	1.49±0.28	1.80±0.29	0.07±0.02	0	0
30	984.03±42.26	1077.84±6.45	117.92±0.44	4.92±0.38	2.29±0.004	0.11±0.0007	0.09±0.05	0.01±0.01
48	36.55±46.38	142.28±126.29	55.65±30.86	8.81±2.29	2.31±0.33	0.05±0.02	1.21±0.53	0.28±0.11
54	38.56±7.07	141.27±11.12	85.86±2.39	12.00±0.38	2.58±0.08	0.06±0.001	1.52±0.12	0.33±0.01
60	32.05±2.55	110.57±12.41	85.43±0.02	12.28±0.18	2.66±0.07	0.07±0.0001	1.49±0.11	0.35±0.01
72	32.70±4.96	68.81±3.61	86.00±5.67	13.61±0.19	2.93±0.07	0.06±0.003	1.74±0.08	0.40±0.002

Table 9: Signal intensity in exposed stimulated cells

Exposure 1	**CYP11A1**	**CYP19***	**β-actin**
Control	1.89777744	0.79571426	3771.154
$1/10^6$	1.69172332	1.6800051	8196.64
$1/10^5$	1.85402318	1.49750345	9516.326
$1/10^4$	1.83163618	1.1006173	11035.518
$1/10^3$	1.57748671	1.3056707	11254.569

* 50 kDa

APPENDIX B

This appendix includes the testing with CyDye conjugated secondary antibodies. All membranes were wet scanned for fluorescence signal at 700 V in Typhoon. Figure B1 and B2 shows the variance in CYP11A1 migration on SDS-PAGE gels, with signal for CY11A1 at both approximately 50 and 75 kDa.

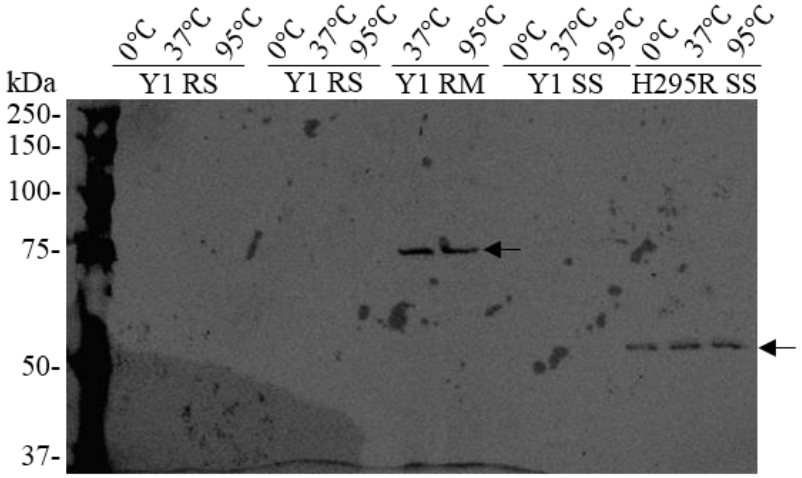

Figure B 1: Fluorescent detection of P40scc (CYP11A1) in Y1 and H295R cells. RS = Ripa supernatant (without mitochondria). RM = Ripa mitochondria, mitochondria isolated in Ripa buffer. SS = Sucrose supernatant (without mitochondria). Membrane was incubated with rabbit polyclonal anti-CYP11A1 IgG primary antibody (1:1000) overnight at 4℃ and detected with anti-rabbit Cy5 secondary antibody (1:2500). There was a detected signal for Y1 and H295R, but at different band sizes indicated with arrows. The Y1 cells are untreated, and the H295R cells have been stimulated with forskolin.

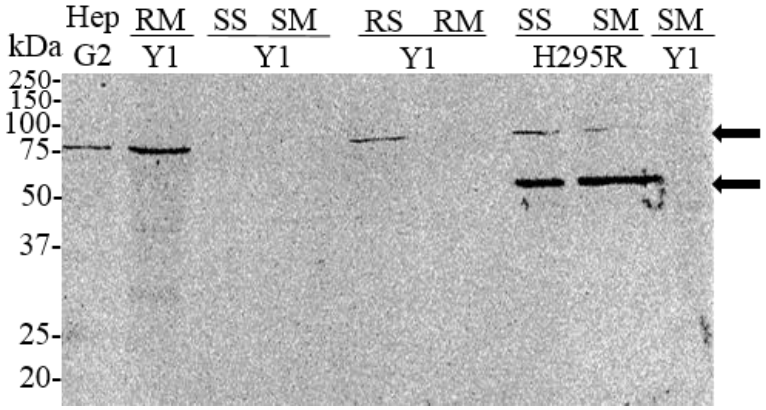

Figure B 2: Fluorescent detection of P40scc (CYP11A1) in HepG2, H295R and Y1 cell lines. Membrane was incubated with fresh rabbit polyclonal anti-CYP11A1 IgG primary antibody (1:1000) overnight at 4℃ and detected with anti-rabbit Cy5 secondary antibody (1:2500). Signal for CYP11A1 indicated with arrows.

Testing anti-beta actin on RIPA whole cell lysate (RL) and mitochondria isolated pellet (SM) and the protein supernatant (SS) showed that beta-actin was not detected in the SS (Fig. B 3). Beta actin could be used for protein loading quantification in RIPA whole cell lysates and mitochondria enriched pellet.

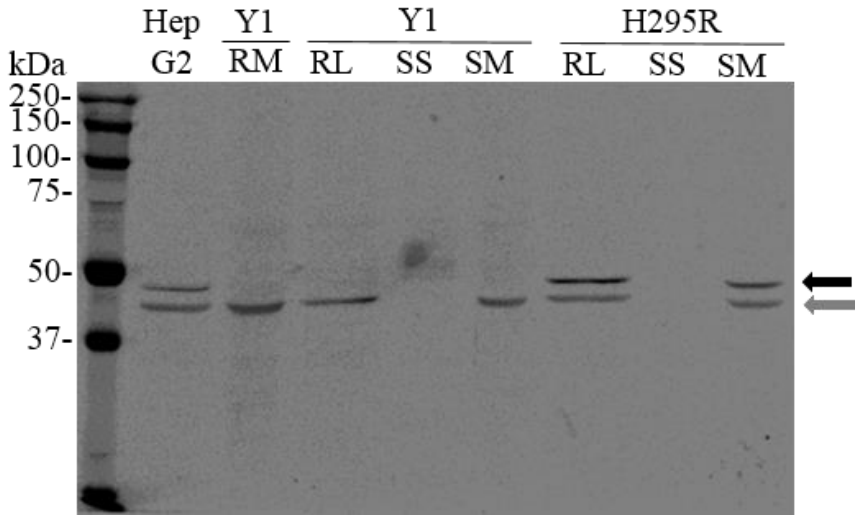

Figure B 3: Multiplex fluorescent detection of P450c11AS (CYP11B2) and StAR in HepG2, H295R and Y1 cell lines. Membrane was incubated with rabbit monoclonal anti-CYPB2 IgG primary antibody (1:1000) and goat anti-StAR (1:1000). Signal was detected with goat anti-rabbit Cy5 and donkey anti-goat Cy5 secondary antibodies, respectively. Black arrow indicate CYP11B2 just below 50 kDa. Grey arrow indicate β-actin. No detection of StAR. Picture taken with Cy5. β-actin is visible on Cy5 even though the β-actin secondary antibody is Cy3. The membrane was wet scanned for fluorescence signal at 700 V in Typhoon.

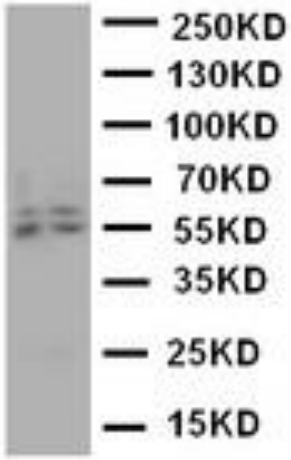

Figure B 4: Incubation of anti-CYP19 detected in human placenta tissue lysate. Two bands are visible on the blot as seen with incubation of CYP19 in this thesis. Antibody epitope aa485-503. Catalogue no. LS-C312646. Figure from LifeSpan BioSciences (2015).

APPENDIX C

Tables and method description provided by Ralf Kellmann.

Table C 1: MS method

Metabolite	Q1	Q3	Dwell time (s)	Cone (V)	CE eV	Period start (min)	Period end (min)	
Estrone sulfate	349.1235	145.0585	0.034	2	52	0	1.4	qualifier
Estrone sulfate	349.1235	269.0857	0.034	2	30	0	1.4	quantifier
Estrone sulfate-d4	353.17	147.05	0.034	2	50	0	1.4	qualifier
Estrone sulfate-d4	353.17	273.2	0.034	2	32	0	1.4	quantifier
DHEA sulfate	367.1681	79.956	0.034	12	76	0	2.5	qualifier
DHEA sulfate	367.1681	96.9341	0.034	12	30	0	2.5	quantifier
DHEAS-d6	373.2	80.01	0.034	10	70	0	2.5	qualifier
DHEAS-d6	373.2	98	0.034	10	31	0	2.5	quantifier
Estriol	287.15	145.05	0.072	26	42	2.5	3.1	qualifier
Estriol	287.15	171.05	0.072	26	36	2.5	3.1	quantifier
13C3-estriol-272	290.18	148.15	0.072	10	40	2.5	3.1	qualifier
13C3-estriol-272	290.18	174.15	0.072	10	35	2.5	3.1	quantifier
Aldosterone	359.025	189.0408	0.046	2	18	3.1	3.7	quantifier
Aldosterone	359.025	331.1674	0.046	2	16	3.1	3.7	qualifier
Aldosterone-d8	367.2	194.27	0.046	10	18	3.1	3.7	quantifier
Aldosterone-d8	367.2	304.24	0.046	10	14	3.1	3.7	qualifier
Cortisone	329.25	123.1	0.046	40	25	3.4	4.5	qualifier
Cortisone	329.25	137.08	0.046	40	26	3.4	4.5	quantifier
Cortisol	331.25	282.15	0.047	10	25	3.75	4.5	qualifier
Cortisol	331.25	297.2	0.047	10	19	3.75	4.5	quantifier
D4-cortisol	335.3	286.15	0.047	10	25	3.75	4.5	qualifier
D4-cortisol	335.3	301.2	0.047	10	21	3.75	4.5	quantifier
Corticosterone	347.15	97.08	0.047	15	31	4.5	5.05	qualifier

Corticosterone	347.15	121.05	0.047	15	18	4.5	5.05	quantifier
11-deoxycortisol	347.2365	97.0961	0.047	2	24	4.5	5.1	quantifier
11-deoxycortisol	347.2365	109.1361	0.047	2	26	4.5	5.1	qualifier
D2-11DOC	349.2042	97.0993	0.047	2	24	4.5	5.1	quantifier
D2-11DOC	349.2042	109.0748	0.047	2	26	4.5	5.1	qualifier
Estrone	269.1425	145.0776	0.034	2	34	5.1	5.45	quantifier
Estrone	269.1425	183.131	0.034	2	32	5.1	5.45	qualifier
D4-estrone	273.21	147.08	0.034	8	38	5.1	5.45	quantifier
D4-estrone	273.21	187.14	0.034	8	36	5.1	5.45	qualifier
Estradiol	271.2	145.05	0.034	25	39	5.1	5.45	quantifier
Estradiol	271.2	183.07	0.034	25	39	5.1	5.45	qualifier
D4-estradiol	275.2	147.16	0.034	25	38	5.1	5.45	quantifier
D4-estradiol	275.2	187.1	0.034	25	37	5.1	5.45	qualifier
Androstenedione	287.1765	97.0994	0.026	4	20	5.45	5.8	quantifier
Androstenedione	287.1765	109.0729	0.026	4	22	5.45	5.8	qualifier
D7-Androstenedione	294.16	100.1	0.026	2	22	5.45	5.8	quantifier
D7-Androstenedione	294.16	113.12	0.026	2	26	5.45	5.8	qualifier
21OHP	331.15	97.05	0.026	25	22	5.6	6	quantifier
21OHP	331.15	109.05	0.026	25	21	5.6	6	qualifier
Testosterone	289.1965	97.1004	0.021	6	22	5.65	6.1	quantifier
Testosterone	289.1965	109.1375	0.021	6	24	5.65	6.1	qualifier
D3-Testosterone	292.1681	97.0436	0.021	56	20	5.65	6.1	quantifier
D3-Testosterone	292.1681	109.0863	0.021	56	24	5.65	6.1	qualifier
17OHP	331.1958	97.1009	0.021	8	22	5.95	6.4	quantifier
17OHP	331.1958	109.1398	0.021	8	26	5.95	6.4	qualifier
17-OHP-13C3	334.2958	100.1032	0.021	10	26	5.95	6.4	quantifier
17-OHP-13C3	334.2958	112.142	0.021	10	30	5.95	6.4	qualifier
DHEA	271.2	213.18	0.021	20	16	6	6.4	qualifier

DHEA	271.2	253.17	0.021	20	12	6	6.4	quantifier
DHEA-d6	277.25	219.39	0.021	10	18	6	6.4	qualifier
DHEA-d6	295.25	258.3	0.021	10	10	6	6.4	quantifier
Dihydrotestosterone	291.2	159.1	0.048	30	20	6.3	6.95	qualifier
Dihydrotestosterone	291.2	255.2	0.048	30	15	6.3	6.95	quantifier
Progesterone	315.1088	97.043	0.047	4	20	6.95	7.6	quantifier
Progesterone	315.1088	109.1432	0.047	4	28	6.95	7.6	qualifier
Pregnenolone	317.2	159.13	0.047	24	24	7.25	9.45	quantifier
Pregnenolone	317.2	281.23	0.047	24	14	7.25	9.45	qualifier
D9-Progesterone	324.2319	100.0929	0.047	10	20	6.95	7.6	quantifier
D9-Progesterone	324.2319	113.1707	0.047	10	28	6.95	7.6	qualifier

The metabolites in each calibrator was made based on levels found in H295R cells and Y1 cells when being run with LC-MS/MS method.

Table C 2: Calibrators (standards) in methanol

Metabolites	**S1**	**S2**	**S3**	**S4**	**S5**	**S6**
Cortisol	1.4648	5.8594	23.4375	93.7500	375.0000	1500.0000
Cortisone	0.4883	1.9531	7.8125	31.2500	125.0000	500.0000
17-hydroxypregnenolone	0.4883	1.9531	7.8125	31.2500	125.0000	500.0000
21-OHP	0.1953	0.7813	3.1250	12.5000	50.0000	200.0000
Corticosterone	0.1953	0.7813	3.1250	12.5000	50.0000	200.0000
11-DOC	0.0977	0.3906	1.5625	6.2500	25.0000	100.0000
Testosterone	0.0977	0.3906	1.5625	6.2500	25.0000	100.0000
Androstenedione	0.2441	0.9766	3.9063	15.6250	62.5000	250.0000
17OHP	0.4883	1.9531	7.8125	31.2500	125.0000	500.0000
Progesterone	0.2441	0.9766	3.9063	15.6250	62.5000	250.0000
Aldosterone	0.0195	0.0781	0.3125	1.2500	5.0000	20.0000
Estradiol	1.4648	5.8594	23.4375	93.7500	375.0000	1500.0000
DHEA	1.9531	7.8125	31.2500	125.0000	500.0000	2000.0000
DHT	0.0977	0.3906	1.5625	6.2500	25.0000	100.0000
Pregnenolone	0.3906	1.5625	6.2500	25.0000	100.0000	400.0000
DHEAS	0.4883	1.9531	7.8125	31.2500	125.0000	500.0000
Estrone sulphate	0.8803	3.5212	14.0847	56.3388	225.3552	901.4206
Estrone	0.4883	1.9531	7.8125	31.2500	125.0000	500.0000
Estriol	0.4883	1.9531	7.8125	31.2500	125.0000	500.0000

Table C 3: Quality Controls (QC)

Testosterone	
QC Low	0.23
QC Medium	3.40415094
QC High	35.8924812

Table C 4: Internal Standard (IS)

Metabolite	**IS µM (8.5 X final concentration)**
Dehydroepiandrosterone-d4 sulphate	0.2550
Estrone-d4 sulphate	0.4597
Aldosterone-d8	0.0102
Cortisol-d4	0.7650
11-deoxycortisol-d4	0.0510
Estrone-d4	0.2550
Estradiol-d4	0.7650
Estriol-13C3	0.2550
Dehydroepiandrosterone-d6	1.0200
Androstenedion-d7	0.1275
Testosterone-d3	0.0510
17-hydroxyprogesterone-13C3	0.2550
Progesterone-d9	0.1275

Table C 5: LC gradient, flow-rate of 400 µl/min

Time (min)	**% B**
0-0.25	30
0.25 - 7.75	75
7.75-10	95
10-15	30

The following conditions were applied to the ion source (tune page):

ESI voltages: -2.0 kV (negative mode) or 1.0 kV (positive mode)

Desolvation temperature: 650°C

Desolvation gas: 1000 L/h

Cone gas: 150 L/h

Nebuliser gas: 7 bar

Collision gas: argon, 0.5 mL/h

APPENDIX D

These are the results from one 72 hour timeline measurement. Since the 72-hour time line required a longer incubation for cells to be in culture, 1.5 mL media was added in each well to ensure that the cells had enough nutrients. Even though the 72 hour time line was only done once, steroid profiling results showed that the highest levels of pregnenolone and progesterone was highest after 30 hours.

Table D 1: Overview of cells and media sampling

	Time points (h)								
Timeline	0	9	12	24	30	48	54	60	72

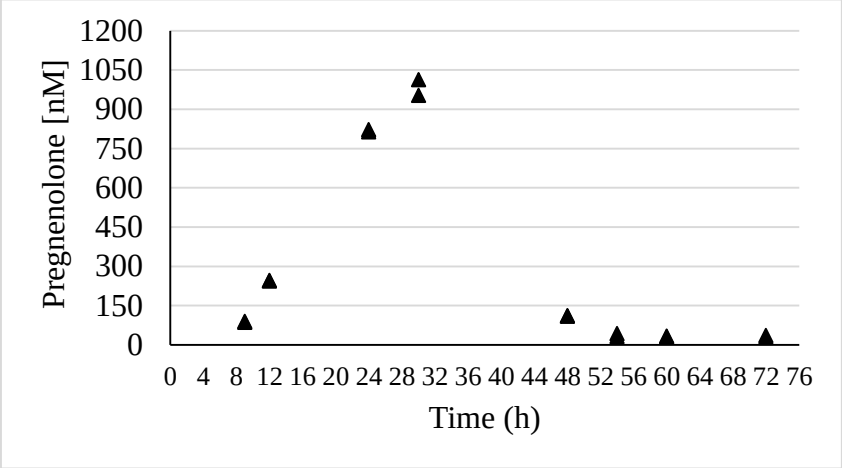

Figure D 1: Levels of pregnenolone in medium of forskolin stimulated Y1 cells.

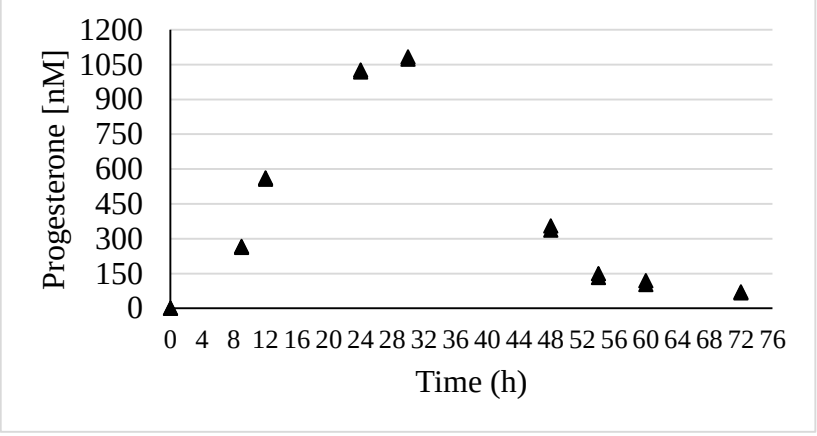

Figure D 2: Levels of progesterone in medium of forskolin stimulated Y1 cells.

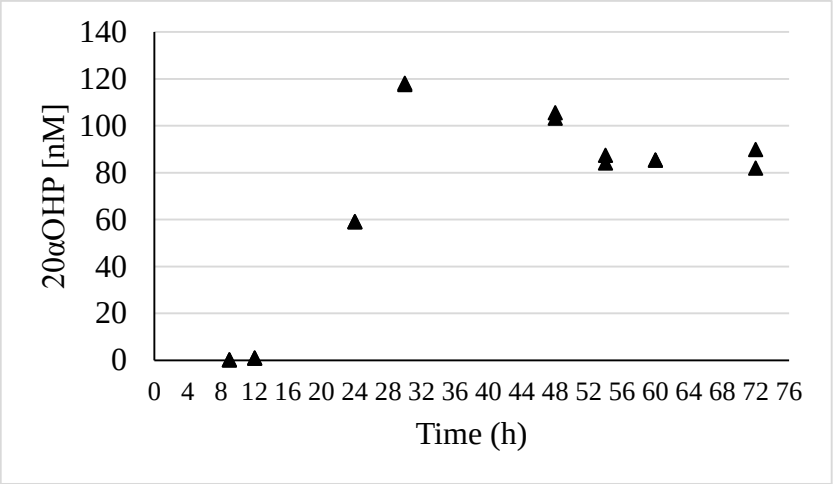

Figure D 3: Levels of 20α-dihydroxyprogesterone (20αOHP) in medium of forskolin stimulated Y1 cells.

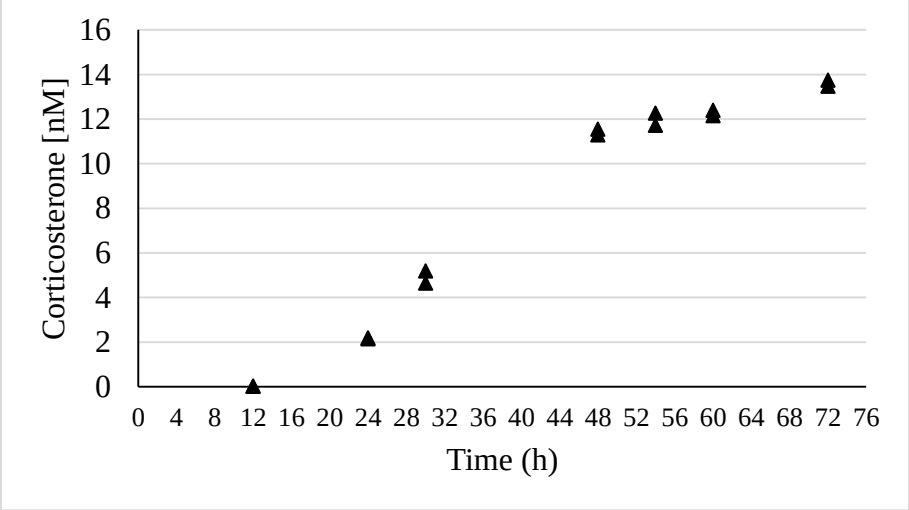

Figure D 4: Levels of corticosterone in medium of forskolin stimulated Y1 cells.

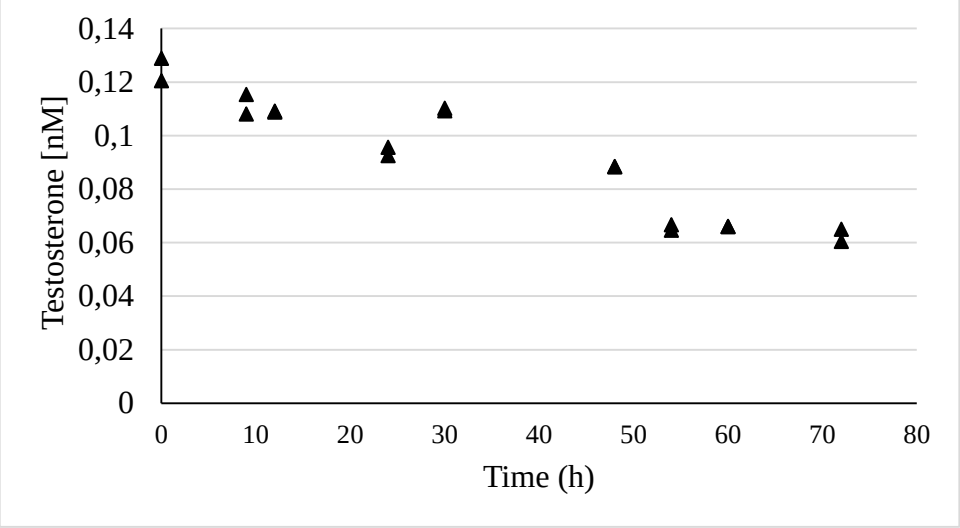

Figure D 5: Levels of testosterone in medium of forskolin stimulated Y1 cells.

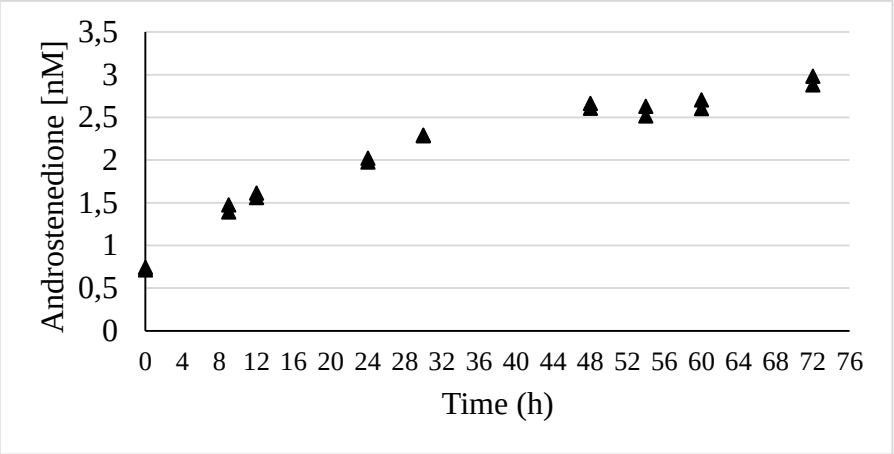

Figure D 6: Levels of androstenedione in medium of forskolin stimulated Y1 cells.

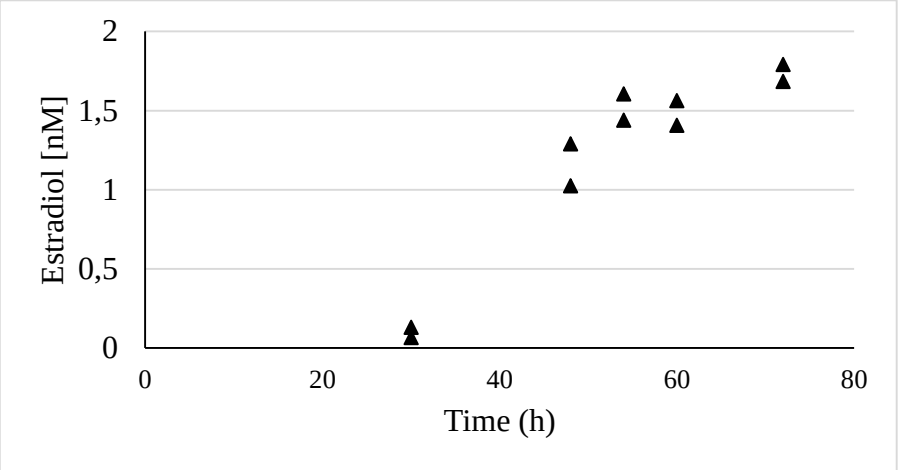

Figure D 7: Levels of estradiol in medium of forskolin stimulated Y1 cells.

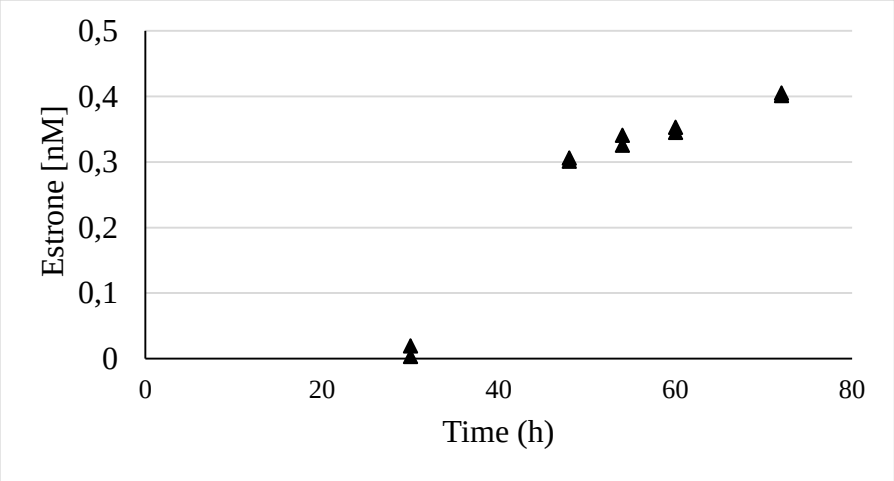

Figure D 8: Levels of estrone in medium of forskolin stimulated Y1 cells.

REFERENCES

Alaee, M., Arias, P., Sjödin, A., & Bergman, Å. (2003). An overview of commercially used brominated flame retardants, their applications, their use patterns in different countries/regions and possible modes of release. *Environment International, 29*(6), 683-689. doi: http://dx.doi.org/10.1016/S0160-4120(03)00121-1

Amor, M., Parker, K. L., Globerman, H., New, M. I., & White, P. C. (1988). Mutation in the CYP21B gene (Ile-172----Asn) causes steroid 21-hydroxylase deficiency. *Proceedings of the National Academy of Sciences, 85*(5), 1600-1604.

Arnold, J. (1866). Ein Beitrag zu der feineren Structur und dem Chemismus der Nebennieren. *Virchows Archiv, 35*(1), 64-107.

ATCC. (2015). from http://www.lgcstandards-atcc.org/Products/All/CCL-79.aspx#generalinformation

Aumo, L., Rusten, M., Mellgren, G., Bakke, M., & Lewis, A. E. (2010). Functional roles of protein kinase A (PKA) and exchange protein directly activated by 3′, 5′-cyclic adenosine 5′-monophosphate (cAMP) 2 (EPAC2) in cAMP-mediated actions in adrenocortical cells. *Endocrinology, 151*(5), 2151-2161.

Barber, J. L., Sweetman, A. J., van Wijk, D., & Jones, K. C. (2005). Hexachlorobenzene in the global environment: Emissions, levels, distribution, trends and processes. *Science of The Total Environment, 349*(1–3), 1-44. doi: http://dx.doi.org/10.1016/j.scitotenv.2005.03.014

Bergman, Å., Heindel, J. J., Jobling, S., Kidd, K. A., Zoeller, R. T., & Jobling, S. K. (2013). *State of the science of endocrine disrupting chemicals 2012: an assessment of the state of the science of endocrine disruptors prepared by a group of experts for the United Nations Environment Programme and World Health Organization*: World Health Organization.

Biosciences, A. (2002). *Ettan DIGE User Manual* (AA ed. Vol. 18-1164-40): Amersham Biosciences AB.

Bloch, E., & Cohen, A. I. (1960). Steroid production in vitro by normal and adrenal tumor-bearing male mice. *Journal of the National Cancer Institute, 24*, 97-107.

Borner, M. M., Schneider, E., Pirnia, F., Sartor, O., Trepel, J. B., & Myers, C. E. (1994). The detergent Triton X-100 induces a death pattern in human carcinoma cell lines that resembles cytotoxic lymphocyte-induced apoptosis. *FEBS letters, 353*(2), 129-132.

Brion, L., Gorostizaga, A., Gomez, N. V., Podesta, E. J., Cornejo Maciel, F., & Paz, C. (2011). Valproic acid alters mitochondrial cholesterol transport in Y1 adrenocortical cells. *Toxicol In Vitro, 25*(1), 7-12. doi: 10.1016/j.tiv.2010.08.006

Buonassisi, V., Sato, G., & Cohen, A. I. (1962). Hormone-producing cultures of adrenal and pituitary tumor origin. *Proceedings of the National Academy of Sciences of the United States of America, 48*(7), 1184.

Cao, Z., West, C., Norton-Wenzel, C. S., Rej, R., Davis, F. B., Davis, P. J., & Rej, R. (2009). Effects of resin or charcoal treatment on fetal bovine serum and bovine calf serum. *Endocrine Research, 34*(4), 101-108.

Charmandari, E., Tsigos, C., & Chrousos, G. (2005). Endocrinology of the stress response 1. *Annu. Rev. Physiol., 67*, 259-284.

Chiang, E. F.-L., Yan, Y.-L., Guiguen, Y., Postlethwait, J., & Chung, B.-c. (2001). Two Cyp19 (P450 aromatase) genes on duplicated zebrafish chromosomes are expressed in ovary or brain. *Molecular Biology and Evolution, 18*(4), 542-550.

Clark, A. J., & Cammas, F. M. (1996). The ACTH receptor. *Baillière's clinical endocrinology and metabolism, 10*(1), 29-47.

Clark, B. J., Wells, J., King, S. R., & Stocco, D. M. (1994). The purification, cloning, and expression of a novel luteinizing hormone-induced mitochondrial protein in MA-10 mouse Leydig tumor cells. Characterization of the steroidogenic acute regulatory protein (StAR). *Journal of Biological Chemistry, 269*(45), 28314-28322.

Cohen, A. I., Bloch, E., & Celozzi, E. (1957a). In vitro Response of Functional Experimental Adrenal Tumors to Corticotropin (ACTH). *Experimental Biology and Medicine, 95*(2), 304-309.

Cohen, A. I., Furth, J., & Buffett, R. F. (1957b). Histologic and physiologic characteristics of hormone-secreting transplantable adrenal tumors in mice and rats. *The American journal of pathology, 33*(4), 631.

Colonna, C., & Podesta, E. J. (2005). ACTH-induced caveolin-1 tyrosine phosphorylation is related to podosome assembly in Y1 adrenal cells. *Exp Cell Res, 304*(2), 432-442. doi: 10.1016/j.yexcr.2004.11.019

Compagnone, N. A., Bair, S. R., & Mellon, S. H. (1997). Characterization of adrenocortical cell lines produced by genetically targeted tumorigenesis in transgenic mice. *Steroids, 62*(2), 238-243.

de Boer, J., Wester, P. G., Klamer, H. J. C., Lewis, W. E., & Boon, J. P. (1998). Do flame retardants threaten ocean life? *nature, 394*(6688), 28-29.

Dedovic, K., Duchesne, A., Andrews, J., Engert, V., & Pruessner, J. C. (2009). The brain and the stress axis: The neural correlates of cortisol regulation in response to stress. *NeuroImage, 47*(3), 864-871. doi: http://dx.doi.org/10.1016/j.neuroimage.2009.05.074

Domalik, L. J., Chaplin, D. D., Kirkman, M. S., Wu, R. C., Liu, W., Howard, T. A., . . . Parker, K. L. (1991). Different Isozymes of Mouse 11/ss-Hydroxylase Produce Mineralocorticoids and Glucocorticoids. *Molecular Endocrinology, 5*(12), 1853-1861.

Farrell, S. O., & Taylor, L. E. (2006). *Experiments in Biochemistry: A Hands-On Approach* (Second ed.): Brooks/Cole Cengage Learning.

Fay, A. P., Elfiky, A., Teló, G. H., McKay, R. R., Kaymakcalan, M., Nguyen, P. L., . . . Choueiri, T. K. (2014). Adrenocortical carcinoma: The management of metastatic disease. *Critical Reviews in Oncology/Hematology, 92*(2), 123-132. doi: http://dx.doi.org/10.1016/j.critrevonc.2014.05.009

Fisher, J. S. (2004). Are all EDC effects mediated via steroid hormone receptors? *Toxicology, 205*(1–2), 33-41. doi: http://dx.doi.org/10.1016/j.tox.2004.06.035

Fromme, H., Tittlemier, S. A., Völkel, W., Wilhelm, M., & Twardella, D. (2009). Perfluorinated compounds – Exposure assessment for the general population in western countries. *International Journal of Hygiene and Environmental Health, 212*(3), 239-270. doi: http://dx.doi.org/10.1016/j.ijheh.2008.04.007

Gorrochategui, E., Pérez-Albaladejo, E., Casas, J., Lacorte, S., & Porte, C. (2014). Perfluorinated chemicals: Differential toxicity, inhibition of aromatase activity and alteration of cellular lipids in human placental cells. *Toxicology and Applied Pharmacology, 277*(2), 124-130. doi: http://dx.doi.org/10.1016/j.taap.2014.03.012

Han, J.-D., & Rubin, C. S. (1996). Regulation of cytoskeleton organization and paxillin dephosphorylation by cAMP studies on murine Y1 adrenal cells. *Journal of Biological Chemistry, 271*(46), 29211-29215.

Han, T. S., Walker, B. R., Arlt, W., & Ross, R. J. (2014). Treatment and health outcomes in adults with congenital adrenal hyperplasia. *Nat Rev Endocrinol, 10*(2), 115-124. doi: 10.1038/nrendo.2013.239

He, Y., Murphy, M. B., Richard, M., Lam, M. H., Hecker, M., Giesy, J. P., . . . Lam, P. K. (2008). Effects of 20 PBDE metabolites on steroidogenesis in the H295R cell line. *Toxicology Letters, 176*(3), 230-238.

Hecker, M., Hilscherova, K., Laskey, J., Buckalew, A., Jones, D. P., Newsted, L. J., & Giesy, P. J. (2007). Culturing of the H295R human adrenocortical carcinoma cell line (ATCC CLR-2128)

Herman, J. P., Figueiredo, H., Mueller, N. K., Ulrich-Lai, Y., Ostrander, M. M., Choi, D. C., & Cullinan, W. E. (2003). Central mechanisms of stress integration: hierarchical circuitry controlling hypothalamo–pituitary–adrenocortical responsiveness. *Frontiers in Neuroendocrinology, 24*(3), 151-180.

Herman, J. P., Ostrander, M. M., Mueller, N. K., & Figueiredo, H. (2005). Limbic system mechanisms of stress regulation: Hypothalamo-pituitary-adrenocortical axis. *Progress in Neuro-Psychopharmacology and Biological Psychiatry, 29*(8), 1201-1213. doi: http://dx.doi.org/10.1016/j.pnpbp.2005.08.006

Hermansson, V., Asp, V., Bergman, A., Bergstrom, U., & Brandt, I. (2007). Comparative CYP-dependent binding of the adrenocortical toxicants 3-methylsulfonyl-DDE and o,p'-DDD in Y-1 adrenal cells. *Arch Toxicol, 81*(11), 793-801. doi: 10.1007/s00204-007-0206-5

Ho, C. S., Lam, C. W. K., Chan, M. H. M., Cheung, R. C. K., Law, L. K., Lit, L. C. W., . . . Tai, H. L. (2003). Electrospray Ionisation Mass Spectrometry: Principles and Clinical Applications. *The Clinical Biochemist Reviews, 24*(1), 3-12.

Hyman, S. E. (2009). How adversity gets under the skin. *Nat Neurosci, 12*(3), 241-243.

Jaroenporn, S., Furuta, C., Nagaoka, K., Watanabe, G., & Taya, K. (2008). Comparative effects of prolactin versus ACTH, estradiol, progesterone, testosterone, and dihydrotestosterone on cortisol release and proliferation of the adrenocortical carcinoma cell line H295R. *Endocrine, 33*(2), 205-209.

Johansson, M., Larsson, C., Bergman, Å., & Lund, B.-O. (1998). Structure-Activity Relationship for Inhibition of CYP11B1–Dependent Glucocorticoid Synthesis in Y1 Cells by Aryl Methyl Sulfones. *Pharmacology & toxicology, 83*(5), 225-230. doi: 10.1111/j.1600-0773.1998.tb01473.x

Johnson, E. O., Kamilaris, T. C., Chrousos, G. P., & Gold, P. W. (1992). Mechanisms of stress: A dynamic overview of hormonal and behavioral homeostasis. *Neuroscience & Biobehavioral Reviews, 16*(2), 115-130. doi: http://dx.doi.org/10.1016/S0149-7634(05)80175-7

Jones, K. C., & de Voogt, P. (1999). Persistent organic pollutants (POPs): state of the science. *Environmental Pollution, 100*(1–3), 209-221. doi: http://dx.doi.org/10.1016/S0269-7491(99)00098-6

Korrick, S. A., Altshul, L. M., Tolbert, P. E., Burse, V. W., Needham, L. L., & Monson, R. R. (2000). Measurement of PCBs, DDE, and hexachlorobenzene in cord blood from infants born in towns adjacent to a PCB-contaminated waste site[ast]. *10*(S6), 743-754.

Kraugerud, M., Zimmer, K. E., Dahl, E., Berg, V., Olsaker, I., Farstad, W., . . . Verhaegen, S. (2010). Three structurally different polychlorinated biphenyl congeners (Pcb 118, 153, and 126) affect hormone production and gene expression in the human H295R in vitro model. *Journal of Toxicology and Environmental Health, Part A, 73*(16), 1122-1132.

Langlois, D., Saez, J. M., & Begeot, M. (1990). Effects of Angiotensin-II On Inositol Phosphate Accumulation And Calicum Influx in Bovine Adrenal And Y-1 Tumor Adrenal Cells. *Endocrine Research, 16*(1), 31-49.

Laville, N., Balaguer, P., Brion, F., Hinfray, N., Casellas, C., Porcher, J.-M., & Aït-Aïssa, S. (2006). Modulation of aromatase activity and mRNA by various selected pesticides in the human choriocarcinoma JEG-3 cell line. *Toxicology, 228*(1), 98-108.

Liebler, D. C. (2000). *Introduction to Proteomics, Tools for the New Biology*: Humana Press Inc, Totowa NJ.

LifeSpan BioSciences, I. (2015). from https://www.lsbio.com/antibodies/anti-cyp19-antibody-aromatase-antibody-aa485-503-ihc-wb-western-ls-c312646/322618

Martinez, A., Erdman, N. R., Rodenburg, Z. L., Eastling, P. M., & Hornbuckle, K. C. (2012). Spatial distribution of chlordanes and PCB congeners in soil in Cedar Rapids, Iowa, USA. *Environmental Pollution, 161*, 222-228.

Mattos, G. E., & Lotfi, C. F. (2005). Differences between the growth regulatory pathways in primary rat adrenal cells and mouse tumor cell line. *Mol Cell Endocrinol, 245*(1), 31-42.

Mellon, S. H., Miller, W. L., Bair, S. R., Moore, C., Vigne, J.-L., & Weiner, R. I. (1994). Steroidogenic adrenocortical cell lines produced by genetically targeted tumorigenesis in transgenic mice. *Molecular Endocrinology, 8*(1), 97-108.

Methlie, P., Hustad, S., Kellman, R., Almås, B., Erichsen, M. M., Husebye, E. S., & Løvås, K. (2013). Multisteroid LC–MS/MS assay for glucocorticoids and androgens and its application in Addison's disease. *Endocrine connections, 2*(3), 125-136.

Miller, W. L. (2013). Steroid hormone synthesis in mitochondria. *Mol Cell Endocrinol, 379*(1–2), 62-73. doi: http://dx.doi.org/10.1016/j.mce.2013.04.014

Miller, W. L., & Auchus, R. J. (2010). The molecular biology, biochemistry, and physiology of human steroidogenesis and its disorders. *Endocrine Reviews, 32*(1), 81-151.

Montaño, M., Zimmer, K. E., Dahl, E., Berg, V., Olsaker, I., Skaare, J. U., . . . Verhaegen, S. (2011). Effects of mixtures of persistent organic pollutants (POPs) derived from cod liver oil on H295R steroidogenesis. *Food and Chemical Toxicology, 49*(9), 2328-2335. doi: http://dx.doi.org/10.1016/j.fct.2011.06.034

Mountjoy, K. G., Bird, I. M., Rainey, W. E., & Cone, R. D. (1994). ACTH induces up-regulation of ACTH receptor mRNA in mouse and human adrenocortical cell lines. *Mol Cell Endocrinol, 99*(1), R17-R20.

Mountjoy, K. G., Robbins, L. S., Mortrud, M. T., & Cone, R. D. (1992). The cloning of a family of genes that encode the melanocortin receptors. *Science, 257*(5074), 1248-1251.

Mukai, K., Mitani, F., Shimada, H., & Ishimura, Y. (1995). Involvement of an AP-1 complex in zone-specific expression of the CYP11B1 gene in the rat adrenal cortex. *Molecular and Cellular Biology, 15*(11), 6003-6012.

Osawa, S., Betz, G., & Hall, P. F. (1984). Role of actin in the responses of adrenal cells to ACTH and cyclic AMP: inhibition by DNase I. *The Journal of cell biology, 99*(4), 1335-1342.

Otchere, F. A. (2005). Organochlorines (PCBs and pesticides) in the bivalves Anadara (Senilis) senilis, Crassostrea tulipa and Perna perna from the lagoons of Ghana. *Science of The Total Environment, 348*(1), 102-114.

Pagotto, R. M., Pereyra, E. N., Monzon, C., Mondillo, C., & Pignataro, O. P. (2014). Histamine inhibits adrenocortical cell proliferation but does not affect steroidogenesis. *J Endocrinol, 221*(1), 15-28. doi: 10.1530/JOE-13-0433

Parker, K. L., Chaplin, D. D., Wong, M., Seidman, J. G., Smith, J. A., & Schimmer, B. P. (1985). Expression of murine 21-hydroxylase in mouse adrenal glands and in transfected Y1 adrenocortical tumor cells. *Proceedings of the National Academy of Sciences, 82*(23), 7860-7864.

Parmar, J., Kulharya, A., & Rainey, W. (2011). Adrenocortical Cell Lines *Adrenocortical Carcinoma* (pp. 305-324): Springer.

Pesticideinfo. (2015). from http://www.pesticideinfo.org/Detail_Chemical.jsp?Rec_Id=PC35419

Pierson Jr, R. W. (1967). Metabolism of Steroid Hormones in Adrenal Cortex Tumor Cultures 1. *Endocrinology, 81*(4), 693-707.

Pitt, J. J. (2009). Principles and Applications of Liquid Chromatography-Mass Spectrometry in Clinical Biochemistry. *The Clinical Biochemist Reviews, 30*(1), 19-34.

Poli, G., Guasti, D., Rapizzi, E., Fucci, R., Canu, L., Bandinelli, A., . . . Luconi, M. (2013). Morphofunctional effects of mitotane on mitochondria in human adrenocortical cancer cells. *Endocrine-Related Cancer, 20*(4), 537-550.

Rahman, F., Langford, K. H., Scrimshaw, M. D., & Lester, J. N. (2001). Polybrominated diphenyl ether (PBDE) flame retardants. *Science of The Total Environment, 275*(1–3), 1-17. doi: http://dx.doi.org/10.1016/S0048-9697(01)00852-X

Rainey, W. E., Saner, K., & Schimmer, B. P. (2004). Adrenocortical cell lines. *Mol Cell Endocrinol, 228*(1-2), 23-38. doi: 10.1016/j.mce.2003.12.020

Rath, A., Glibowicka, M., Nadeau, V. G., Chen, G., & Deber, C. M. (2009). Detergent binding explains anomalous SDS-PAGE migration of membrane proteins. *Proceedings of the National Academy of Sciences, 106*(6), 1760-1765. doi: 10.1073/pnas.0813167106

Rehfuss, R. P., Walton, K. M., Loriaux, M. M., & Goodman, R. (1991). The cAMP-regulated enhancer-binding protein ATF-1 activates transcription in response to cAMP-dependent protein kinase A. *Journal of Biological Chemistry, 266*(28), 18431-18434.

Rocha, K. M., Forti, F. L., Lepique, A. P., & Armelin, H. A. (2003). Deconstructing the molecular mechanisms of cell cycle control in a mouse adrenocortical cell line: Roles of ACTH. *Microscopy Research and Technique, 61*(3), 268-274. doi: 10.1002/jemt.10336

Rui, X., Al-Hakim, A., Tsao, J., Albert, P. R., & Schimmer, B. P. (2004). Expression of adenylyl cyclase-4 (AC-4) in Y1 and forskolin-resistant adrenal cells. *Mol Cell Endocrinol, 215*(1-2), 101-108. doi: 10.1016/j.mce.2003.11.019

Sanderson, J. T., Boerma, J., Lansbergen, G. W. A., & van den Berg, M. (2002). Induction and Inhibition of Aromatase (CYP19) Activity by Various Classes of Pesticides in H295R Human Adrenocortical Carcinoma Cells. *Toxicology and Applied Pharmacology, 182*(1), 44-54. doi: http://dx.doi.org/10.1006/taap.2002.9420

Schimmer, B. P., Cordova, M., Cheng, H., Tsao, A., Goryachev, A. B., Schimmer, A. D., & Morris, Q. (2006). Global Profiles of Gene Expression Induced by Adrenocorticotropin in Y1 Mouse Adrenal Cells. *Endocrinology, 147*(5), 2357-2367. doi: doi:10.1210/en.2005-1526

Schimmer, B. P., Kwan, W. K., Tsao, J., & Qiu, R. (1995). Adrenocorticotropin-resistant mutants of the Y1 adrenal cell line fail to express the adrenocorticotropin receptor. *Journal of cellular physiology, 163*(1), 164-171.

Schimmer, B. P., & Schulz, P. (1985). The roles of cAMP and cAMP-dependent protein kinase in forskolin's actions on Y1 adrenocortical tumor cells. *Endocrine Research, 11*(3-4), 199-209.

Song, R., He, Y., Murphy, M. B., Yeung, L. W., Richard, M., Lam, M. H., . . . Wu, R. S. (2008). Effects of fifteen PBDE metabolites, DE71, DE79 and TBBPA on steroidogenesis in the H295R cell line. *Chemosphere, 71*(10), 1888-1894.

Stahl, T., Mattern, D., & Brunn, H. (2011). Toxicology of perfluorinated compounds. *Environmental Sciences Europe, 23*(1), 1-52.

Temel, R. E., Trigatti, B., DeMattos, R. B., Azhar, S., Krieger, M., & Williams, D. L. (1997). Scavenger receptor class B, type I (SR-BI) is the major route for the delivery of high density lipoprotein cholesterol to the steroidogenic pathway in cultured mouse adrenocortical cells. *Proceedings of the National Academy of Sciences, 94*(25), 13600-13605.

Terashima, M., Toda, K., Kawamoto, T., Kuribayashi, I., Ogawa, Y., Maeda, T., & Shizuta, Y. (1991). Isolation of a full-length cDNA encoding mouse aromatase P450. *Archives of Biochemistry and Biophysics, 285*(2), 231-237.

Towbin, H., Staehelin, T., & Gordon, J. (1979). Electrophoretic transfer of proteins from polyacrylamide gels to nitrocellulose sheets: procedure and some applications.

Proceedings of the National Academy of Sciences of the United States of America, 76(9), 4350-4354.

Tsigos, C., & Chrousos, G. P. (2002). Hypothalamic–pituitary–adrenal axis, neuroendocrine factors and stress. *Journal of Psychosomatic Research, 53*(4), 865-871. doi: http://dx.doi.org/10.1016/S0022-3999(02)00429-4

Whitehouse, B., Gyles, S., Squires, P., Sayed, S., Burns, C., Persaud, S., & Jones, P. (2002). Interdependence of steroidogenesis and shape changes in Y1 adrenocortical cells: studies with inhibitors of phosphoprotein phosphatases. *Journal of Endocrinology, 172*(3), 583-593.

Wikimedia. (2015). from https://commons.wikimedia.org/wiki/File:PFOS-2D-skeletal.png

Xu, Y., Richard, M., Zhang, X., Murphy, M. B., Giesy, J. P., Lam, M. H., . . . Yu, H. (2006). Effects of PCBs and MeSO 2–PCBs on adrenocortical steroidogenesis in H295R human adrenocortical carcinoma cells. *Chemosphere, 63*(5), 772-784.

Yasumura, Y., Buonassisi, V., & Sato, G. (1966). Clonal analysis of differentiated function in animal cell cultures I. Possible correlated maintenance of differentiated function and the diploid karyotype. *Cancer research, 26*(3 Part 1), 529-535.

Zimmer, K. E., Montaño, M., Olsaker, I., Dahl, E., Berg, V., Karlsson, C., . . . Verhaegen, S. (2011). In vitro steroidogenic effects of mixtures of persistent organic pollutants (POPs) extracted from burbot (Lota lota) caught in two Norwegian lakes. *Science of The Total Environment, 409*(11), 2040-2048. doi: http://dx.doi.org/10.1016/j.scitotenv.2011.01.055